Natural Resources Canada | Ressources naturelles Canada

GEOLOGICAL SURVEY OF CANADA
OPEN FILE 8239

Seismic operations report for the 2016 Canada–Sweden Polar Expedition in the Arctic Ocean

J. Shimeld and K. Boggild

2017

GEOLOGICAL SURVEY OF CANADA
OPEN FILE 8239

Seismic operations report for the 2016 Canada–Sweden Polar Expedition in the Arctic Ocean

J. Shimeld and K. Boggild

2017

doi:10.4095/300670

This publication is available for free download through GEOSCAN (http://geoscan.nrcan.gc.ca/).

Recommended citation
Shimeld, J. and Boggild, K., 2017. Seismic operations report for the 2016 Canada–Sweden Polar Expedition in the Arctic Ocean; Geological Survey of Canada, Open File 8239, 68 p. doi:10.4095/300670

Publications in this series have not been edited; they are released as submitted by the author.

Table of Contents

List of Figures

List of Tables

Executive Summary

The 2016 Canada–Sweden Polar Expedition was organized and conducted under the responsibilities of two Canadian federal government departments: Natural Resources Canada and the Department of Fisheries and Oceans. This expedition collected geological, geophysical and bathymetrical data across remote, ice-covered regions of the Arctic Ocean, including the Amundsen Basin, Lomonosov Ridge, Makarov Basin, Marvin Spur, Alpha Ridge, northern Canada Basin, and Chukchi rise. These data will be used to examine the nature of the crust beneath the Arctic Ocean, and to increase scientific understanding of its geologic evolution. The political impetus is to delineate the Extended Continental Shelf of Canada under the United Nations Convention on the Law of the Sea.

Two icebreakers were contracted by Natural Resources Canada for the expedition: the *CCGS Louis S. St-Laurent*, managed by the Canadian Coast Guard, and the *IB Oden*, managed by the Swedish Polar Research Secretariat. Both ships were equipped with gravimetric, seismic and multibeam systems that could be used either in tandem or independently. In addition, the *Louis* carried two helicopters, and the *Oden* carried one helicopter, for working on the sea ice at a maximum range of 60 nMi from the ships. Multibeam and seismic operations were given top priority on the *Louis,* but oceanographic measurements were also collected whenever opportunities arose. A broader scientific program that included seafloor dredging, piston coring, oceanography, sea ice studies, meteorology, and biogeochemistry was managed onboard the *Oden*.

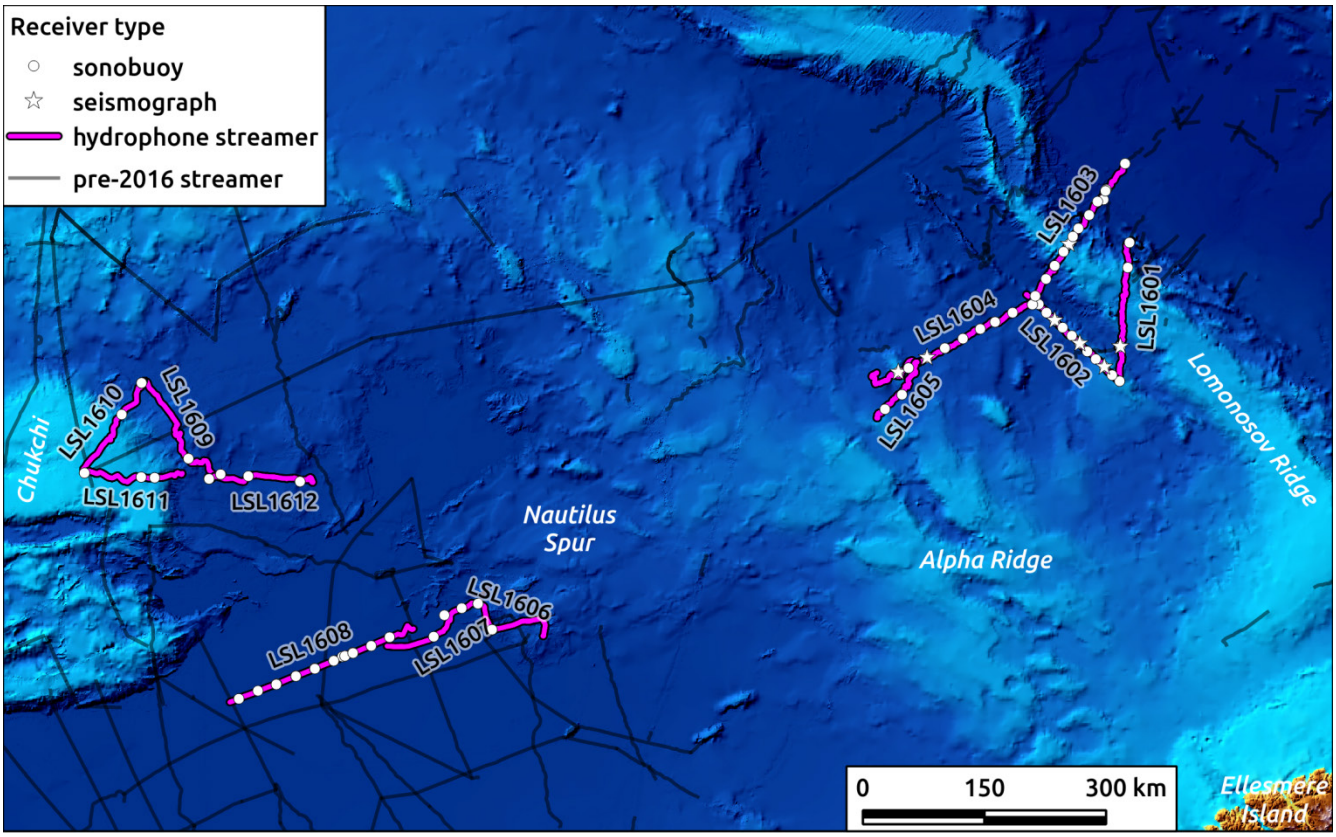

Seismic records collected during the 2016 Canada–Sweden Polar Expedition.

In the first phase of the expedition, between the Amundsen Basin and central Alpha Ridge, the *Oden* acted as the lead icebreaker while the seismic source and hydrophone streamer systems were towed by the *Louis.* In the second phase of the expedition, the two icebreakers operated independently: the *Oden* collected geological samples, multibeam and seismic data over the Makarov and Amundsen basins, while the *Louis* collected multibeam and seismic data over the Nautilus Spur, northern Canada Basin, and Chukchi rise. Gravimetric data were collected continuously on both ships for the duration of the expedition.

Seismic operations conducted onboard the *Louis* during the first and second phases of the expedition produced 12 seismic reflection profiles of the sedimentary succession and upper crust along a total combined distance of 2184 km. They also produced seismic wide-angle reflection and refraction recordings from 62 expendable sonobuoys and 5 ice-station seismometers for investigation of the upper to lower crust. In the first phase, *Oden* seismic operations were vital for deployment and recovery of the ice-station seismometers, and they also produced duplicate recordings of the sonobuoys. In the second phase, the *Oden* collected four seismic reflection profiles in the Amundsen Basin, totalling 197 km in length, along with recordings from 14 sonobuoys and 2 ice-station seismometers.

The *Louis* operations are documented in Chapter 1, and signal processing of the resulting seismic reflection records is described in Chapter 2. Seismic acquisition and processing reports for the data collected on the *Oden* will be published by staff members of that program.

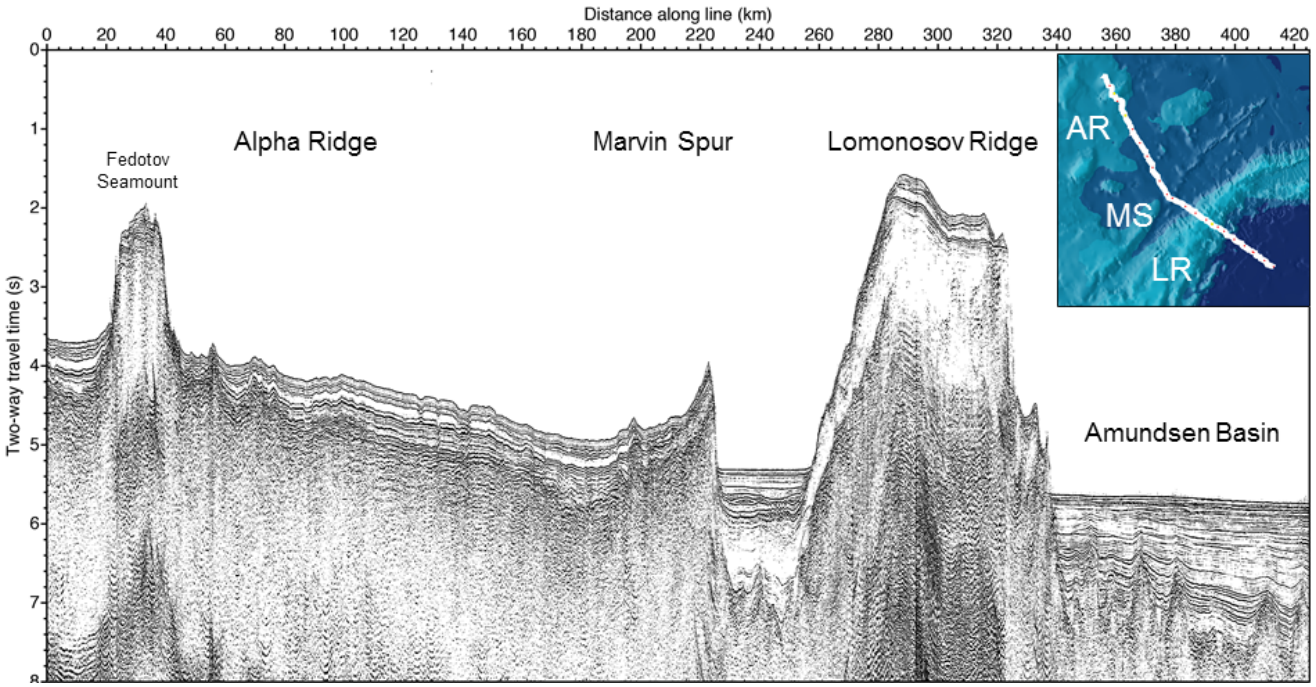

Filtered and migrated record section showing merged lines LSL1603 and LSL1604.

Acknowledgements

The authors thank Lead Scientist Mary-Lynn Dickson, Co-Lead Scientist Katarina Gårdfeldt, and Liaison Officers Gary Sonnichsen and Åsa Lindgren for their efforts to maximize the scientific success of the expedition, which involved personnel from the Geological Survey of Canada, the Swedish Polar Research Secretariat, the Canadian Coast Guard, the Canadian Hydrographic Service, the Canadian Ice Service, the Geological Survey of Denmark and Greenland, Global Affairs Canada, Aarhus University, Chalmers University of Technology, and Stockholm University. Captain Anthony Potts of the *CCGS Louis S. St-Laurent*, and Master Erik Andersson of the *IB Oden* skillfully managed the safety of all personnel and the complex two-ship operations, whilst their officers and crew worked with professional dedication for the success of the expedition.

The seismic team onboard the *Oden* contributed enormously to the overall program, adapting rapidly to ever-changing logistical constraints and offering technical support that, at one point, enabled seismic operations onboard the *Louis* to continue despite the loss of critical equipment. The *Oden* team consisted of Thomas Funck, John Hopper, Per Trinhammer, Lars Rasmussen, Tommy Kessler, Anders Dahlin, Andreas Skifter Madsen, Lasse Nygaard Eriksen, and Trine Andreasen.

The authors also express appreciation to the *Louis* seismic team who, through deep experience and perennial inventiveness, kept the equipment and operations running under highly challenging conditions. Thank you Des Manning, Patrick Meslin, Peter Pledge (onshore support), Borden Chapman, Ken Asprey, Robert Garber, Bob Murphy, Stan Myers, Rodger Oulton, Dale Ruben, John Ruben, and Nelson Ruben.

Seismic team members from the two icebreakers.

CHAPTER 1: Seismic data acquisition onboard the *CCGS Louis S. St-Laurent*

J. Shimeld and K. Boggild

1.1 Introduction

Two icebreakers, *IB Oden* and *CCGS Louis S. St-Laurent*, were operated jointly in the Arctic Ocean between August 11th and September 2nd of 2016 to collect seismic data over regions of the Amundsen Basin, Lomonosov Ridge, Marvin Spur, and northern Alpha Ridge. The resulting data set includes seismic reflection recordings from a 16-channel hydrophone streamer, and also wide-angle reflection/refraction recordings from expendable sonobuoys and from seismometers on drifting ice floes. Some of the wide-angle recordings are fully-reversed (*i.e.* they were made while shooting both towards and away from the receiver) and they exhibit signals at offsets of greater than 40 km. To our knowledge, the seismic data set collected during the first phase of the expedition is the most comprehensive of any that have been collected in these remote regions of the Arctic Ocean.

During the second phase of the expedition, after September 2nd, the icebreakers were operated independently. The *Oden* was used to collect geological samples, multibeam and seismic data over the Makarov and Amundsen basins, while the *Louis* was used to collect multibeam and seismic data over the Nautilus Spur, northern Canada Basin, and Chukchi rise. Single-ship operations with the *Oden* finished on September 10th, and those with the *Louis* were finished on September 11th.

In this chapter we document the seismic operations conducted onboard the *Louis* during the first and second phases of the expedition. In total, this work yielded 2183.9 line-km of seismic reflection shot records at an average shotpoint density of 34.0 m/shot along 12 line segments. There are also 62 sonobuoy and 5 seismometer records spaced irregularly at distances of 15 to 80 km along each of the line segments.

1.2 Seismic sources

Two seismic sources, designed specifically for towing behind the *Louis*, were assembled using Sercel G-guns suspended beneath specially designed tow-sleds, which were fabricated in 2007 from lead-filled artillery shell casings (Hutchinson *et al.*, 2009). Each assembly, including the G-guns and tow-sled, has a mass of about 2300 kg, allowing it to be towed almost vertically behind the stern of the ship, well protected from ice, at a nominal depth of 11.2 m.

The standard seismic source used for the operations has a total volume of 1150 in^3, comprised of a cluster of two 500 in^3 G-guns and one 150 in^3 G-gun (Figure 1-1). This is the same basic configuration that was used for each of the seismic surveys conducted by the Geological Survey of Canada in various regions of the Arctic Ocean since 2007. In regions of thick sedimentary cover, such as the Canada Basin, the 1150 in^3 source yields a seismic penetration of greater than 6 km (Shimeld *et al.*, 2016). It is fired at a pressure of 1800 psi (124 bar) and at intervals of between 12 and 20 s, with shorter intervals generally being used in shallower water for increased shotpoint density.

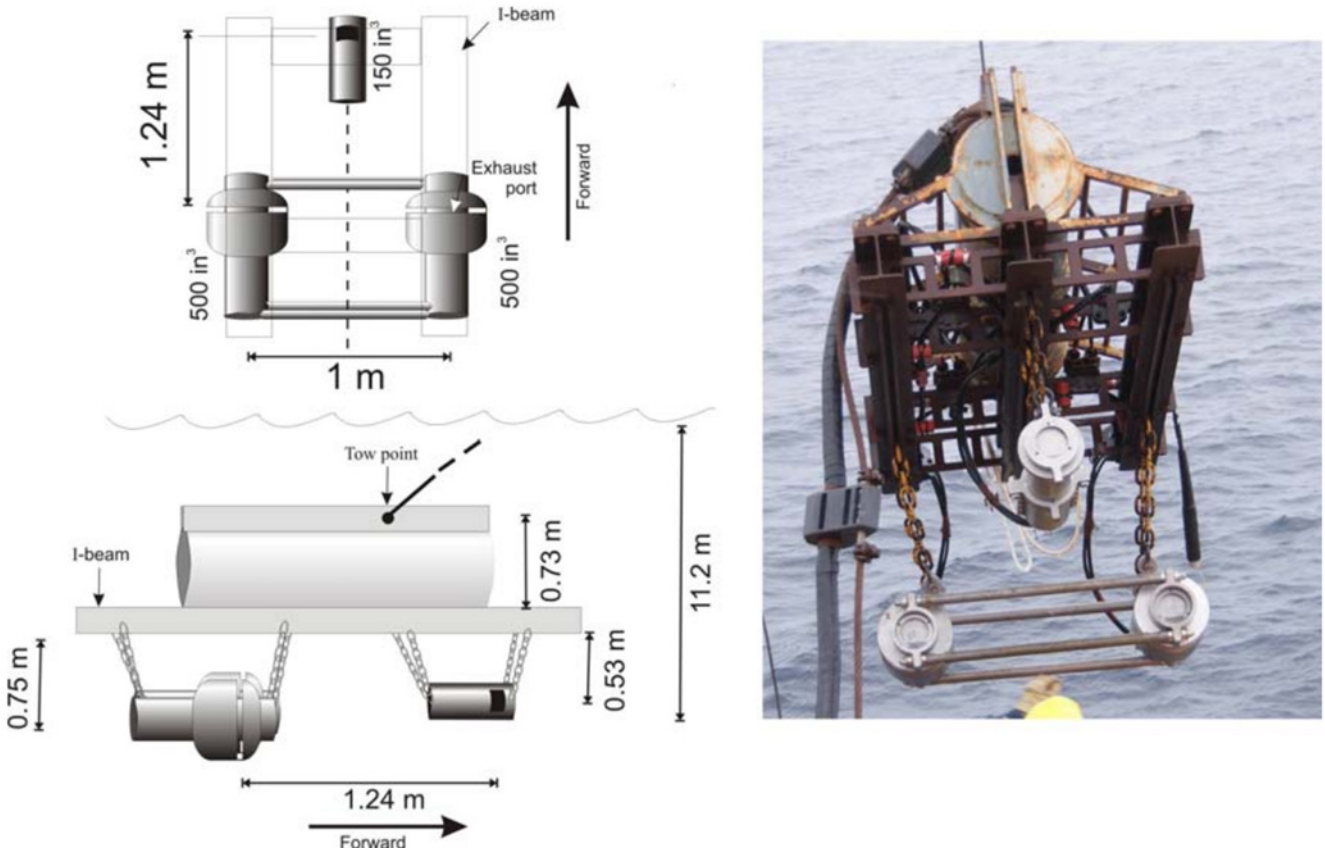

Figure 1-1: Schematic diagram and photograph of the 1150 in^3 seismic source being deployed.

A second seismic source was assembled using a cluster of four 500 in^3 G-guns, for a total volume of 2000 in^3 (Figure 1-2). The intention of utilizing this source was to generate reflections and refractions from mid to upper crustal levels, and possibly as deep as the Moho. Initially it was fired every 20 s, but the interval was increased to 30 s in order to prevent contamination of the shot records by wrap-around multiple energy and to reduce the risk of premature failure from repetitive mechanical strain. With its significantly greater power, the 2000 in^3 source was expected to be less durable than the other source. There were also concerns that it would be vulnerable to damage from sea ice because mounting the four 500 in^3 G-guns on the tow-sled required high pressure air lines and control cables to be routed to the fore and aft, rather than to the centre, of the tow-sled. Nonetheless, the 2000 in^3 source proved to be both mechanically reliable and operationally robust for operations in ice.

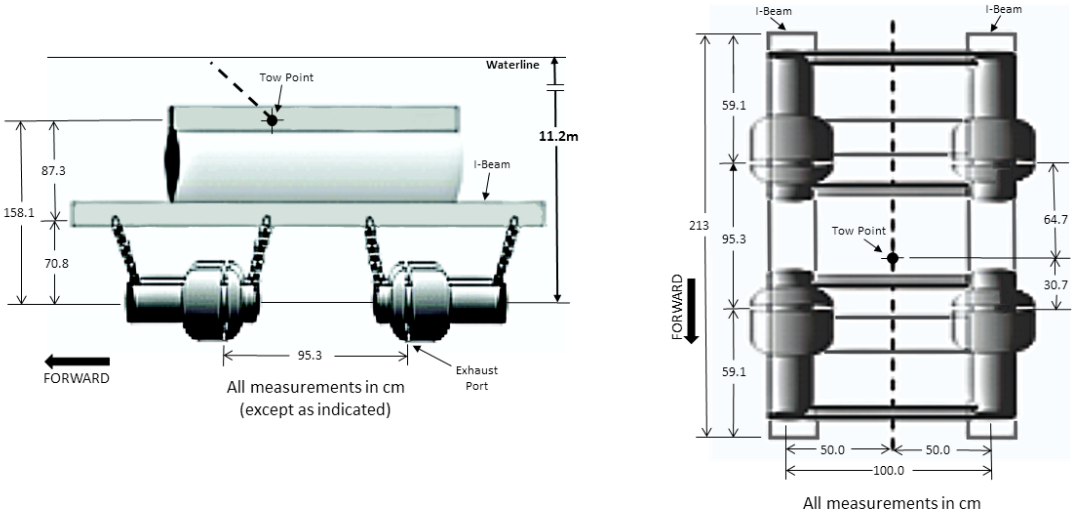

Figure 1-2: Schematic diagram of the 2000 in^3 seismic source.

1.3 Receiver systems

Hydrophone streamers towed by the *Louis* were used for seismic reflection profiling, while expendable sonobuoys deployed immediately astern of the icebreaker were used to obtain non-reversed (*i.e.* one-sided) records of wide-angle reflections and refractions. Fully-reversed records were collected using expendable sonobuoys deployed in open water pools and leads ahead of the survey, both by advance icebreaker and by helicopter. Non-expendable seismometer stations installed and later recovered by helicopter on multiyear ice floes were also used, and these yielded high quality, fully-reversed records both from hydrophones suspended beneath the ice and from geophones placed on the ice. Each of these receiver systems is described in more detail below.

1.3.1 Hydrophone streamers

Two hydrophone streamers were assembled using identical components of the GeoEel system from Geometrics Inc. (Figure 1-3). The standard streamer assembly includes two active sections, each 50 m long, and each with eight groups of four Benthos Geopoint hydrophones spaced at regular intervals of 6.25 m. The groups are configured into eight channels per active section, for a total of 16 channels.

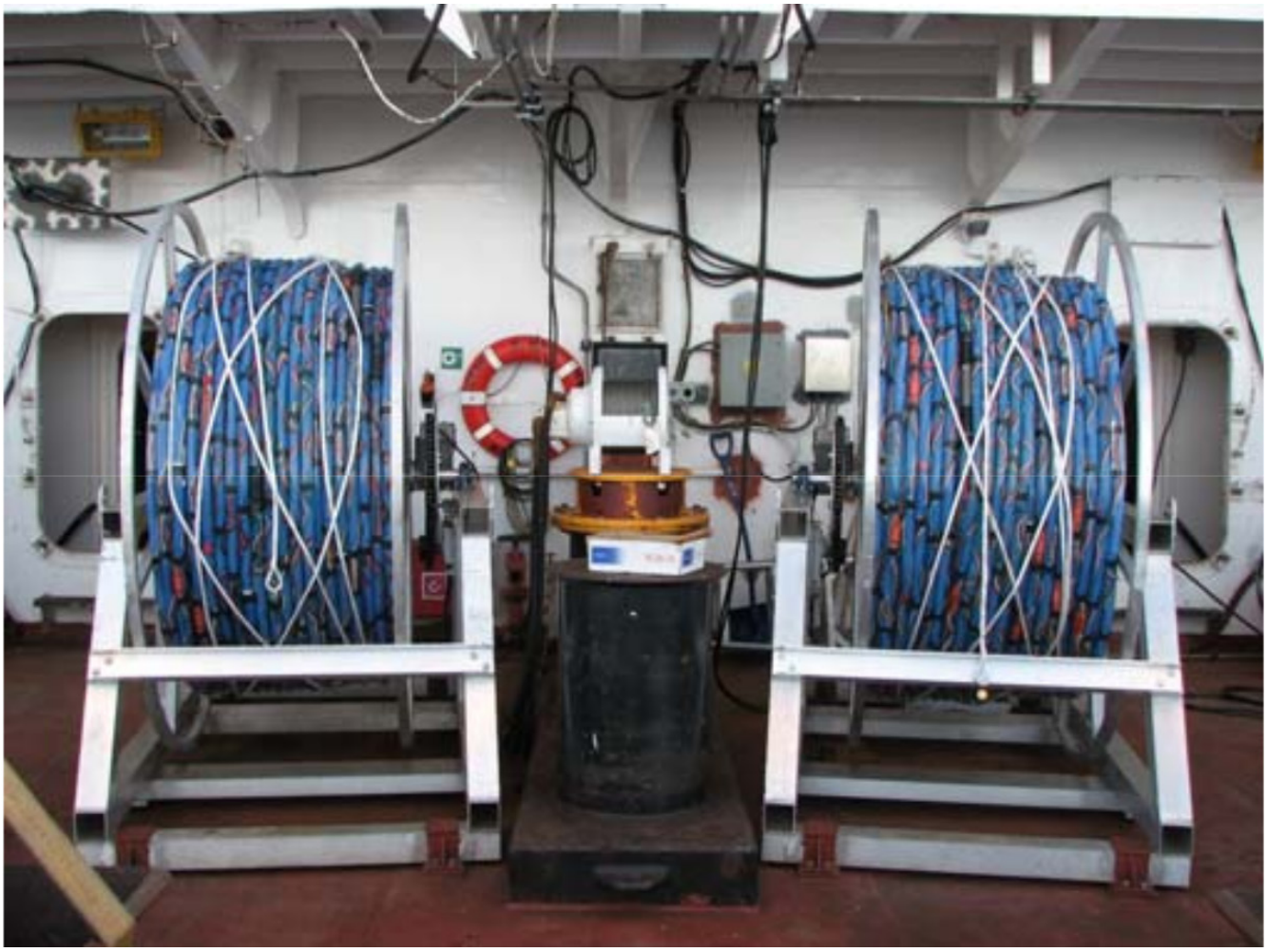

Figure 1-3: Photograph of the two 16-channel digital streamers onboard the Louis, assembled using GeoEel system components from Geometrics Inc.

Normally a hydrophone streamer is flown beneath the ice by attaching it directly to the tow-sled (Figure 1-4). However, the loss of some streamer components during the operations, coupled with damage to critical sections in the umbilical package connecting deck units to the tow sled, necessitated the improvised assembly of a third streamer that was flown from a pull point on the steel tow cable just above the sled. The lead-in section where this improvised streamer entered the water could not be fully protected from ice within the umbilical package, so that system had to be used only in regions of open water or very light ice with small isolated floes in concentrations of less than about 3/10.

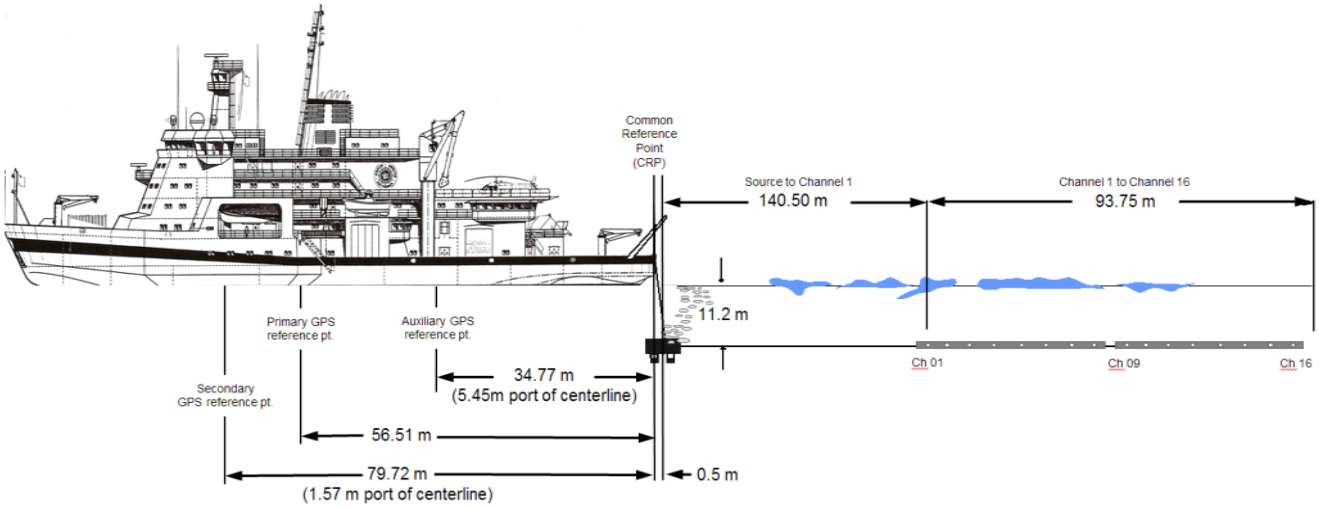

Figure 1-4: Reference points, source-to-receiver offsets, and towing arrangement for the standard streamer assembly. The improvised streamer assembly had the same reference points and offsets, but the towing arrangement was modified slightly such that the streamer was flown from the tow cable just above the gun sled.

Analog hydrophone signals in the Geometrics GeoEel system are automatically summed for each receiver group and converted to 24-bit digital traces by digitizing units in the streamer. The trace data from each receiver group are broadcast, via ethernet connection in the streamer, to the Geometrics digital multithreaded software controller and recording system (GeoEel Controller version 5.36), which runs under the Windows XP operating system (service pack 3) on a personal computer in the seismic lab.

The GeoEel Controller software provides a user interface for configuring the streamer system, for monitoring the data quality during acquisition, for testing the receiver array, and for recording the data to magnetic disk drive and/or magnetic tape. Additional data, such as measurements from the streamer depth sensors, can also be logged by the Controller software through a serial communications port. The recording parameters that were used during the survey are listed in Table 1-1.

Table 1-1: Parameters used with version 5.37 of the GeoEel Controller software.

Parameter	Value
Sampling interval	2 ms
Record length	11.5 s
Recording delay	0.05 s
Recording format	SEG-D 8058 revision 1
Active channels	1 through 16 (near trace = 1; far trace = 16)
Reset file timestamp to GPS time	disabled for LSL1601 through LSL1605 enabled for LSL1606 through LSL1612
Shot/file number comparison	disabled
Time window for capturing NMEA strings from serial port	±5.0 s for LSL1601 through LSL1605 ±2.5 s for LSL1601 through LSL1605
AC coupling	disabled
Preamp gains	18 dB on all channels for all lines, except 8 dB on all channels for LSL1603
Transconductance	20 Volt/bar

1.3.2 Sonobuoy and seismometer receivers for wide-angle recording

Wide-angle reflection and refraction records were acquired along each of the survey lines to investigate seismic velocity in the crust, and to enable time-to-depth conversions. These data were collected with expendable sonobuoys, deployed from the stern of either the *Oden* or the *Louis*, and also non-expendable seismometers on drifting ice floes, which were installed and recovered by helicopter.

A unique instrument code, as illustrated on Figure 1-5, was assigned to each wide-angle receiver that was deployed during the seismic operations, and these codes were used in all associated field logs and data files.

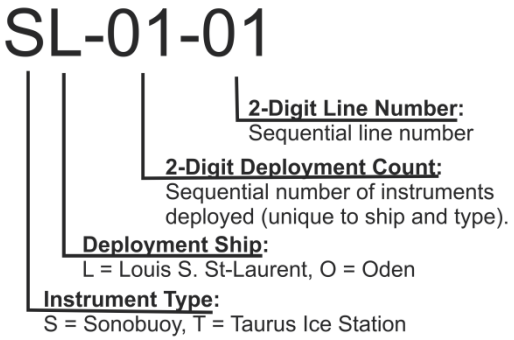

Figure 1-5: Instrument code assigned to each wide-angle receiver.

Example instrument codes are as follows:

SL-01-01 —first sonobuoy launched from Louis, line 01
SL-03-02 —third sonobuoy launched from Louis, line 02
SO-23-07 —twenty-third sonobuoy from Oden, line 07
TL-11-05 —eleventh Taurus seismometer from Louis, line 05

Data files from the ice-station seismometers are labelled with the one of the following channel names: GEO (Geophone, channel 1), HY1 (Hydrophone, channel 2), or HY2 (hydrophone, Channel 3).

1.3.3 Expendable sonobuoys

Ultra-Electronics Model 53C sonobuoys were used to collect wide-angle seismic signals that were then rebroadcast to radio receivers and digitizing systems onboard the ships. All sonobuoys were programmed with a hydrophone depth setting of D1 (30 m) and a duration setting of 8 hours prior to deployment, with the exception of SL-45-12 which was set to a D4 depth setting. Sonobuoys were deployed both from the stern, and ahead of the ship to acquire reversed records.

During two-ship operations, sonobuoy transmissions were recorded by both vessels to provide data redundancy and to maximize the signal received. Onboard the *Louis*, sonobuoy signals were received by two stacked Yaggi arrays mounted on the crow's nest: one forward facing array (elevation: 88.5 ft) and one aft-facing array (elevation: 92 ft). Each array was split three ways for a total of six available channels received on three ICOM radios and digitized using GSCA Portable Digitizer units #1 and #3.

Sonobuoys were recorded onboard the *Oden* using a GeoEel digitizer that was synchronized by Zyfer atomic clock to the shot times onboard the *Louis*. Backup recordings were also made using a Taurus seismometer. A full description of the recording equipment on the *Oden* will be provided by the staff involved in those operations.

1.3.4 Non-expendable seismometers on drifting ice floes

In an effort to acquire high quality, fully-reversed wide-angle reflection/refraction records with long offsets, seismometer stations were flown by helicopter and installed on drifting ice floes ahead of the seismic operation, and then subsequently recovered by helicopter once the operation had proceeded past the seismometer station. The ice-stations consisted of the following equipment: one seismometer cooler; one CarteNav ETS-1500 satellite beacon; one flag pole for attaching the satellite beacon antenna; and, several snow-filled garbage bags to increase visibility of the site (Figure 1-6). Inside each seismometer cooler was: one Nanometrics Taurus Portable Seismometer; two 14 V battery packs; built-in Trimble GPS receiver antenna; bubble wrap insulation; power/GPS cables; and, a sensor cable assembly for two hydrophones and one geophone.

The original 28-pin sensor extension cables built into the cooler boxes were incompatible with the sensor cable configuration. When these original extension cables were used, noise spikes were produced roughly every 3.3 s on both of the hydrophone channels. For this reason, the original extension cables were removed from every cooler box and modified cables were installed. For

deployment, sensor cables were passed into the box through the sensor cable hole, which was then insulated using Duct Seal. Silicon caulk was applied to the seams of the cooler boxes where necessary to prevent additional heat leakage. Also, coin cell batteries were replaced in each CarteNav ETS-1500 beacons prior to testing and deployment. Testing of these units revealed that two of the beacons were non-operational (serial numbers 06017, 06015).

Figure 1-6: Photograph of a seismometer installation on the sea-ice (ice-station TL-01-02).

Each Taurus seismometer was configured by uploading a configuration file via ethernet connection. For acquisition of wide-angle data, the seismometers were configured to record at a sample rate of 250 Hz in buffered mode. Geophone data were digitized on channel 1 (GEO), and hydrophone data were digitized on channels 2 and 3 (HY1 and HY2). Other relevant configuration settings for the Taurus seismometers are listed in Table 1-2.

Table 1-2: Configuration parameters used to program each Taurus seismometer.

	Setting	Configuration
General	Taurus Running Mode	Buffered
	SOH Report Interval [s]	60
	UI Timeout [min]	10
	GPS Duty Cycle Mode	Auto
Digitizer	Sample Rate [Hz]	250
	Output Channels	3
	Enable DC Removal	Yes
	DC Removal [Hz]	0.001
	Frames Per Packet	7
Timing	Resynchronization Mode	Discard Samples
	Require Good Time	Yes
Front End	Input Range, diff p-to-p [V]	8
	Input Impedance	High
	Common Mode Range	Extended
	Enable Dither	No
	Software Gain	1
	Enable Hard Clip	No
Power Manager	High Voltage Disconnect [mV]	36000
	High Voltage Reconnect [mV]	35000
	Low Voltage Reconnect [mV]	11800
	Low Voltage Disconnect [mV]	11500
Sensor Library	Sensor Name	Default Passive Sensor

Ice-stations were deployed within 10–15 m of the ice edge on medium-sized floes so that the hydrophones could reach the water. The geophone sensor was coupled to the ice surface near the insulated seismometer box. The CarteNav ETS-1500 satellite beacons were then activated, with the transmitting antenna mounted to the flag pole. Snow-filled black garbage bags were used to add visibility for recovery of the site.

Positions for deployed ice-stations were reported every three hours by the ETS-1500 beacons over an Iridium network. These positions were delivered by email as binary-encoded files to personnel onboard the *Louis* and *Oden*, and then converted to ASCII-encoded geographic coordinates using in-house software (Iridium Decoder v1.1, Peter Pledge, 2016). The output files contained a true GPS position for the first hour, and derived positions for the second and third reported hours.

Upon recovery of the instruments, backups were made of all Taurus seismometer data files stored on compact flash memory cards. The memory cards themselves were collected for storage in the GSCA physical archives at the Bedford Institute of Oceanography. Positional information for each seismometer station is available in the state-of-health file that is created by each Taurus instrument. These positions were updated every time the Taurus updated its clock using Global Positioning Satellite information, roughly every 30 to 60 minutes during the deployment. These positions can be interpolated to calculate receiver coordinates at the firing time of every seismic shot.

1.4 Navigational systems

Navigational information was available from three different Global Positioning System (GPS) receiver systems. The primary source of information was an Applanix POS-MV, which is high-precision inertial navigation unit that is an integral component of the multibeam echosounding equipment onboard the *Louis*. Under ideal conditions, the POS-MV is capable of generating cm-scale positional accuracy and can resolve angular information such as heading, pitch, heave, and roll to within 0.002° (Applanix, 2015). A secondary source of navigational information was provided by a Marine Star system that is used by the bridge crew for ship operations and which can generally attain metre-scale positional accuracy. These two GPS receiver systems provide a high degree of reliability and back-up capacity. However, experience from previous Arctic Ocean surveys, has demonstrated that it is also advisable to have a receiver system dedicated solely to seismic operations. Therefore a Trimble BX982 was also installed and operated as an auxilliary GPS receiver system for the duration of the cruise.

Serial communication strings from each of GPS receiver systems were broadcasted at an update rate of 1 Hz to the GSCA NavNet server and logged in ASCII-encoded text files. Each receiver reported positional information for different reference locations on the ship. Those for the primary system were professionally surveyed to a precision of 0.005 m during installation of the multibeam echosounding equipment (Cunningham, 2014), but they were not tied to the reference locations of the secondary and auxiliary navigational systems. Offsets between each of the reference locations had to be determined from scaled engineering drawings of the ship and verified using simple tape measurements, so the values shown on Figure 1-7 are known only to a precision about 0.15 m.

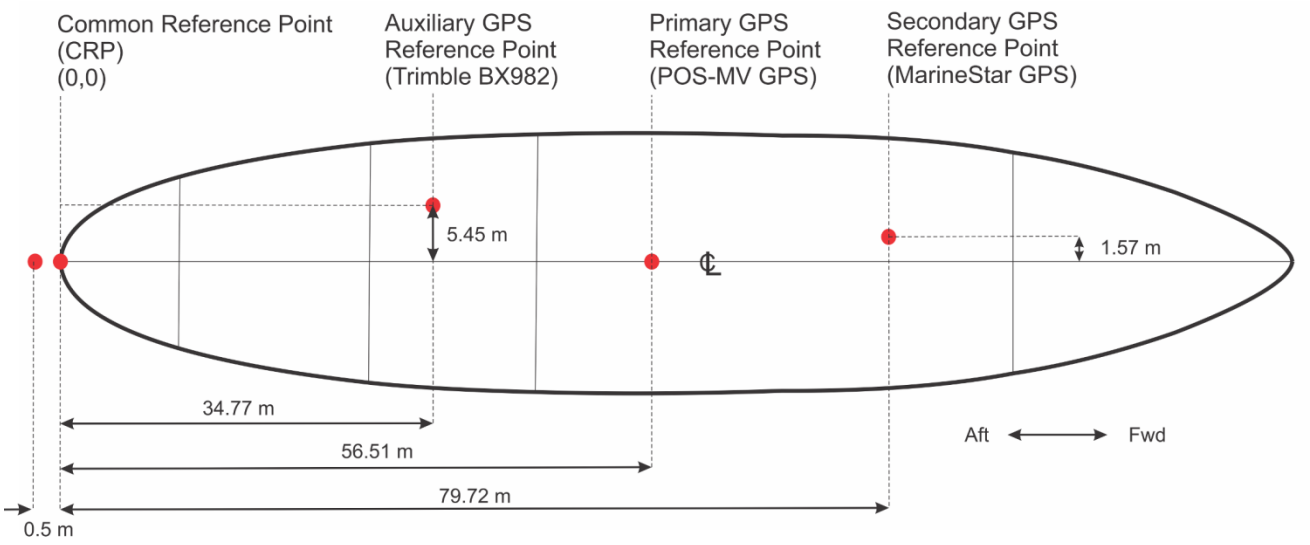

Figure 1-7: Global positioning system reference locations on the Louis. The centre of the seismic source was located at an estimated distance of 0.5 m from the aft face of the stern roller sheave, which serves as the common reference point.

1.5 Field results

The seismic program commenced with a calibrated hydrophone recording and test of the towing arrangement for the 2000 in^3 source. This work was conducted between Thursday August 11th and Friday August 12th, as the *Louis* moved to join the *Oden* at the edge of the icepack over the western slope of the Yermak Plateau. The 2000 in^3 source was fired at 30 s intervals and wide-angle reflections and refractions were recorded onboard the Oden using a sonobuoy deployed from that ship. The calibrated recording and towing test helped to establish that the 2000 in^3 source is sufficiently durable to be operated in the ice, and that it provides almost exactly double the seismic amplitude as the 1150 in^3 source.

Principal seismic operations onboard the *Louis* commenced on Wednesday August 17th, and continued until Sunday September 11th. Production during the 25.3 day period was continuous, with the exceptions listed below in Table 1-3.

Table 1-3: Time intervals during which seismic production was stopped.

Downtime interval	Hours	Comments
eol-02 to sol-03	47.4	Ceremonial visit to North Pole and transit.
eol-03 to sol-04	21.5	Transit.
eol-04 to sol-05	33.1	Dredging operations at eol-04 and transit.
eol-05 to sol-06	123.7	Transit to Nautilus Spur, detailed multibeam echosounding, and rafting of the *Oden* and *Louis* for farewell ceremonies with staff from both icebreakers.
eol-07 to sol-08	23.3	Transit and sonobuoy deployments.
eol-08 to sol-09	16.8	Transit.
eol-11 to sol-12	3.5	Transit to avoid difficult ice conditions.

Note: eol and sol are abbreviations for end-of-line and start-of-line. Thus eol-01 refers to the geographic location of the end of line LSL1601.

The *Oden* and *Louis* were operated jointly between August 17th and September 2nd to collect seismic data along lines LSL1601 through LSL1605. Afterwards, the *Oden* headed northward to conduct multibeam echosounding, dredging, and other scientific activities over the Makarov Basin, Marvin Spur, and Lomonosov Ridge, and also to collect seismic data in the Amundsen Basin along lines OD1601 through OD1604. Seismic operations with the *Louis* after September 2nd had to be conducted in essentially open water because there was no way to protect the improvised streamer from possible ice damage. After gaining confidence and experience with the improvised streamer system, it was occasionally operated under very light ice conditions with small isolated floes in concentrations of less than about 3/10.

The geographic distribution and types of seismic records acquired during the operations is illustrated on Figure 1-8, and data acquisition statistics are summarized in Table 1-4. This work produced 66,654 16-channel shot records along 12 line segments totaling 2183.9 km in length with an average density of 34.0 m per shotpoint. There are also 62 sonobuoy and 5 seismometer records of wide-angle reflections and that were collected at irregular intervals of 15 to 80 km along each of the line segments. Two additional seismometers were installed on the ice, but not successfully recovered. Positions for these drifting instruments were still being broadcast by satellite beacons at the end of the program, so there is some—albeit small—possibility that the instruments could still be recovered.

Data integrity and quality were monitored continuously throughout the program by reading the shot records, generating brute stack plots, inspecting the amplitude and frequency characteristics of signal and noise on the records, and troubleshooting the cause of any irregularities. The following sections provide more detail about the data sets and results that have been produced.

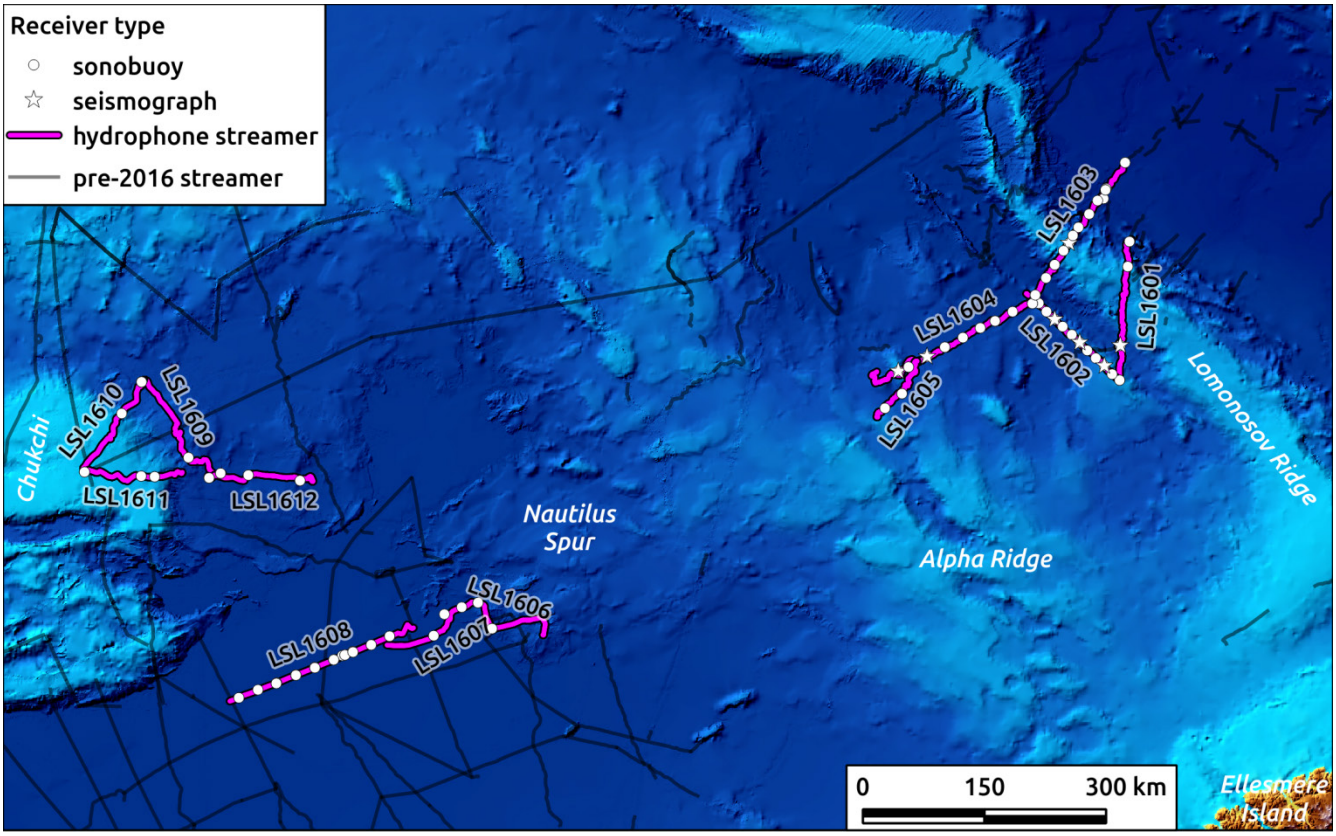

Figure 1-8:Geographic distribution and types of seismic records collected onboard the Louis.

Table 1-4: Seismic data acquisition managed onboard the Louis.

	LSL1601	LSL1602	LSL1603	LSL1604	LSL1605	LSL1606	LSL1607	LSL1608	LSL1609	LSL1610	LSL1611	LSL1612
Start date (UTC)	JD230 11:42	JD232 07:23	JD235 08:51	JD237 11:11	JD240 17:26	JD246 19:01	JD247 14:55	JD249 10:43	JD251 16:51	JD252 22:09	JD253 20:37	JD254 20:33
End date (UTC)	JD231 19:26	JD233 09:30	JD236 13:40	JD239 08:20	JD241 15:17	JD247 14:52	JD248 11:24	JD251 00:01	JD252 22:06	JD253 20:35	JD254 19:59	JD255 19:33
Start lat/lon	89.33 -65.71	87.79 -84.89	89.69 +51.04	88.88 -121.96	87.12 -137.15	81.98 -141.43	81.60 -146.46	78.71 -149.52	79.68 -161.92	79.10 -168.55	78.22 -164.34	79.52 -162.06
End lat/lon	87.88 -86.21	88.49 -126.61	88.79 -123.42	86.70 -140.95	86.37 -134.70	81.60 -146.45	80.52 -147.41	80.89 -147.45	79.10 -168.55	78.22 -164.35	79.26 -162.74	80.57 -159.63
Bathymetric range (m)	1113 4069	1015 3490	1059 4492	1516 3993	1580 3496	2556 3733	3314 3999	3515 3982	1470 3596	396 3109	342 2712	3078 3996
Seismic source (in^3)	1150	1150 & 1000	2000	1150	1150	1150	1150	1150	1150	1150	1150	1150
Average field time break[A] (ms)	60.5	60.0	59.9	56.0	56.2	56.3	56.3	56.1	56.2	56.2	56.3	55.9
First shot[B]	5	11060	17594	21331	30860	35350	39097	42812	49527	54792	58834	62513
Last shot	8851	17592	21323[C]	30855	35249	39096	42870	49526	54791	58833	62511	66654
# shots	8847	6533	3730	9525	4390	3747	3684	6715	5265	4038	3678	4142
Line-km	205.4	195.3	192.8	325.1	113.8	129.8	134.6	257.7	191.0	151.0	136.6	150.8
Shotpoint density (m/shot)	23.2	29.9	51.9	34.1	25.9	34.6	36.5	38.4	36.3	37.4	37.2	36.4
# sonobuoys	2	8	12	7	2	1	4	16	2	2	3	3
# seismometers	1	3	1	2	0	0	0	0	0	0	0	0

NOTES:

A Field time breaks could not be digitized by the recording system so, instead, they were monitored and recorded manually by the seismic watchkeepers. The values reported here include an additional 10 ms delay because the airguns were fired on the down-going pulse of the trigger signal. This delay was confirmed in the field using oscilloscope measurements.

B Shot numbers generated by the gun controller are not logged by the data recording system and are not automatically written into shot records. Therefore, the field file identification (FFID) numbers are considered to be the same as the shot number.

C The streamer system failed after shot number 21323, but transit along the line and firing of the source was continued because wide-angle sonobuoy and seismometer records were still being collected. Shots fired after failure of the streamer are numbered in the navigation log as 21323.001, 21323.002, 21323.003, *etc.*

1.5.1 Seismic navigation

Positional information was carefully monitored during the seismic operations and verified through comparisons between the primary, secondary, and auxiliary systems. Apart from some notable exceptions, described in the following sections, the positional information is generally accurate to within about a metre.

1.5.2 Verification of positional information and GPS reference points

GPS data logged while the *Louis* was tied to the wharf in Tromsø provided an opportunity to examine the reference points for each GPS receiver system. The centre-line of the ship was determined using time-averaged positions and headings from the primary navigation system since, although tied to the wharf, the ship was never perfectly at rest. Relative GPS reference points for the three systems could then be calculated and are plotted onFigure 1-9. As expected, the primary and secondary systems yielded metre-scale precision. The auxiliary system exhibited poorer measurement precision, but still better than about 5 m.

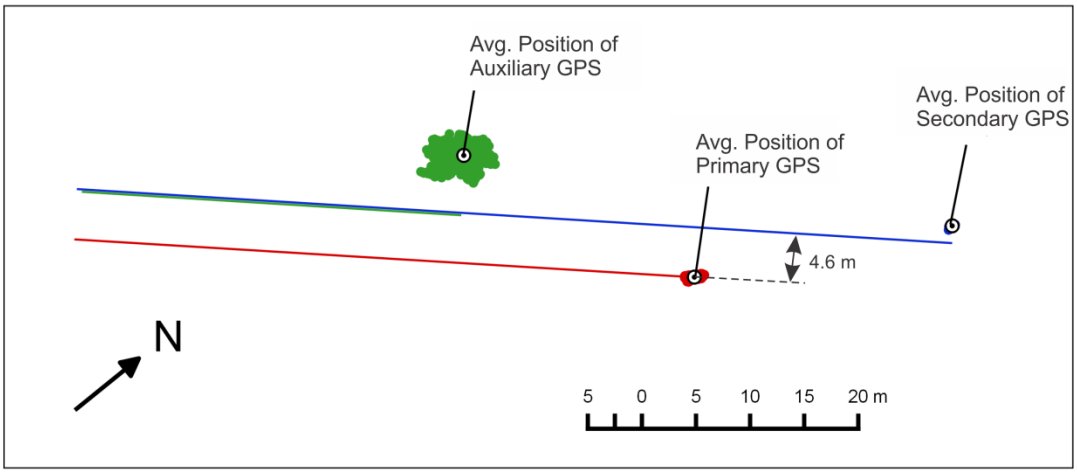

Figure 1-9: Time-averaged positions logged between 09:00 and 10:00 UTC on August 8th by the primary, secondary, and auxiliary navigational systems while the Louis was tied to the wharf in Tromsø. The blue and green lines are the centre-line of the ship calculated using reference points and offsets for the secondary and auxiliary systems. These are assumed to be correct because they overlap and because of other verifications done in the field. The red line, calculated for the primary system, reveals an unexpected discrepancy of 4.6 m to the starboard of the assumed centre-line.

The test conducted in Tromsø indicates that the primary reference location is offset laterally to the starboard from the centre-line of the ship by an average distance of 4.6 m when compared to the secondary and auxiliary reference locations. Further evidence of this discrepancy is obtained from inspection of the shotpoint navigation for each seismic line, as shown in the example on Figure 1-10.

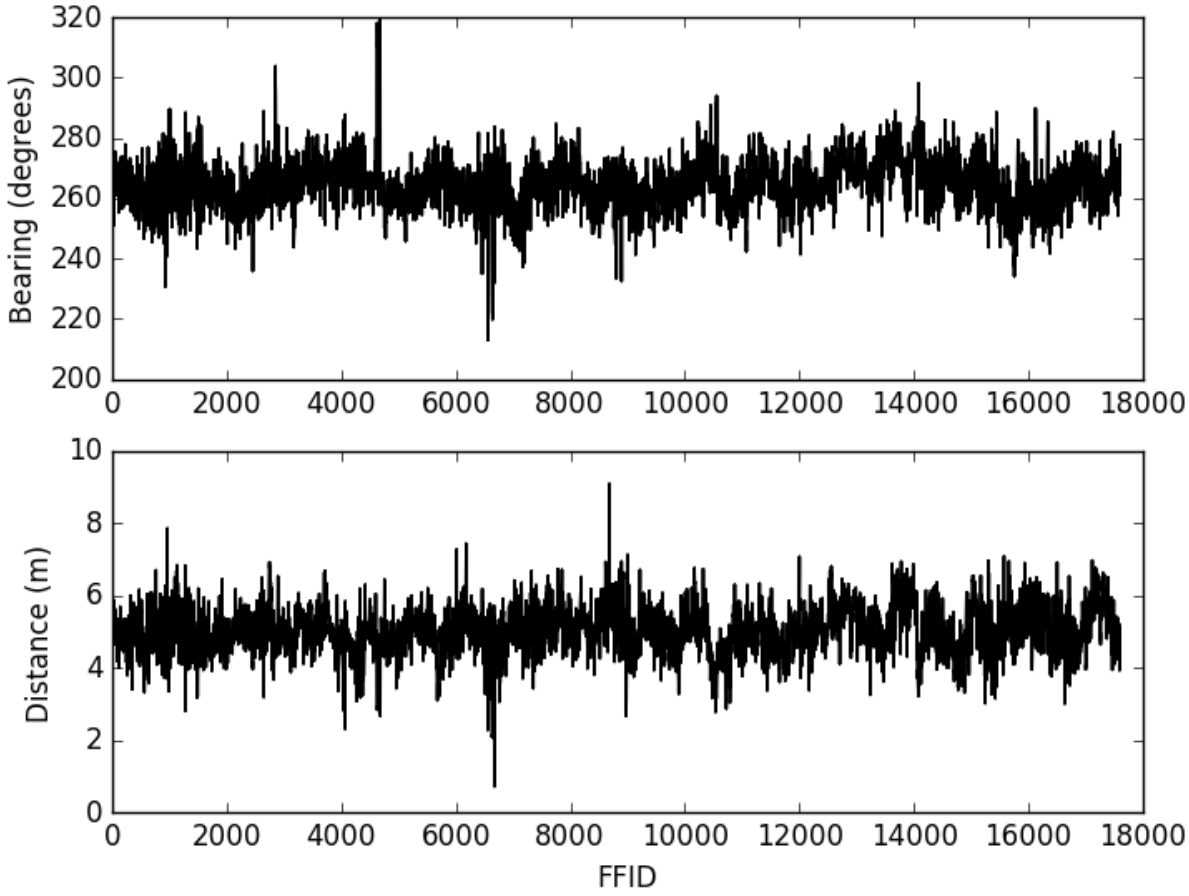

Figure 1-10: Bearing (top panel) and distance (bottom panel) between common reference points calculated from the primary and auxiliary navigation systems for lines LSL1601 and LSL1602.

Repeated efforts were made during the cruise to investigate the cause of the apparent offset, but no satisfactory explanation was determined. A line-by-line summary of the average offset and bearing discrepancies between the positions from the primary navigation system and the other two systems is given in Table 1-5. The magnitude of the apparent offset is not considered significant for processing or interpretation of the seismic data so, for seismic navigation, the primary reference point is assumed to lie on the centre-line of the ship. However, it is possible that the 4.6 m offset—if real—could affect multibeam echosounding operations. It would be best if reference points for all GPS receiver systems are tied by precise survey methods, or are at least established relative to known points that can be measured on scaled engineering drawings.

Table 1-5: Average discrepancies observed between positions from the primary navigation system and those from the other two navigation systems.

Line	Average offset (m) from secondary	StDev	Average bearing (°) from secondary	StDev	Average offset (m) from auxiliary	StDev	Average bearing (°) from auxiliary	StDev
LSL1601	4.859	0.748	272.692	10.35	4.950	0.548	263.002	7.016
LSL1602	5.181	0.539	274.956	6.623	5.139	0.618	265.793	7.478
LSL1603	5.034	0.526	272.127	5.770	5.013	0.554	262.667	6.411
LSL1604	4.964	0.531	271.69	7.086	5.016	0.578	262.562	6.954
LSL1605	5.090	0.672	272.466	6.210	5.045	0.597	262.723	6.438
LSL1606	4.944	0.666	273.019	8.533	4.904	0.652	263.671	7.515
LSL1607	5.430	0.728	273.017	6.246	5.345	0.670	264.703	6.128
LSL1608	5.013	0.693	270.271	8.264	4.825	0.670	261.958	8.475
LSL1609	5.277	0.757	272.857	8.357	5.060	0.667	263.931	8.065
LSL1610	5.199	0.832	275.918	8.635	5.056	0.739	267.342	8.092
LSL1611	4.941	0.753	272.898	7.809	4.890	0.724	263.503	7.670
LSL1612	5.048	0.626	272.547	8.272	4.969	0.578	263.640	7.820

1.5.3 Navigational errors and data gaps

Accurate data from the primary navigational system are available for the entire period of seismic operations, except for the beginning of line LSL1603. Between shotpoints 17594 and 19647, positions from the primary navigation system are offset by up to 75 m from those provided by the secondary and auxiliary systems. Attitudinal information from the primary system, such as heading, does not appear to have been affected.

Although this single failure of the primary navigation system requires further investigation, it is thought that heavy use of Iridium satellite communication systems in the vicinity of the North Pole caused blanking of GPS radio reception by the POS-MV antennae and therefore caused a loss of satellite connectivity. Under such circumstances, the POS-MV system operates in a dead-reckoning mode that relies on inertial data to derive positions. Errors in the positions were likely accumulated while the system remained in this mode along the beginning of line LSL1603. Once satellite connectivity was re-established, at shotpoint 19648, the primary navigation system generated accurate positions that have been verified through comparison with the secondary and auxiliary systems.

Data from the auxiliary navigation system were not recorded for the period between 19:52:52 and 21:58:25 UTC during September 6th, coinciding with shotpoints 48782 through 49157 on line LSL1608, as a result of a network cable becoming disconnected.

1.5.4 Post-processing of shotpoint positions

Shotpoint positions were post-processed using a Python script called *shotlog_create.py*, which is listed in Appendix A. This script is used to scan the seismic log files recorded by the GeoEel controller software and then index each shot number with an independent log of the Zyfer trigger times using the start time of the field record. Once indexed, each trigger time is used in a binary search for the nearest logged strings, heading, vessel speed and water depth before exporting these data to a comma-delimited shotlog, stored as one ASCII-encoded file for each seismic line. The nearest positional information for each index entry is then linearly interpolated to the exact trigger time using a Python script called *shotlog_interpolate.py*, which is listed in Appendix B.

The interpolated positions provide an increase in positional accuracy and resolve small apparent navigational errors associated with assigning GPS locations sampled at 1 Hz to shotpoints at arbitrary trigger times (Figure 1-11). Finalized shotlogs for each seismic line were produced using a third Python script called *shotlog_finalize.py*, listed in Appendix C, which applies the offset from the navigational reference point to the centre of the seismic source as shown on figures 1-4 and 1-7.

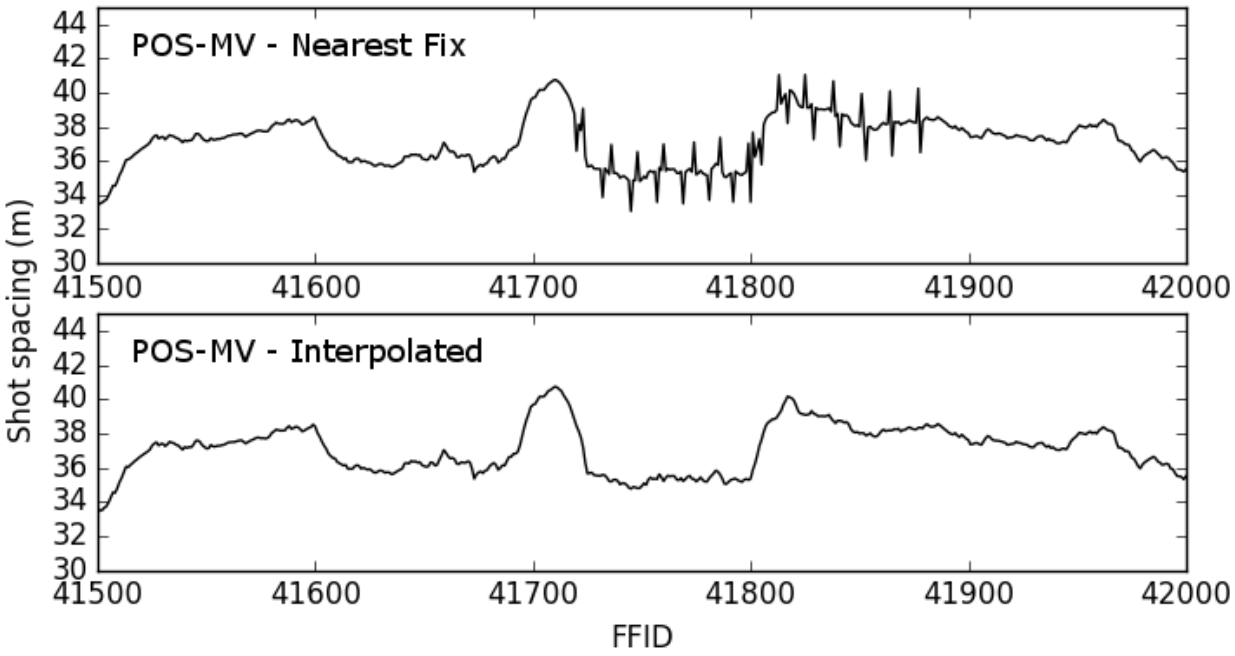

Figure 1-11: Example of small apparent navigational errors caused by assignment of the nearest GPS location to an arbitrary shot time (top panel), which were then corrected by linear interpolation of the navigational information (bottom panel).

Several erroneous duplicate entries in the finalized shotlogs were identified and removed. These entries, listed in Appendix D, were the result of extraneous data in the Zyfer trigger log, errors in the GeoEel controller logs, or shots that were triggered before the full record length of the previous shot had elapsed (*e.g.* during a change in fire interval). Partial file errors were encountered during LSL1602 and LSL1610. The resultant partial files and their contents are summarized in Appendix E. In these cases, only the initial shot number is listed in the finalized shot log.

1.5.5 Calibrated recording of the 2000 in^3 source

Date: August 11, 2016
Water depth: 1240 m
Nominal tow depth: 11.2 m
Timing system: Zyfer atomic clock
Nominal field time break: 49.8 ms
Location: western Yermak Plateau (80.25°N, 8.00°E)
Seismic source: 4x500 in^3 G-gun cluster
Firing pressure: 2000 psi
Gun controller: Realtime Systems LongShot

Receiver:
- calibrated hydrophone (Serial no. NRCan H022)
- Sensitivity: -200.3 dB//1V/uPa (Measured by Peter Simpkin, June 11, 2010 using SCU-6 w/gain=1.0)
- suspended from stern rail at a depth of 400 ft (121.92 m)

Receiver Depths:
- SeaStar mini-CTD (serial no. S8028), attached to cable 9.86 m above the hydrophone
- sampling interval: 20 s
- mean receiver depth during calibrated recording: 117.33 m (stdDev 0.92 m)
- mean water temperature: 3.73 °C (stdDev 0.04 °C)

Signal conditioning unit:
- SCU-6 (serial no.: 025); input: Seistec J1; output: input A; DC power
- no gain (low) switch setting

GSC portable digitizer 4:
- channel 1: nil
- channel 2: calibrated hydrophone (gain = 1.0)
- channel 3: clock time break (gain = 1.0)
- channel 4: nil
- sampling frequency: 25.6 kHz (interval = 0.0390625 ms)
- samples/trace: 30720
- record length: 1199.9609375 ms
- calibration factor: unknown
- data files:
    CalPhone_2016_224_09_08_07.sgy (36 shot records)
    CTB_2016_224_09_08_07.sgy (digitized clock time break)

<u>*Preliminary analysis*</u>

The 36 unfiltered shot records were aligned, debiased, and stacked. The first arrival of seismic energy on the resulting trace occurs at a time of 80.8 ms. The average sound speed in the uppermost 117.3 m of the water column is 1471.47 m/s (CTD measurement d2016-15_0001, *pers. comm.* Jane Eert), so the calculated source-to-receiver offset is 118.9 m.

Trace amplitudes of the shot records are in raw counts, measured in 24-bit samples over a range of +/- 10 V. Therefore each count is equivalent to 5.9605E-07 V. The maximum trace amplitude is 0.7571 V, which corresponds to a maximum pressure at the hydrophone of -2.417 dB//1V, or 197.9 dB//1µPa. Please note that these are preliminary results only, and that it may be necessary to measure and apply a correction factor for the digitizing unit. Assuming that the dissipation of seismic energy in the water column can be accurately described using a spherical spreading model of 20·*log*(radius of travel), the estimated maximum pressure is 239.7 dB//1µPa·m. The maximum peak-to-peak amplitude is 17.6 bar·m, and the maximum zero-to-peak amplitude is 9.71 bar·m.

The amplitude and frequency characteristics of the stacked source signature trace are plotted on Figure 1-12. For comparison, the preliminary maximum peak-to-peak amplitude reported above is just over twice the value of 8.5 bar·m that was measured in 2010 for the 1150 in^3 source (Mosher *et al.,* 2010).

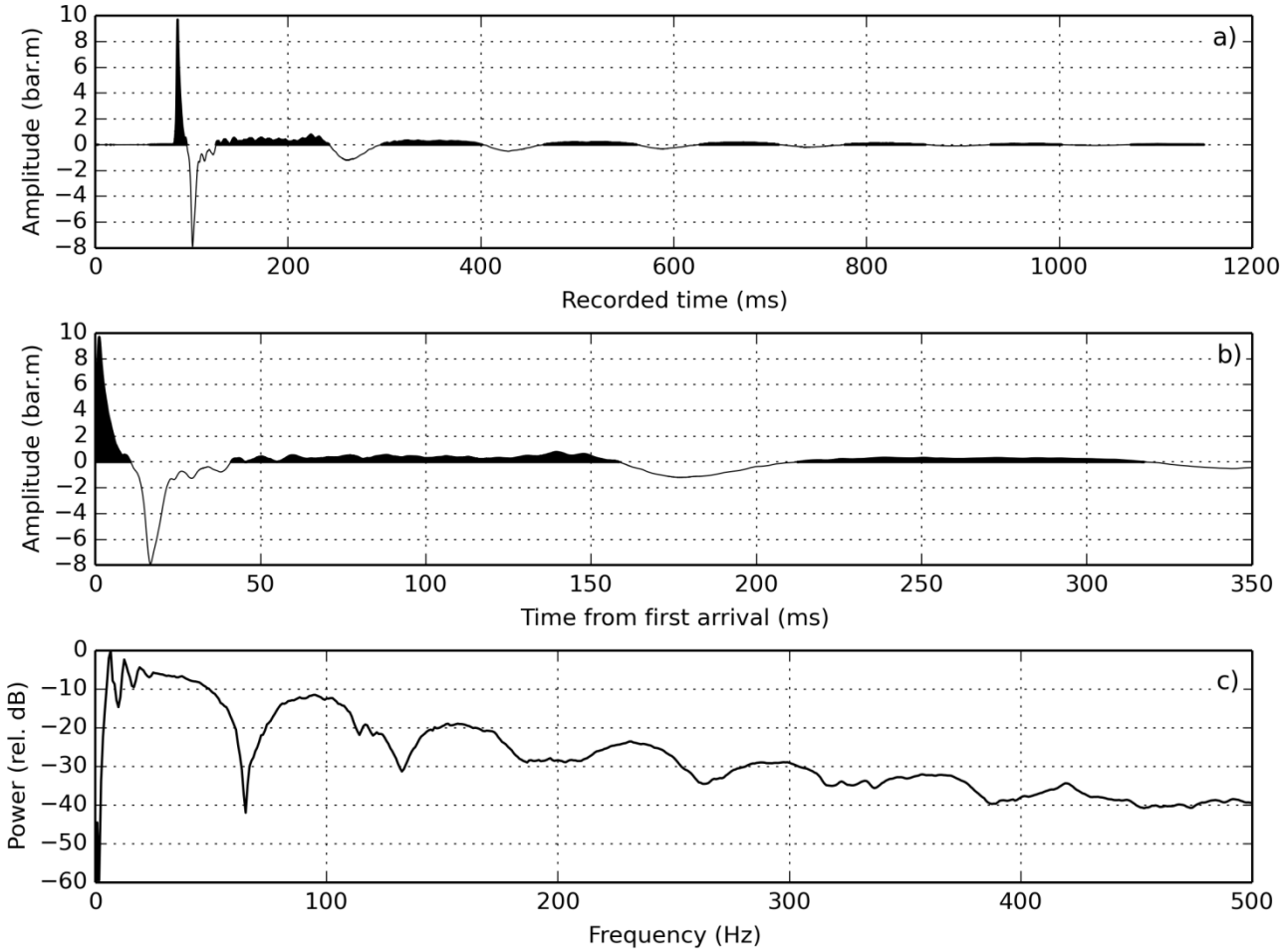

Figure 1-12: Amplitude and frequency characteristics of 2000 in^3 source. a) Amplitude time series for the full recorded interval. b) Amplitudes starting at the first arrival. c) Relative power spectrum.

1.5.6 Hydrophone streamer depths

Icebreaking operations require frequent course deviations, changes in speed, and even complete stops, and there can be significant changes in water temperature and salinity around the icepack. As a result, correct balancing of the streamer is not possible over the duration of the survey. Neither is active streamer control since the associated hardware would be at risk of getting caught in the ice. As a result, receiver depths can vary significantly along the length of the streamer and also from one shot to the next. Differences of several metres between the inboard and outboard receiver groups are common, and the average depth along the streamer can change by 20 m in the space of 10 minutes when the ship encounters difficult patches of ice.

Receiver depths were measured in two ways: 1) using Star ODDI mini-CTD sensors housed in plastic casings attached to the outside of the streamer with waterproof tape; and 2) using pressure transducers that are built into the GeoEel streamer at receiver groups 1 and 16.

Attempts to calibrate depth measurements from the Star ODDI mini-CTD sensors failed because the instruments were being operated outside their designed depth and temperature ranges, so inaccuracies are expected in the measurements. Unfortunately the GeoEel streamer sensors also exhibited unreliable behaviour, so all the streamer depth information must be used with caution and, if possible, verified using independent measures. A summary of streamer depth data is listed in Table 1-6. Negative depth values on the inboard sensor are instances in which the sensor was not working properly until reconfiguration of the streamer after LSL1605.

Table 1-6: Average streamer depths from built-in GeoEel transducers (inboard and outboard) and Star ODDI mini-CTD sensor S8026 (where available), with the static depth correction values applied to the ODDI mini-CTD data during reconversion.

Line #	Avg. Inboard Depth (m)	Avg. Outboard Depth (m)	Avg. ODDI Depth (m)	ODDI position	ODDI depth correction applied (m)
LSL1601	-0.84	11.01	17.84	Ch. 09	2.57 m
LSL1602	-0.83	12.30	13.33	Ch. 09	2.57 m
LSL1603	-0.81	10.82	13.79	Ch. 16	2.57 m
LSL1604	-0.81	10.40	11.98	Ch. 09	2.97 m
LSL1605	-1.70	7.93	-	N/A	N/A
LSL1606	8.78	8.18	-	N/A	N/A
LSL1607	5.89	6.23	-	N/A	N/A
LSL1608	6.99	7.13	-	N/A	N/A
LSL1609	8.43	7.84	-	N/A	N/A
LSL1610	7.37	6.87	-	N/A	N/A
LSL1611	7.86	7.54	-	N/A	N/A
LSL1612	8.12	7.62	-	N/A	N/A

Star ODDI mini-CTD sensor data

Star ODDI mini-CTDs are small sensors that collect depth, temperature and salinity data. All the sensors used during the 2016 survey were manufactured to be calibrated for use between depths of 4.5 to 1230 m and temperatures of -1 °C to 40 °C. Prior to deployment of seismic gear, the mini-CTD sensors were activated to collect measurements at 30 second intervals before being attached to the streamer. Sensors were attached inside a protective plastic housing and taped to the outside of the streamer using heavy-duty waterproof tape. After gear was recovered, the sensors were removed to download the data in SeaStar software via USB/serial port connection.

Loss of the streamer during the first deployment prior to the start of LSL1601 resulted in the loss of three mini-CTD sensors (serial numbers S8025, S8029, S8027). A fourth mini-CTD was irreparably damaged while attached to the source calibration hydrophone during this deployment (serial number S8028). The remaining mini-CTD (serial number S8026) was used to collect streamer depth measurements along LSL1601 through LSL1604, and was lost along with the streamer at the end of LSL1605.

A series of calibrations were attempted using the mini-CTD sensors prior to seismic operations by lowering the sensors to a known depth and calculating the offset from measured values. For sensor S8026, static depth corrections obtained from these calibrations were between 4.41 and 5.57 m offset (Table 1-7).

Table 1-7: Correction offsets for S8026 determined from calibration tests performed under different temperature conditions.

Date	Calibration Depth (m)	Average Temperature (°C)	Offset (m)	Offset (mbar)
2016-07-21	10	10.32	4.41	493.54
2016-08-08	9	9.28	4.84	450.18
2016-08-11	8	5.81	5.58	568.28
2016-08-20	8	-1.54	5.31	541.39

Application of the above calibrations to the mini-CTD data, however, results in streamer depth values that are unrealistically low for the towing configuration, or even negative. This is likely due to the fact that seawater temperatures were regularly below the lower bound of the calibrated temperature range (-1 °C). For this reason data were instead corrected using static offsets obtained from durations during which the mini-CTD sensors were sitting on deck after gear recovery (assuming atmospheric pressure, 0 m depth). This correction resulted in more reasonable results, despite the fact that the depth measurements made while on deck were collected under atmospheric pressure, and thus outside of the calibrated depth range of the sensor. After this correction, streamer depths were linearly interpolated between samples to the nearest second of the trigger time.

Comparison between the streamer depth sensor systems

During acquisition of line LSL1603, mini-CTD S8026 was placed adjacent to the aft streamer depth sensor for direct depth comparison of results. However, both of the streamer depth sensors malfunctioned along this line. The inboard sensor (Ch. 01) measured negative depths for the entirety of the line, whereas measurements from the outboard depth sensor (Ch. 16) gradually became more reasonable several hours into acquisition (Figure 1-13). Comparison of depth values between FFIDs 19500 and 21323 produce a weak positive correlation (Figure 1-14).

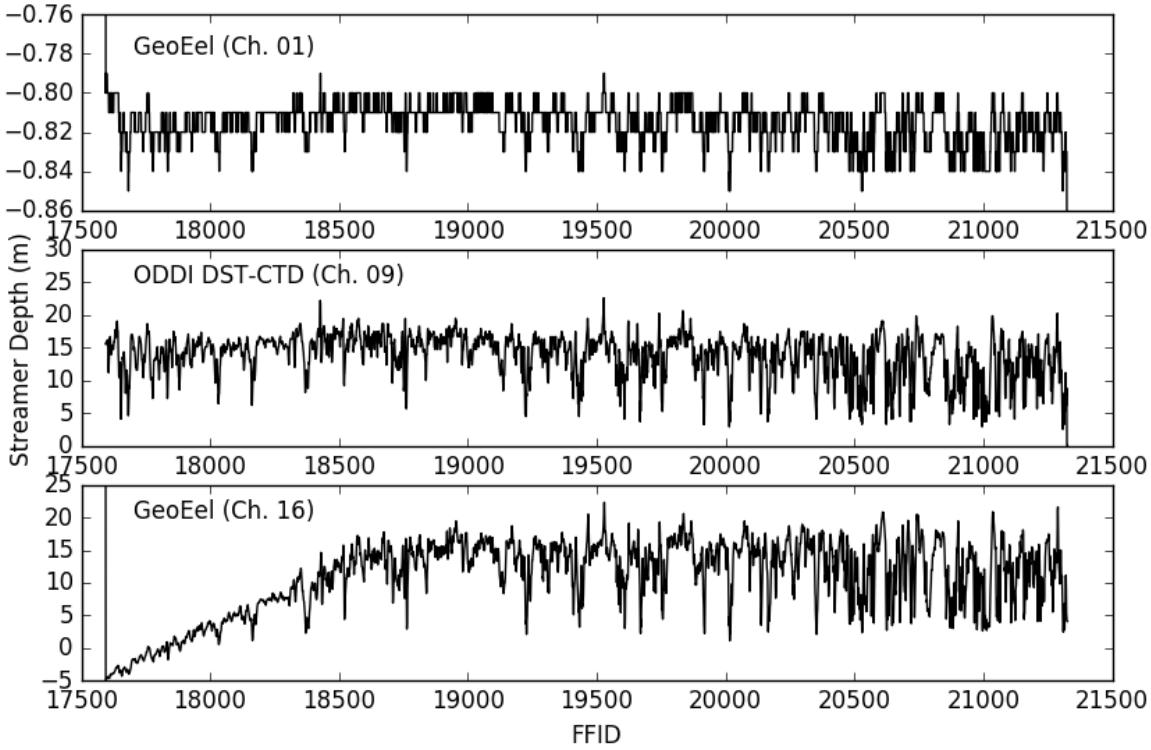

Figure 1-13: Streamer depths measured along line LSL1603 using the built-in sensor near receiver group 01 (top panel), a Star ODDI mini-CTD sensor (#S8026; middle panel), and the built-in sensor near group 16.

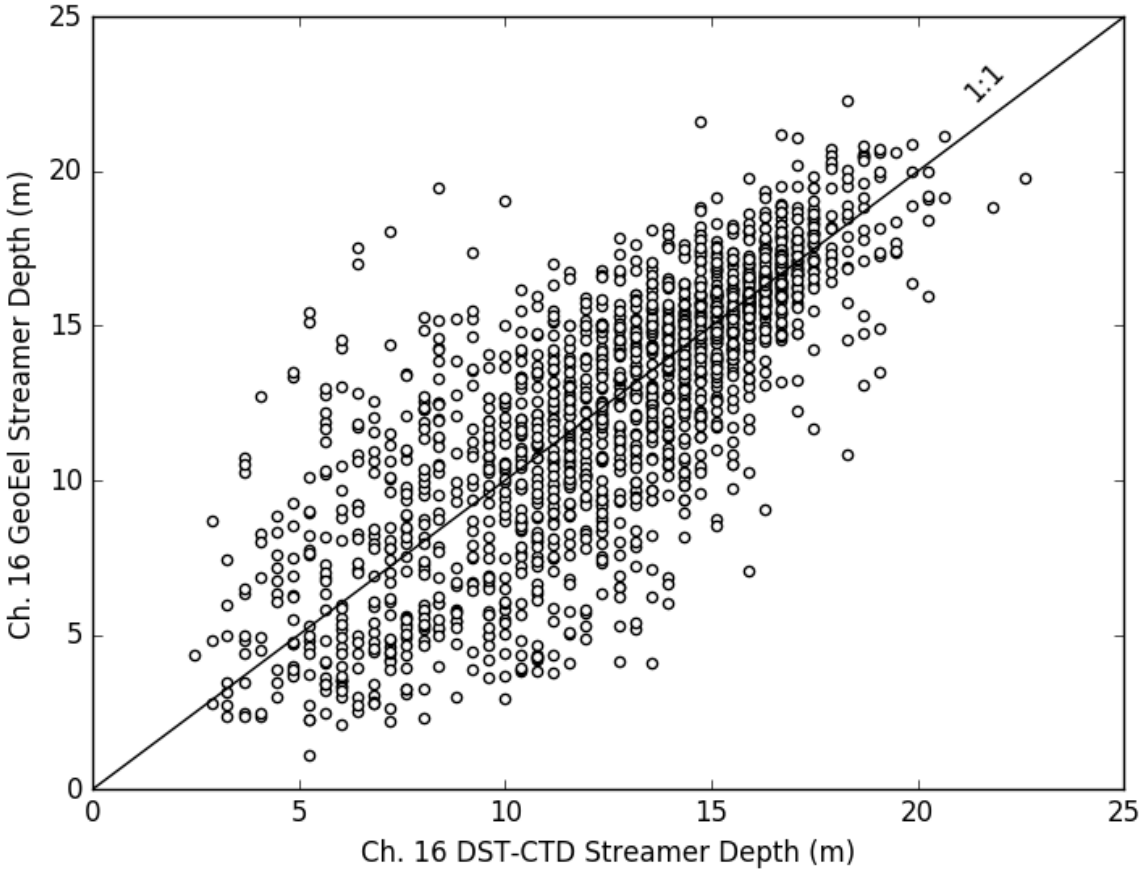

Figure 1-14:Example scatter plot of streamer depth measurements from the built-in and mini-CTD sensors between shotpoints 19500 and 21323.

1.5.7 Seismic reflection records

Digital shot records were stored on a solid-state disk drive, one file per shot record, in the Society of Exploration Geophysicists SEG-D 8058 Revision 1 format. The records were automatically copied every 15 minutes over the internal network onto a separate magnetic disk drive installed on the seismic processing computer. Upon completion of each line, all associated shot records and log files were copied onto two additional hard drives.

Watchkeepers kept a half-hourly log of the following system parameters: calendar day, UTC time, latitude, longitude, line segment, water depth, course over ground, heading, speed over ground, speed through water, streamer system (port/starboard), streamer leakage, streamer current, streamer voltage, streamer depth information, shot number, total source volume, field time break, firing interval, recording delay, record length, field file identification number, NMEA string verification, and comments.

Shot records contain 16 channels, one from each of the streamer hydrophone groups. Included in each SEG-D file is a variable-sized external header containing the following NMEA strings from the auxiliary GPS navigation system: GGA (offset corrected to the common reference point), DBT, VTG, and HDT. These strings document at each shotpoint useful GPS information such as UTC time, geographic position, water depth, heading, and course over ground. In addition, serial port information from the two streamer depth sensors is also appended to the external SEG-D header for each shot record.

During acquisition of seismic reflection shot records, the GeoEel Controller user interface was used to automatically plot shot gathers, the amplitude spectra of each trace, a log of diagnostic messages, and a simple brute-stack record section. An example monitor display is shown on Figure 1-15. This provided immediate, shot-by-shot feedback on the GeoEel system performance and confirmation that the data were of acceptable quality.

Shot numbers generated by the gun controller are not logged by the data recording system and are not written to the trace headers of the shot records. Therefore, for the purposes of data processing and interpretation, the reflection field file identification (FFID) numbers are considered to be the same as the shot number. An exception occurs for line LSL1603 because the GeoEel streamer system failed at JD236 13:40 UTC after recording FFID 21323. Transit along the line and firing of the source was continued, even though no seismic reflection shot records were acquired, because the sonobuoys that were deployed were still operational and because there was a seismometer recording the seismic signals from a drifting ice floe. Shots fired after failure of the streamer are numbered in the navigation log using a decimal system such that the first post-failure shot is 21323.001, the second is 21323.002, the third is 21323.003, *etc*.

Note that the Controller option to reset the file timestamp to GPS time (Table 1-1) should be enabled, as is recommended in the Geometrics software manual. This was not done during the seismic operations in 2015, which caused significant drift of up to 3 s in the file timestamps. When the Controller software was initialized for the 2016 operations, the reset timestamp option was mistakenly left disabled which, as in 2015, caused significant drift in the file timestamps. The problem was discovered and corrected during transit between eol-05 and sol-06.

An additional factor that may have contributed to the drift is that, in 2015, the time window for capturing NMEA strings from serial input to the Controller software was set to ±5.0 s, which is unrealistically long considering that the record length is 11.5 s. There may have been a misunderstanding in 2015 that the time window parameter specifies only +5 s from the beginning of the recording window. Again, for the 2016 operations this parameter was initially left at the 2015 setting, and was then changed to ±2.5 s before sol-06.

A problem with the primary navigational system occurred on line LSL1603 in the vicinity of the North Pole (please refer to Section 1.5.1). It was quickly confirmed that the erroneous primary navigation could be fixed using information from the alternate GPS systems. However, the NMEA GGA string was mistakenly omitted from the GPS serial input to the GeoEel controller during acquisition of line LSL1604. This situation was corrected for the remaining line segments in the program.

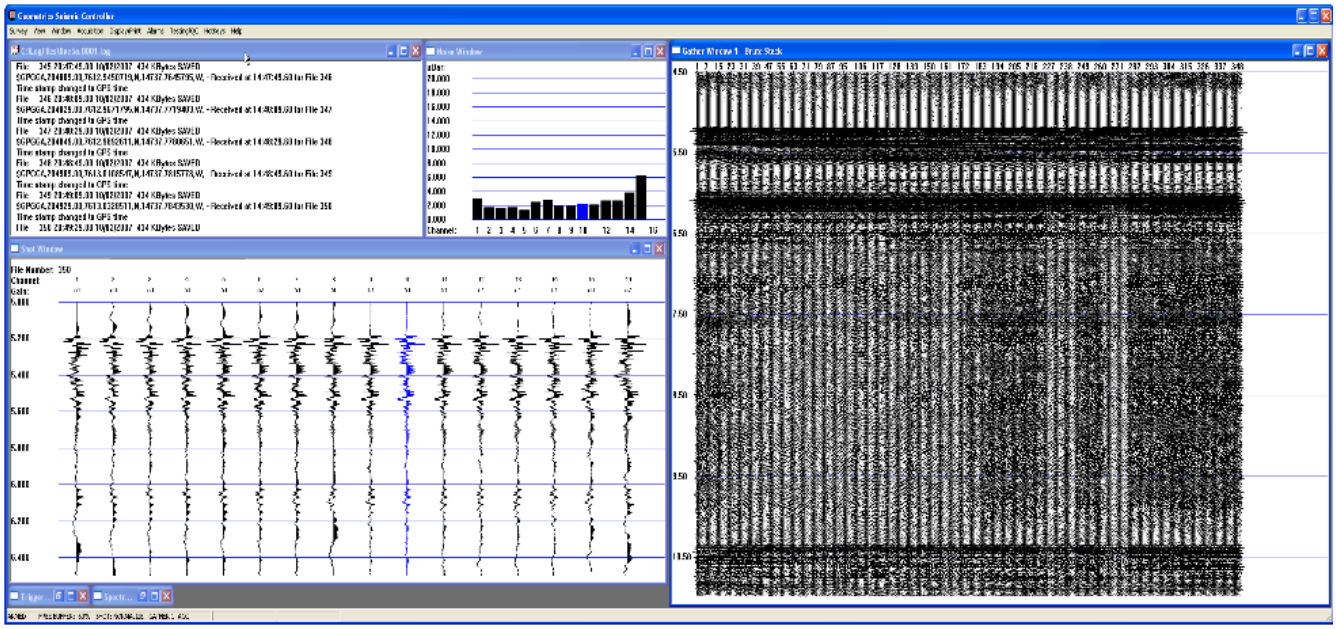

Figure 1-15: Screen capture of the GeoEel Controller software for system configuration and real-time monitoring of field records.

To further verify the integrity and quality of the seismic reflection field records, the SEG-D formatted files were regularly inspected using the Globe Claritas commercial software package (version 6.4) running on a Dell Precision M6800 laptop (Intel Core i74800MQ CPU@ 2.70 GHz x 8) running the 64-bit Ubuntu Linux operating system (version 14.04 LTS). The following workflow was used to produce a scaled raster plot of a simple brute stack for each line segment:

1. read SEG-D shot records, channels 1 to 16
2. extract navigation from SEG-D headers and inspect
3. debias traces by subtracting the mean amplitude
4. check for large values (> 1.0E+15) and NaNs
5. check amplitude range
6. apply zero-phase Butterworth low-cut filter (taper = 6/12 Hz)
7. apply bulk shift for recording delay
8. normalized trace sum, channels 1 to 16
9. automatic gain control (500 ms)
10. scaled raster plot

An example plot is shown on Figure 1-16. No further onboard processing of the seismic reflection data was attempted because the field operations and GPS navigational troubleshooting kept the staff fully occupied. Final shotlogs, keyed on times from the Zyfer atomic clock, were completed near the end of the cruise, and full signal processing, including stacking and migration, was completed within four months of the end of the cruise. The processing workflow and results are described in Chapter 2.

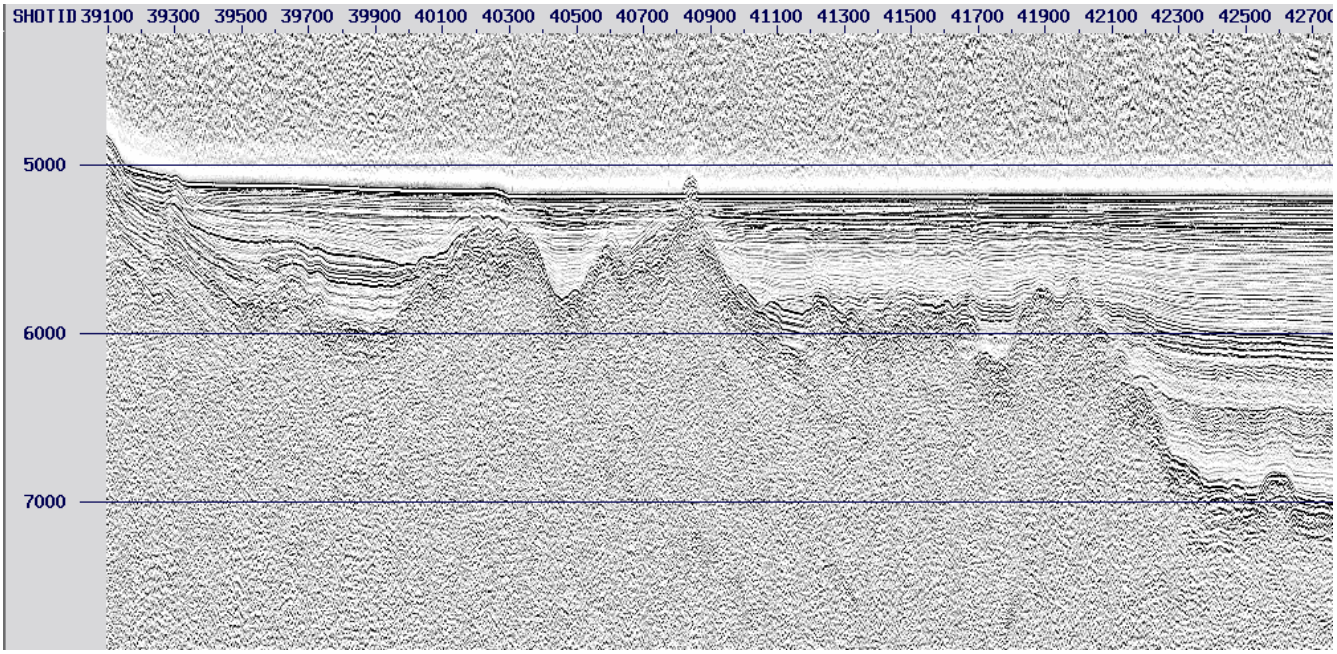

Figure 1-16: Brute stack record section for a segment of line LSL1607.

1.5.8 Seismic wide-angle reflection and refraction records

As is summarized on Table 1-8, 33 sonobuoys were deployed during the two-ship operations along lines LSL1601 through LSL1605, and a further 32 sonobuoys were deployed during single-ship operations along LSL1606 through LSL1612. Seven seismometer ice-stations were deployed during the two-ship operations, with five successful recoveries (Table 1-9).

Unfavourable weather prevented recovery of instruments TO-03-02 and TO-04-03. The satellite beacons at these drifting ice-stations continue to transmit GPS positions more than 4 weeks after they were initially deployed. As of October 4th 2016, the latest reported positions are over the Lomonosov Ridge (Figure 1-17), with each seismometer having drifted more than 360 km from its deployment position. In the hopes that the seismometers may yet be recovered, their positions will continue to be monitored and communicated to the *RV Polarstern*, which will be operating in the Amundsen Basin until early October.

Table 1-8: Sonobuoys recorded onboard the Louis during the first and second expedition phases.

Instrument Code	Deployment Time (UTC)	Deployment Latitude (°)	Deployment Longitude (°)	Channel	Deployment Type
SL-01-01	2016.08.17 12:17:55	89.322341° N	068.523385° W	81	Stern
SL-02-01	2016.08.17 17:45:16	89.062989° N	075.845033° W	85	Stern
SO-01-01	2016.08.18 03:42:46	88.20805° N	085.32371° W	90	Helicopter
SL-03-02	2016.08.19 08:33:22	87.823227° N	086.343893° W	81	Stern
SO-02-02	2016.08.19 09:41:22	87.89414° N	088.50841° W	83	Helicopter
SO-03-02	2016.08.19 10:14:39	88.06895° N	093.76432° W	90	Helicopter
SO-04-02	2016.08.19 16:06:18	88.14537° N	096.85189° W	66	Helicopter
SO-05-02	2016.08.19 16:40:13	88.28786° N	103.28775° W	58	Helicopter
SO-06-02	2016.08.19 21:59:56	88.34782° N	107.42008° W	87	Helicopter
SO-07-02	2016.08.19 22:08:59	88.43651° N	115.57632° W	28	Helicopter
SL-04-02	2016.08.20 05:30	88.479104° N	120.027379° W	81	Stern
SL-05-03	2016.08.22 08:47:04	89.681661° N	051.186643° E	81	Stern
SL-06-03	2016.08.22 11:34:44	89.842571° N	046.767988° E	85	Stern
SO-08-03	2016.08.22 11:49:00	89.95670° N	104.78776° W	58	Helicopter
SO-09-03	2016.08.22 11:58:00	89.79557° N	121.55754° W	28	Helicopter
SL-07-03	2016.08.22 15:35:42	89.941062° N	108.162224° W	77	Stern
SL-08-03	2016.08.22 21:30	89.618317° N	121.739940° W	81	Stern
SO-10-03	2016.08.22 22:16:54	89.42961° N	124.07438° W	62	Helicopter
SO-11-03	2016.08.22 22:22:52	89.32005° N	124.12395° W	83	Helicopter
SL-09-03	2016.08.23 06:52:52	89.121458° N	123.546771° W	79	Stern
SL-10-03	2016.08.23 10:43:45	88.937180° N	123.293160° W	81	Stern
SO-12-03	2016.08.23 11:56:59	88.76115° N	123.31835° W	66	Helicopter
SO-13-03	2016.08.23 12:52:57	88.53766°N	123.12826°W	87	Helicopter
SL-11-04	2016.08.24 18:48:20	88.440168	122.212456	79	Stern
SO-14-04	2016.08.24 20:17:13	88.24079°N	126.71391°W	83	Helicopter
SO-15-04	2016.08.24 20:27:39	88.03886°N	129.47318°W	87	Helicopter
SL-12-04	2016.08.25 05:11:28	87.873277° N	131.555032° W	79	Stern
SL-13-04	2016.08.25 09:39:35	87.662982° N	133.360406° W	85	Stern
SO-16-04	2016.08.25 11:31:52	87.44739°N	135.00691°W	90	Helicopter
SO-17-04	2016.08.25 18:52:00	87.00300°N	137.47699°W	83	Helicopter
SO-18-04	2016.08.25 21:24:26	86.75906°N	138.75337°W	75	Helicopter
SL-14-05	2016.08.28 05:04:00	86.744761° N	134.496309° W	81	Stern
SL-15-05	2016.08.25 09:29:40	86.496823° N	134.850338° W	77	Stern
SL-16-06	2016.09.03 08:44:48	81.578359° N	144.187509° W	81	Stern
SL-17-07	2016.09.03 14:40:49	81.613647° N	146.410551° W	77	Stern
SL-18-07	2016.09.03 15:21:23	81.435700° N	146.800100° W	83	Helicopter
SL-19-07	2016.09.03 15:31:52	81.232600° N	147.061200° W	85	Helicopter
SL-20-07	2016.09.04 02:15:00	81.003357° N	146.197449° W	81	Stern
SL-21-08	2016.09.04 18:05:47	80.154532° N	148.259336° W	77	Stern
SL-22-08	2016.09.04 20:09:46	79.929520° N	148.444909° W	81	Stern
SL-23-08	2016.09.04 22:18:50	79.705771° N	148.669308° W	79	Stern
SL-24-08	2016.09.05 00:29:27	79.484196° N	148.863746° W	87	Stern
SL-25-08	2016.09.05 02:38:11	79.259045° N	149.050504° W	83	Stern
SL-26-08	2016.09.05 05:09:20	79.042452° N	149.262051° W	85	Stern
SL-27-08	2016.09.05 12:29:23	78.816713° N	149.425419° W	80	Stern
SL-28-08	2016.09.05 19:17:10	79.253104° N	149.031663° W	90	Stern
SL-29-08	2016.09.05 22:56:22	79.485078° N	148.848108° W	88	Stern

Instrument Code	Deployment Time (UTC)	Deployment Latitude (°)	Deployment Longitude (°)	Channel	Deployment Type
SL-30-08	2016.09.06 00:21	80.037778° N	148.384444° W	85	Helicopter
SL-31-08	2016.09.06 02:22:21	79.706089° N	148.638172° W	80	Stern
SL-32-08	2016.09.06 06:17:22	79.929690° N	148.448462° W	82	Stern
SL-33-08	2016.09.06 08:33:51	80.062626° N	148.333027° W	85	Stern
SL-34-08	2016.09.06 10:03:15	80.155493° N	148.220495° W	87	Stern
SL-35-08	2016.09.06 13:22:04	80.368219° N	147.991039° W	83	Stern
SL-36-08	2016.09.06 17:09:18	80.591127° N	147.828020° W	80	Stern
SL-37-09	2016.09.07 17:12:34	79.657531° N	161.977399° W	85	Stern
SL-38-09	2016.09.08 02:30:00	79.370375° N	163.464133° W	83	Stern
SL-39-09	2016.09.08 12:34:02	79.347086° N	165.729548° W	85	Stern
SL-40-10	2016.09.08 22:42:20	79.070486° N	168.463696° W	84	Stern
SL-41-10	2016.09.09 06:30:30	78.782138° N	166.937443° W	81	Stern
SL-42-11	2016.09.09 20:41:28	78.225482° N	164.315134° W	83	Stern
SL-43-11	2016.09.10 08:49:29	78.812639° N	163.219696° W	81	Stern
SL-44-11	2016.09.10 11:15:36	78.951919° N	162.963617° W	85	Stern
SL-45-12	2016.09.10 20:55:05	79.520839° N	161.927952° W	88	Stern
SL-46-12	2016.09.11 05:15:44	79.941488° N	161.323050° W	81	Stern
SL-47-12	2016.09.11 15:33:26	80.460343° N	159.875097° W	83	Stern

Table 1-9: Seismometer stations installed on drifting ice floes during the first expedition phase.

Station #	Taurus SN	Beacon ID	Deployment/Recovery Day	Time (UTC)	Latitude	Longitude	Comments
TO-01-01	0427	-	2016-08-18	03:42:46	88.20805°N	85.32371°W	Beacon did not activate properly during deployment.
			2016-08-18	19:15:07	88.21402°N	84.11829°W	
TO-02-02	0544	06009	2016-08-19	10:00:00	87.98800°N	90.89881°W	
			2016-08-19	17:51:04	88.02351°N	90.27274°W	
TO-03-02	0453	06022	2016-08-19	16:30:00	88.22169°N	99.88160°W	Unable to attempt recovery. Still on the ice (as of 2016-10-03)
			-	-	-	-	
TL-01-02	0399	06024	2016-08-19	18:59:00	88.39450°N	111.31333°W	Recovered during LSL1604. Field record contains shots from LSL1603 and LSL1604 as well
			2016-08-24	18:53:00	88.71939°N	101.24476°W	
TO-04-03	0416	06020	2016-08-22	22:49:08	89.22598°N	123.24917°W	Deployed at large (km-scale) open lead. High winds, snow, breaking waves. Station not recovered. Still on the ice (as of 2016-10-03)
			-	-	-	-	
TO-05-04	0544	06009	2016-08-25	12:00:29	87.23333°N	136.38167°W	
			2016-08-25	20:53:21	87.26835°N	135.53067°W	
TO-06-04	0820	06021	2016-08-25	19:18:52	86.88851°N	138.27145°W	
			2016-08-26	10:42:55	86.96297°N	137.11926°W	

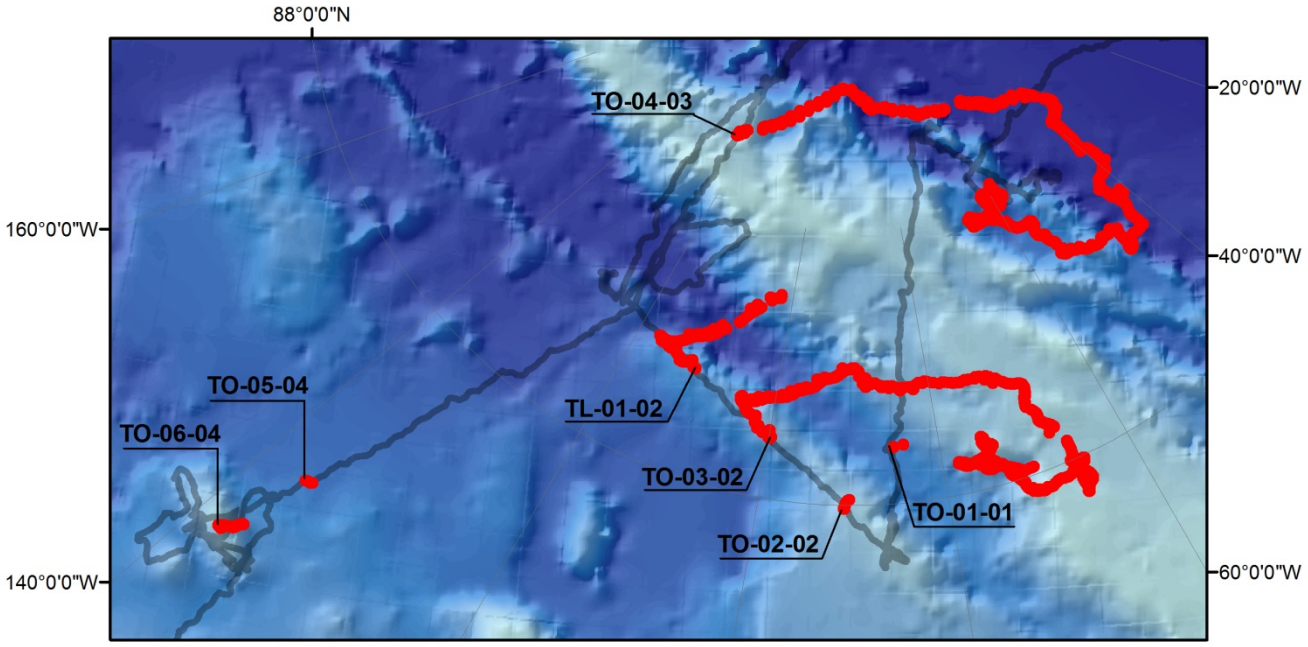

Figure 1-17: Map of the drifting ice-stations deployed during the first phase of the expedition. Hourly positions are plotted in red, while the ship's track is shown in grey.

Expendable sonobuoy records

Sonobuoy data quality varied substantially with environmental conditions. The cleanest signal was obtained in open water conditions in which a consistent heading could be maintained (*e.g.* Figure 1-18). Some of these records exhibit signal reception at 40 km offset. Records acquired in heavy ice were generally noisier and signal reception suffered from strong changes in heading necessary to navigate through the ice. As in previous surveys, radio communication on HF bands introduced blanking to the sonobuoy records. Repetitive coherent noise also occurs in several sonobuoy records (generally those transmitted over channels 81, 87, and 90), which is likely caused by interference from the ship's radar system mounted close to the Yaggi array. An example of this behaviour is illustrated on Figure 1-19.

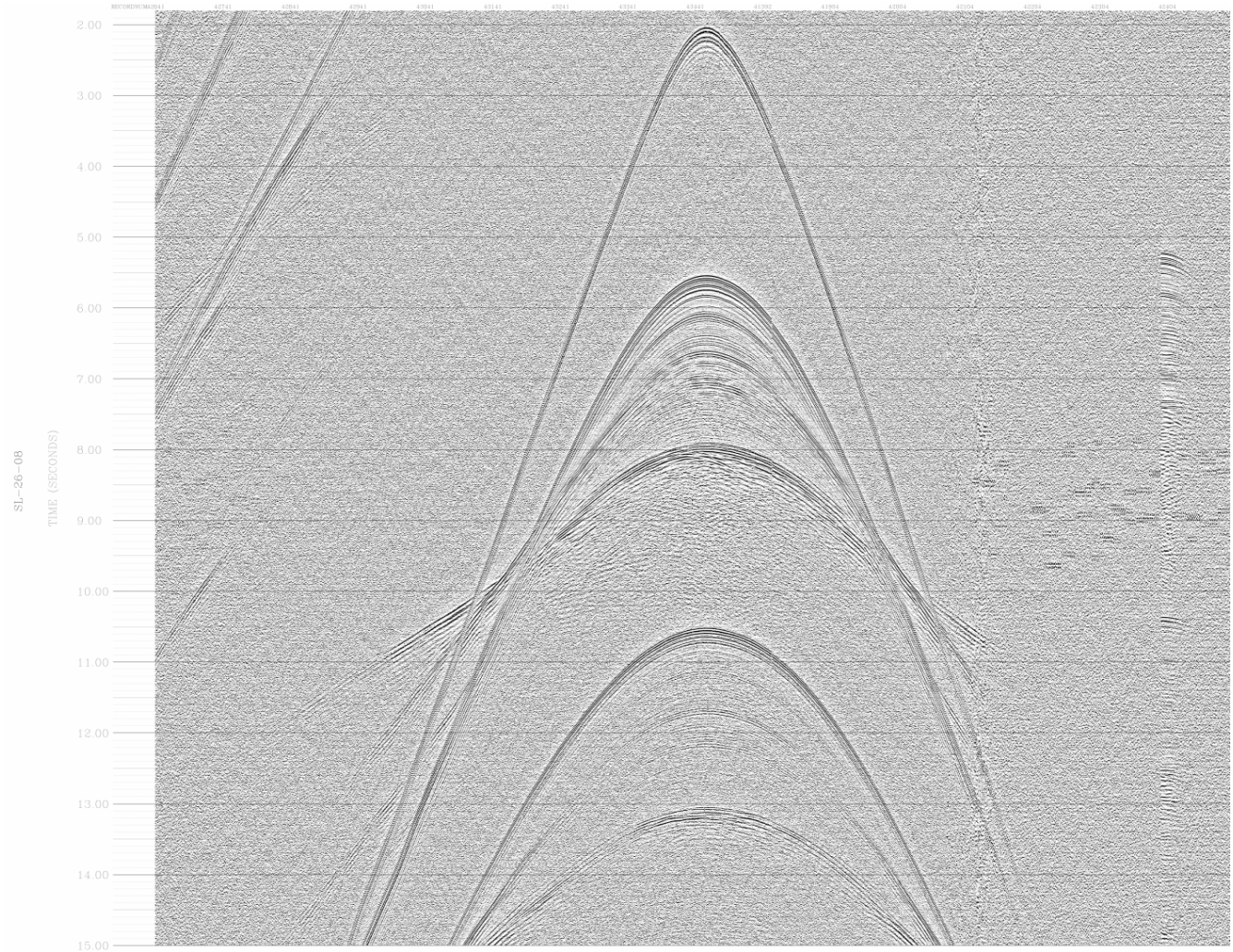

Figure 1-18: Example of an excellent quality sonobuoy record (SL-26-08) acquired in the northern Canada Basin during the second phase of the expedition.

During the two-ship operations, there was miscommunication of the fact that instrument SO-13-03 had failed. This failed instrument was assigned an instrument code by staff on the *Oden*, as per policy, but not by staff on the *Louis*. As a result, all sonobuoys deployed and logged onboard the *Oden* after SO-13-03 were assigned an instrument code that was one instrument number greater than the corresponding number assigned onboard the *Louis*. In other words, the numbers assigned onboard the ship are out-of-synchronization by one after SO-13-03. These discrepancies are listed in Table 1-10. The discrepancies were not corrected in the field since it was necessary to limit the potential for any further confusion during busy seismic operations. It is recommended, though, that the logging information and field records be carefully inspected and properly renumbered before commencing any data processing or interpretation. We believe that field records of all sonobuoys deployed from the *Louis* (*i.e.* instrument codes starting with SL) are correctly numbered, but this too should be carefully verified.

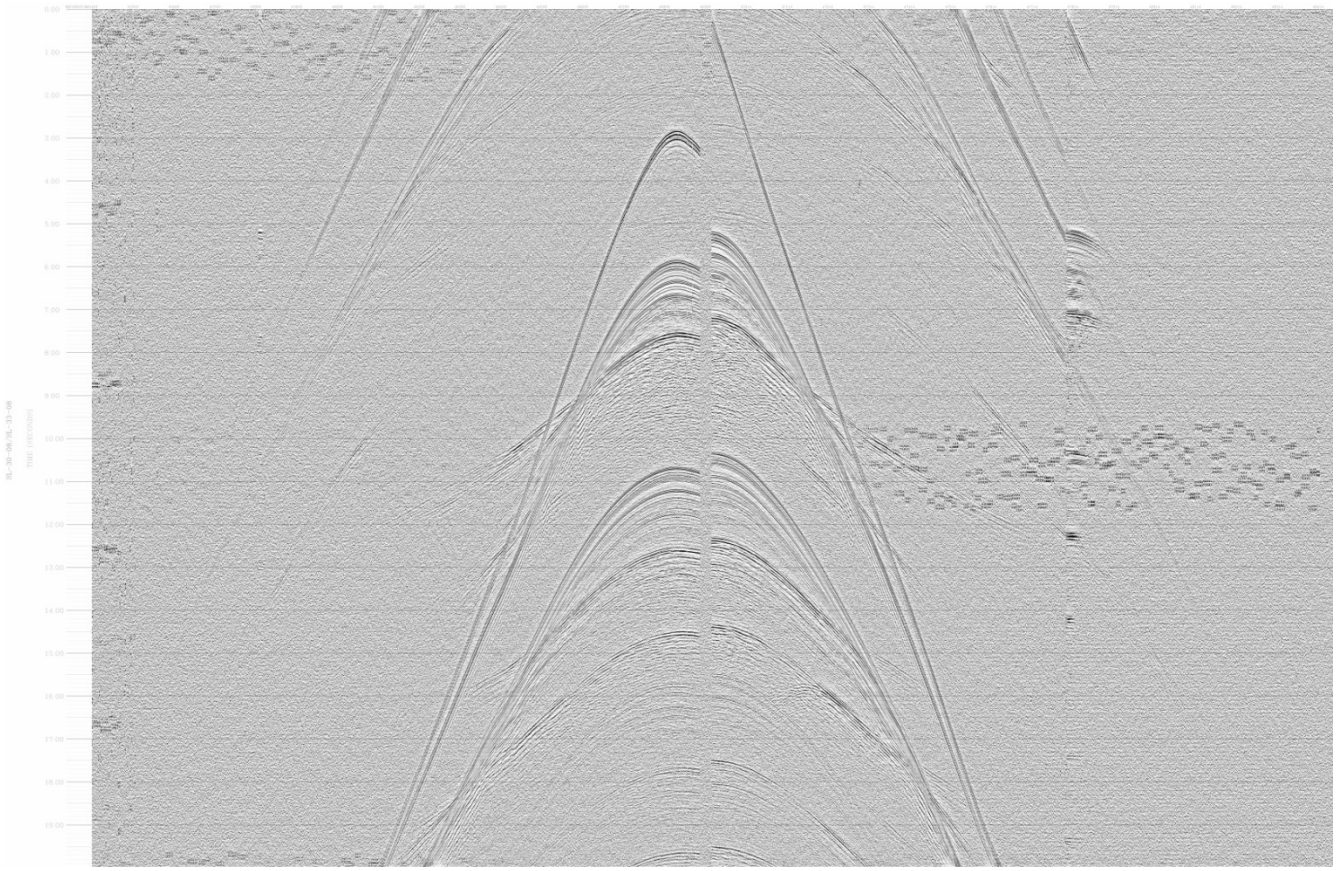

Figure 1-19: Composite of two sonobuoy records (SL-30-08 and SL-33-08) illustrating coherent noise from radar interference.

Table 1-10: Discrepancies in instrument codes assigned onboard the Louis versus onboard the Oden. Instrument codes used for naming all field records should be carefully verified before beginning any processing or interpretation of the data.

Deployment Date (UTC)	Instrument Codes		Comments
	Louis Log	Oden Log	
2016-08-23 (236) 11:56:59	SO-12-03	SO-12-03	
2016-08-23 (236) 12:08:28	N/A	SO-13-03	Failed deployment
2016-08-23 (236) 12:52:57	SO-13-03	SO-14-03	
2016-08-24 (237) 20:17:13	SO-14-04	SO-15-04	
2016-08-24 (237) 20:27:39	SO-15-04	SO-16-04	
2016-08-25 (238) 11:31:52	SO-16-04	SO-17-04	
2016-08-25 (238) 18:52:00	SO-17-04	SO-18-04	
2016-08-25 (238) 21:24:26	SO-18-04	SO-19-04	

Non-expendable seismometer records

Installation and recovery of seismometers on the drifting Arctic icepack using helicopters from a ship has, to our knowledge, been attempted in only one other expedition (Jackson *et al.* 1995), although similar work is commonly accomplished from ice camps (*e.g.,* Funck *et al.*, 2011). We had anticipated, before beginning the seismic operations, that successful deployment and recovery of the seismometers would be unlikely because of the generally foggy weather that persists over the Arctic Ocean during most of August and September. However, we benefitted from a highly adaptable capacity to operate helicopters from both ships, which allowed us to respond quickly to brief weather improvements and to make multiple attempts for both deployment and recovery of the instruments.

During recovery, it is important to incorporate the latest wind direction in establishing a search area. More than once, the winds changed just before a planned recovery. This was enough to shift the trajectory of the ice drift and greatly increase search times. Ideally, recoveries would be planned using last-known satellite beacon positions that are less than an hour old. Of course, radio beacons at each seismometer station would virtually eliminate any time requirement for searching.

The ETS-1500 satellite beacons performed well, overall, which was a crucial factor enabling successful recovery of the seismometers from the drifting ice floes. Under some conditions, however, it was noted that only the first of the three hourly positions reported for each beacon was reliable. Errors in the second and third hourly positions occurred at high latitudes during which the direction of drift was perpendicular lines of longitude, and also when the beacons were being tested on a moving ship. The beacons use differential latitude and longitudes to calculate the second and third hourly positions. Apparently the calculation accrues errors at high latitudes (where the lines of longitude converge) and when positions change rapidly due to transiting of the ship.

Wide-angle reflection/refraction records from the seismometers appear to be of excellent quality, although it was only possible to extract and inspect a subset of the records because the staff was completely engaged with other priorities during the operations. Fully-reversed records were collected with seismic signals at more than 40 km offset from the source (*e.g.* Figure 1-20).

The battery supply for each of the seismometer stations was more than adequate for the Taurus instrument running in buffered mode. Ice-station TL-01-02, for example, remained active for over five days between LSL1602 and LSL1604, and contains signal recorded from each of those lines.

Some coherent system noise was digitized on the hydrophone channels and is likely the result of the seismometer entering communication mode to write the data buffer to the permanent store. The noise consists of a pulse every 0.5 s and occurs for roughly 10 minutes at a time throughout the record.

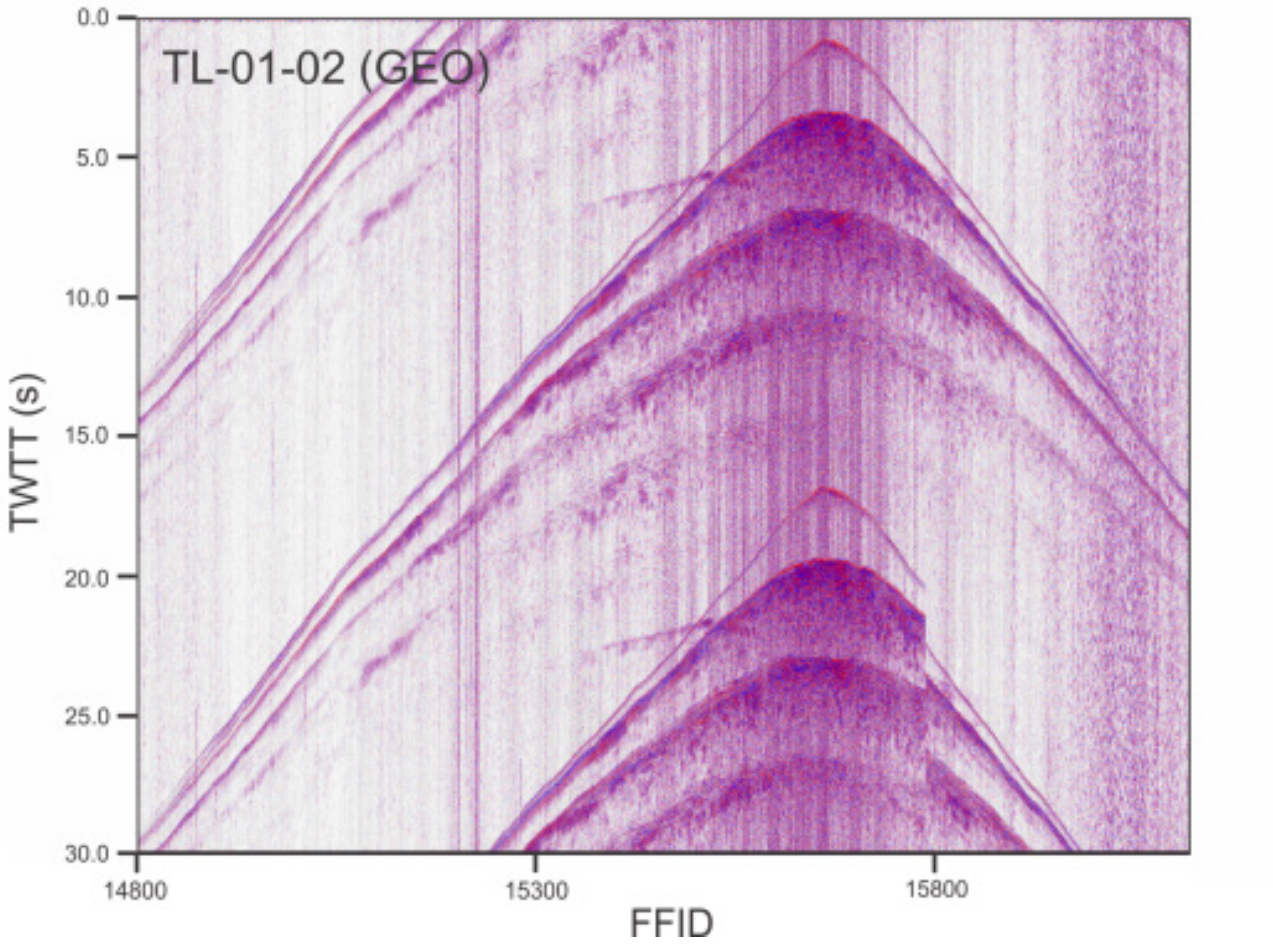

Figure 1-20: Plot of the raw geophone channel from an ice-station seismometer (TL-01-02).

1.6 Summary and recommendations

The data set collected during operations with the *IB Oden* and *CCGS Louis S. St-Laurent* comprises the first-ever seismic transect to be collected in a single season across the Amundsen Basin, Lomonosov Ridge, Marvin Spur, Alpha Ridge, and northern Canada Basin. The data set is notable in that it includes fully-reversed, long-offset records of wide-angle reflections and refractions from the crust. In the first phase of the expedition, when the ships were operated together, 1032.3 line-km of reflection seismic shot records, 33 sonobuoy records, and 5 seismometer records were collected along lines LSL1601 through LSL1605. During the second phase of the program, when the ships were operated separately, the *Louis* was used to collect a further 1151.6 line-km of reflection seismic shot records and 32 sonobuoy records. Data acquisition achieved using *IB Oden* during the second phase of the program are documented in a separate report by the staff who managed those operations.

We make the following suggestions to improve future seismic operations onboard the *Louis*:

1. Reference locations for every GPS receiver system on the ship should be verified relative to each other using accurate survey methods (section 1.5.1).

2. Critical operational systems, such as GPS receivers and ship-to-ship email communication, should be protected from public-use systems on the ship (section 1.5.1).

3. The computer software developed to produce shot navigation tables should be further developed so that these tables can be produced automatically during the seismic operations (section 1.5.1 and appendices A, B, and C).

4. The ODDI SeaStar mini-CTD sensors can provide accurate measurements of the hydrophone streamer depths, which would enable significant signal processing enhancements. Mini-CTDs lost during the operations should be replaced and properly calibrated before the start of the next program. The replacement sensors should be designed to operate in water depths of 0 to 100 m, and at temperatures as low as -4 °C (section 1.5.6).

5. The ability to log shot numbers separately from field file identification numbers is desirable for future seismic programs since it would simplify the numbering scheme that is needed in cases where either a shot is fired without a field record being generated or *vice versa* (section 1.5.7).

6. As recommended in the Geometrics manual, the “reset timestamp from GPS” parameter should be enabled in the GeoEel Controller software. Otherwise, the timestamps of shot records produced by the Controller can drift by 3 s or more from the actual time (section 1.5.7).

7. The time interval for serial logging of NMEA strings with the GeoEel Controller should be kept to a reasonable range relative to the length of the shot records. The initial setting of ±5.0 s is likely unrealistically long, and may have contributed to drift of the file timestamps. A ±2.5 s serial window is sufficient to ensure capture of GGA strings for all shot records whereas, in previous years, the default setting of ±1.0 s was sometimes too short (section 1.5.7).

8. Network connections to the computer running the GeoEel Controller software should be restricted to a single user who is responsible for inspecting, verifying, archiving, and processing the records. Otherwise, if multiple users are allowed network access, the GeoEel software might crash and data might be lost (section 1.5.7).

9. A few months prior to the seismic program, obtain the latest version of the GeoEel Controller software and manuals, install two copies on removable drives, and create an installation backup. The new version of the software should be tested prior to the start of acquisition. Version 5.36 proved to be reliable and should therefore be kept as a backup in case there are bugs in the latest version (section 1.5.7).

10. Field records and logging information for sonobuoys launched from the *Oden*, from SO-13-03 onwards, are misnumbered. Instrument codes assigned to any of the wide-angle seismic reflection/refraction field records from either ship should be carefully verified before beginning any data processing or interpretation (section 1.5.8).

11. Results from this program demonstrate that it is feasible during a ship-based program in the Arctic Ocean, that it is feasible to deploy and recover seismometers on drifting ice floes. For success, it is essential that the helicopter operations be highly adaptable to rapidly changing weather and ice conditions.

CHAPTER 2: Signal processing of multichannel seismic reflection data collected using the *CCGS Louis S. St-Laurent*

John Shimeld

2.1 Summary

Seismic operations were conducted onboard the *CCGS Louis S. St-Laurent* during two phases of the 2016 Canada–Sweden Polar Expedition (Figure 2-1). The first phase occurred over the Amundsen Basin, Lomonosov Ridge, Marvin Spur, and northern Alpha Ridge, while the second phase occurred over the Nautilus Spur, northern Canada Basin, and Chukchi rise. In total, the work produced 66,654 multichannel shot records along 12 line segments totaling 2183.9 km in length with an average density of 34.0 m per shotpoint (Table 2-1). There are also 62 sonobuoy and 5 seismometer records that were collected at irregular intervals of 15 to 80 km along each of the line segments.

Data integrity and quality were monitored continuously throughout the program by reading the shot records, generating brute stack plots, inspecting the amplitude and frequency characteristics of signal and noise on the records, and troubleshooting the cause of any irregularities. The following sections describe signal processing steps that have been applied to the multichannel seismic data set collected onboard the *Louis*. Processing of the *Oden* data set is documented in a separate report.

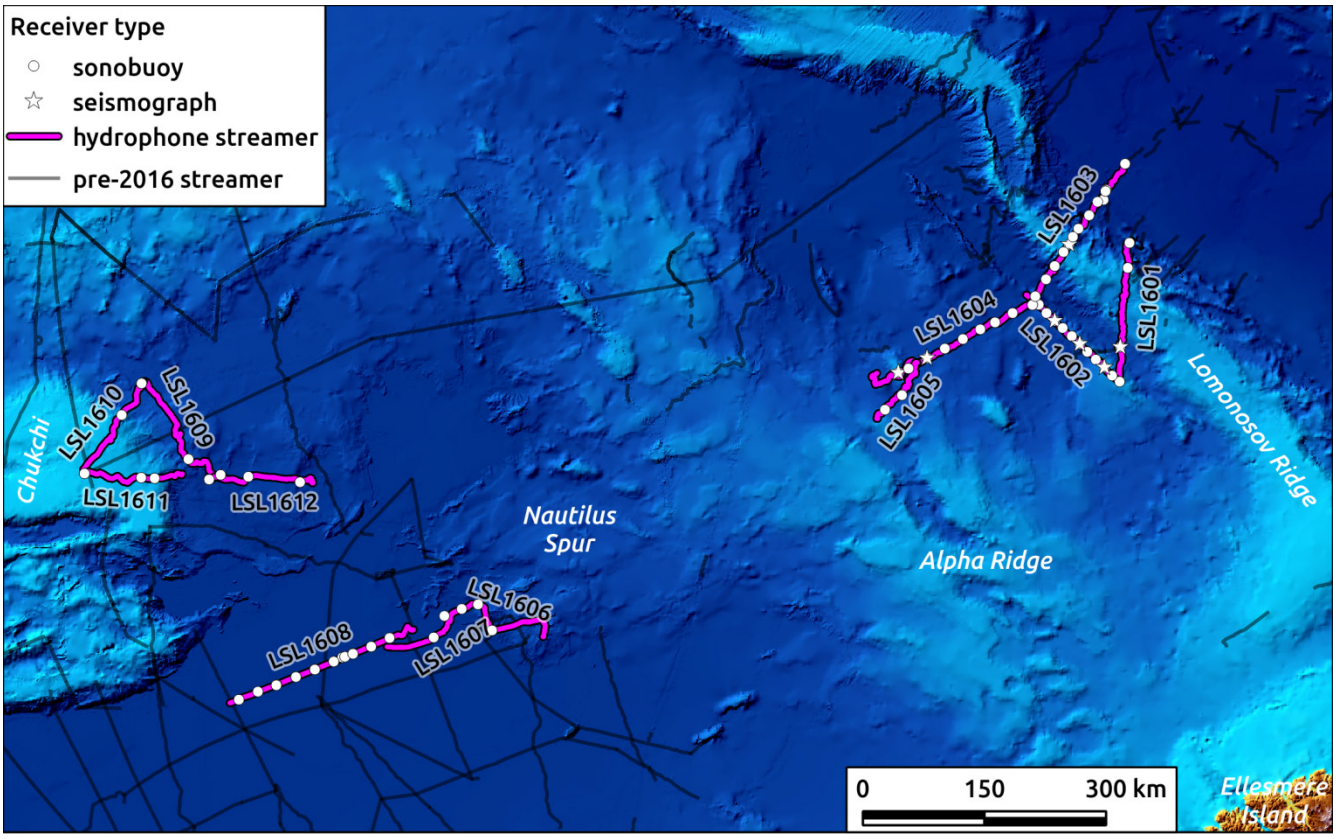

Figure 2-1: Geographic distribution and types of seismic records collected onboard the Louis.

Table 2-1: Seismic data acquisition managed onboard the Louis.

	LSL1601	LSL1602	LSL1603	LSL1604	LSL1605	LSL1606	LSL1607	LSL1608	LSL1609	LSL1610	LSL1611	LSL1612
Start date (UTC)	JD230 11:42	JD232 07:23	JD235 08:51	JD237 11:11	JD240 17:26	JD246 19:01	JD247 14:55	JD249 10:43	JD251 16:51	JD252 22:09	JD253 20:37	JD254 20:33
End date (UTC)	JD231 19:26	JD233 09:30	JD236 13:40	JD239 08:20	JD241 15:17	JD247 14:52	JD248 11:24	JD251 00:01	JD252 22:06	JD253 20:35	JD254 19:59	JD255 19:33
Start lat/lon	89.33 -65.71	87.79 -84.89	89.69 +51.04	88.88 -121.96	87.12 -137.15	81.98 -141.43	81.60 -146.46	78.71 -149.52	79.68 -161.92	79.10 -168.55	78.22 -164.34	79.52 -162.06
End lat/lon	87.88 -86.21	88.49 -126.61	88.79 -123.42	86.70 -140.95	86.37 -134.70	81.60 -146.45	80.52 -147.41	80.89 -147.45	79.10 -168.55	78.22 -164.35	79.26 -162.74	80.57 -159.63
Bathymetric range (m)	1113 4069	1015 3490	1059 4492	1516 3993	1580 3496	2556 3733	3314 3999	3515 3982	1470 3596	396 3109	342 2712	3078 3996
Seismic source (in^3)	1150	1150 & 1000	2000	1150	1150	1150	1150	1150	1150	1150	1150	1150
Average field time break[A] (ms)	60.5	60.0	59.9	56.0	56.2	56.3	56.3	56.1	56.2	56.2	56.3	55.9
First shot[B]	5	11060	17594	21331	30860	35350	39097	42812	49527	54792	58834	62513
Last shot	8851	17592	21323[C]	30855	35249	39096	42870	49526	54791	58833	62511	66654
# shots	8847	6533	3730	9525	4390	3747	3684	6715	5265	4038	3678	4142
Line-km	205.4	195.3	192.8	325.1	113.8	129.8	134.6	257.7	191.0	151.0	136.6	150.8
Shotpoint density (m/shot)	23.2	29.9	51.9	34.1	25.9	34.6	36.5	38.4	36.3	37.4	37.2	36.4
# sonobuoys	2	8	12	7	2	1	4	16	2	2	3	3
# seismometers	1	3	1	2	0	0	0	0	0	0	0	0

NOTES:

A Field time breaks could not be digitized by the recording system so, instead, they were monitored and recorded manually by the seismic watchkeepers. The values reported here include an additional 10 ms delay because the airguns were fired on the down-going pulse of the trigger signal. This delay was confirmed in the field using oscilloscope measurements.

B Shot numbers generated by the gun controller are not logged by the data recording system and are not automatically written into shot records. Therefore, the field file identification (FFID) numbers are considered to be the same as the shot number.

C The streamer system failed after shot number 21323, but transit along the line and firing of the source was continued because wide-angle sonobuoy and seismometer records were still being collected. Shots fired after failure of the streamer are numbered in the navigation log as 21323.001, 21323.002, 21323.003, *etc.*

2.2 Acquisition parameters

The seismic equipment, data acquisition parameters, and field results are described in Chapter 1, and a summary of the parameters that are relevant for processing of the data is given in Table 2-2.

Table 2-2: Parameters used for collection of seismic reflection data onboard the Louis

Seismic source	LSL1603: (4 x 500) in^3 G-gun cluster all other lines: (2 x 500) in^3 + (1 x 150) in^3 G-gun cluster
Shot interval	12 to 20 s depending on water depth and field conditions
Nominal source depth	11.2 m
Airgun firing pressure	1800 psi (124 bar)
Average total firing delay	LSL1601: 60.5 ms LSL1604: 56.0 LSL1607: 56.3 LSL1610: 56.2 LSL1602: 60.0 LSL1605: 56.2 LSL1608: 56.1 LSL1611: 56.3 LSL1603: 59.9 LSL1606: 56.3 LSL1609: 56.2 LSL1612: 55.9
Number of channels	16 (near trace = 1; far trace = 16)
Group interval	6.25 m
Source-to-channel 01	140.50 m
Length of active section	93.75 m
Nominal streamer depth	11.2 (streamer is towed from the source, but there are no birds)
Sampling interval	2 ms
Record length	11.5 s
Recording delay	0.05 s
Recording format	SEG-D 8058 revision 1
Recording filters	none

Shooting was based on time rather than distance in order to minimize stress on the equipment while operating under variable ice conditions. This strategy has an additional benefit of increasing the trace density of the sonobuoy records and increasing the effective fold of the processed seismic reflection profiles. Experience gained in previous surveys has demonstrated that the reflection data can be successfully binned and processed despite the irregular trace spacing in the mid-point and common receiver gathers that is produced by shooting on time rather than distance.

In regions of deep water, such as the Amundsen Basin which can be deeper than 4.3 km, the shot interval should normally be greater than about 28 to 30 s in order to avoid overprinting the records with energy from the third primary multiple of previous shots. This energy, which is commonly called the wrap-around multiple, can be a serious form of coherent noise that is difficult or impossible to eliminate during processing. A 30 s shot interval would translate to a shot spacing of about 60 m at a typical survey speed of 4 knots, which would yield a low trace density and likely cause mid-point binning of the data to be ineffective. Fortunately, multiple energy is attenuated by spherical spreading in the deep water and also by scattering of the reflections from the base of the sea ice (Lykke-Andersen et al., 2010). Thus, in practice, shot intervals of 12 to 20 s can be utilized even in deep water

so long as the position of the wrap-around multiple is carefully monitored and the shot interval is adjusted to minimize contamination of signal.

Icebreaking operations require frequent course deviations, changes in speed, and even complete stops, and there can be significant changes in water temperature and salinity around the icepack. As a result, correct balancing of the streamer is not possible over the duration of the survey. Neither is active streamer control since the associated hardware would be at risk of getting caught in the ice. As a result, receiver depths can vary significantly along the length of the streamer and also from one shot to the next. Differences of several metres between the inboard and outboard receiver groups are common, and the average depth along the streamer can change by 20 m in the space of 10 minutes when the ship encounters difficult patches of ice.

2.3 Processing workflow

The shot records are frequently contaminated with high amplitude noise from cable strumming, propwash, and electro-mechanical interference. Signal processing options are limited, though, by the small number of channels and the relatively short source-to-receiver offsets. As a result, the processing sequence used for seismic reflection profiles from ice-covered regions typically consists of little more than trace editing, frequency filtering, automatic gain control, binning and stacking (Eittreim and Grantz, 1979; Jokat *et al.* 1994; Bruvoll *et al.* 2012).

Additional signal processing techniques such as multiple attenuation, deterministic deconvolution and migration are worthwhile—as has been learned through working with seven other seismic data sets collected in the Arctic Ocean by the Geological Survey of Canada between 2007 and 2015—so long as the high amplitude noise can be eliminated or sufficiently attenuated. The processing sequence, detailed in the following sections, is as follows:

1. input SEG-D shot records;
2. assign geometry;
3. bandpass filter;
4. *F-K* filter for suppression of cable noise;
5. turbulence and swell noise suppression;
6. surface related multiple attenuation;
7. wavelet shaping deconvolution;
8. additional random noise suppression;
9. common midpoint binning and stacking;
10. finite difference migration;
11. amplitude recovery;
12. time-varying bandpass filter and final output of SEG-Y record sections.

2.3.1 Input SEG-D shot records

Channels 1 through 16 were read from the shot records and, for each trace, the mean value was subtracted from the live samples to remove possible DC bias. Traces containing NaNs or values greater than 1.0E+15 were muted. A line-by-line summary of the input traces is provided in Table 2-3.

Table 2-3: Summary of traces input to the signal processing workflow

Line	First SP	Last SP	# SPs	# traces
LSL1601	5	8851	8847	141552
LSL1602	11060	17592	6533	104496
LSL1603	17594	21309	3716	59456
LSL1604	21331	30855	9525	152400
LSL1605	30860	35249	4390	70240
LSL1606	35350	39096	3747	59952
LSL1607	39097	42780	3684	58944
LSL1608	42812	49526	6715	107440
LSL1609	49527	54791	5265	84240
LSL1610	54792	58833	4038	64608
LSL1611	58834	62511	3678	58848
LSL1612	62513	66654	4142	66272

2.3.2 Assign geometry

In the Arctic icepack, shot records are rarely collected along straight tracks; deviations from the planned ship track frequently exceed 500 m. However, uncertainties in the positioning of receivers with respect to the wiggly ship track are generally insignificant because the source-to-receiver offsets are relatively small (< 234 m) and the water depths are relatively large (> 3.5 km).

Information from the shotpoint navigation log was used to design common midpoint bins spaced at a regular 12.5 m interval along the track of each seismic reflection profile. The in-line halfwidth of each bin was 25 m, and the cross-line halfwidth was 75 m. Traces were assigned to all of the multiple overlapping bins in which they were located. This strategy ensured that each bin was assigned traces from multiple shots, typically yielding an effective fold of between 3 and 6 depending on the spatial density of the shotpoints. An example of the mid-point bins and trace assignments is shown on Figure 2-2.

In addition to course deviations, icebreaking operations involve frequent changes in speed—sometimes with complete stops—and there can be significant changes in water temperature and salinity around the icepack. As a result, correct balancing of the streamer is not possible over the duration of the survey. Neither is active streamer control since the associated hardware would be at risk of getting caught in the ice. Consequently, the depth of the streamer usually varies significantly along its length, and from one shot to the next. Differences of several metres between the inboard and outboard receiver groups are common, and the streamer can sink at a rate of about 20 m in 10 minutes when forward progress is hindered by difficult ice conditions.

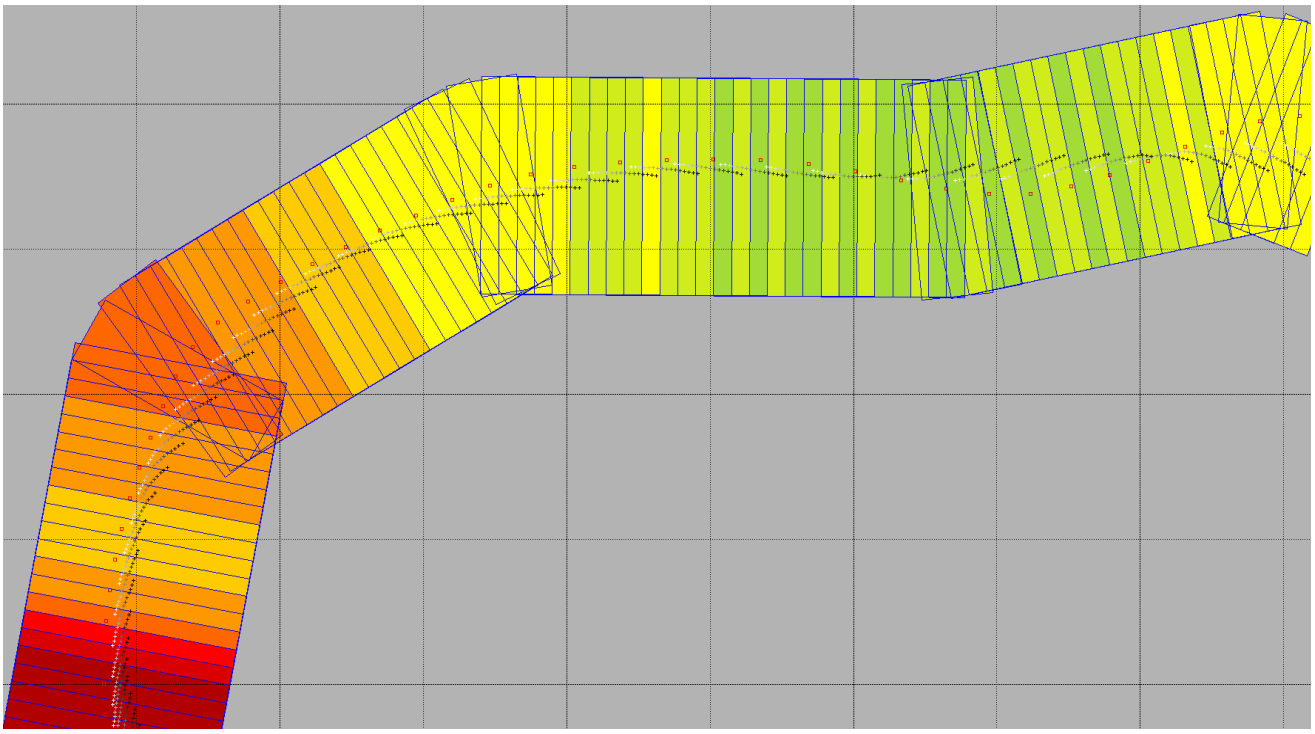

Figure 2-2: Example of trace binning along line LSL1601. The horizontal and vertical grid lines are spaced at 100 m. Shotpoints are indicated by the red boxes. Each bin is outlined in blue and colour-shaded to indicate the number of traces that fall within the bin, which ranges in this example between 20 (green) and 60 (red). Receiver positions are plotted as colour-coded dots from near offset (white) to far offset (black).

Fluctuations in the receiver depths change the way in which the receiver ghost reflection interferes with primary reflections. The depth fluctuations also correspond to significant changes in the two-way travel time with respect to the seismic datum, which causes positioning errors in the reflection events and loss of resolution due to misalignment of the common midpoint gathers. These issues can be corrected during processing if the receiver depths are known with reasonable accuracy.

Receiver depths were measured using sensors installed internally within in the streamer near receiver groups 1 and 16, and also using externally mounted mini-CTD sensors. However, various problems arose with both sensor types and the depth measurements collected during the survey are frequently inaccurate or missing (Chapter 1, section 1.5.6). This problem was solved by interpreting the receiver ghost from the autocorrelation of bandpass filtered traces within a 1.0 s window beneath the seafloor (Figure 2-3), and depth-converting the resultant two-way travel times using sound speed profiles from CTD measurements. Wherever possible, these results were verified using measurements from the streamer and mini-CTD sensors. Depths were interpreted on channels 1, 8 and 16 of all shot records, and then linearly interpolated for the remaining channels.

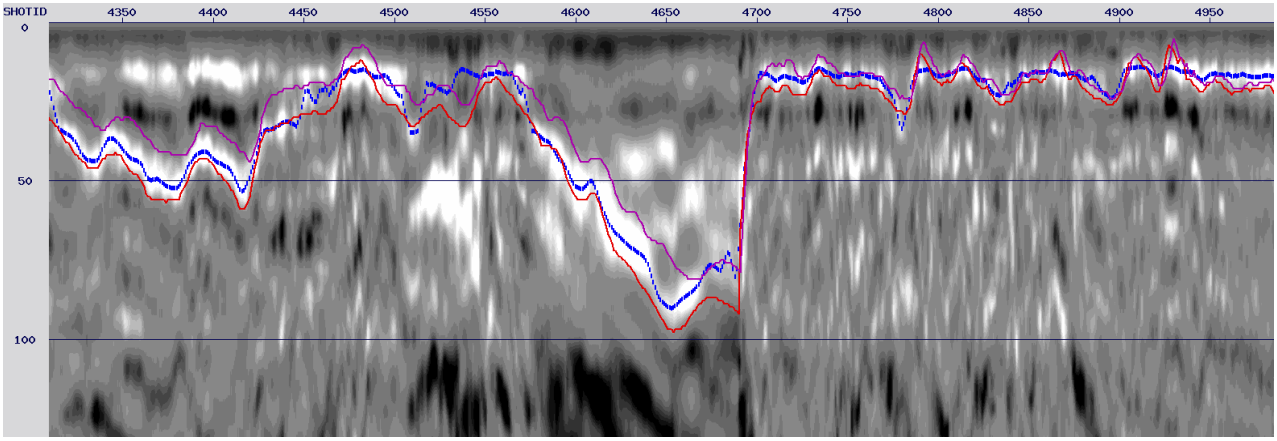

Figure 2-3: Determination of receiver depths along a segment of line LSL1601. The receiver ghost reflection recorded on channel 1 (blue dots) corresponds closely with two-way time converted measurements from the streamer sensor at receiver group 1 (red line), and with those from the Star ODDI mini-CTD (magenta line).

Time shifts were calculated to correct the total two-way travel time to the seismic reference datum of sea level using the recording delay of 50 ms, the nominal source depth delay of between 7 and 8 ms, the calculated receiver depth delays, and the average airgun firing delay for each line. The total time shift calculated for each trace was stored in the trace header so that it could be applied a later stage in the processing. A summary of the time shifts applied to each line is given in Table 2-4.

Table 2-4: Time shifts applied to correct the two-way travel times of seismic traces to sea level. All shifts are in milliseconds.

Line	Recording delay	Source depth delay	Airgun firing delay	Minimum total shift	Maximum total shift
LSL1601	50	8	61	-5	41
LSL1602	50	8	60	-3	3
LSL1603	50	8	60	-4	2
LSL1604	50	8	56	0	13
LSL1605	50	8	56	1	17
LSL1606	50	8	56	-2	3
LSL1607	50	8	56	-1	2
LSL1608	50	7	56	-2	2
LSL1609	50	7	56	-2	2
LSL1610	50	7	56	-2	3
LSL1611	50	7	56	-2	2
LSL1612	50	7	56	-2	3

2.3.3 Bandpass filter

The acquisition system did not apply low- or high-cut filtering, so the raw traces are dominated by high amplitude, low frequency noise. A minimum-phase Butterworth bandpass filter was applied for signal processing in the frequency domain using 1.0% additive noise, a 6.5 Hz low-cut with a slope of 24 dB/octave, and a 116 Hz high-cut with a slope of 48 dB/octave.

2.3.4 F-K filter for suppression of cable noise

Tugging and strumming of the streamer during seismic acquisition causes longitudinal waves within the streamer that manifest on shot gathers as high amplitude linear noise with apparent velocities of typically between 200 and 800 m/s. Fortunately, primary reflection events are essentially horizontal on the shot gathers since the combination of small offsets and deep water means that the moveout of primary reflection events is close to zero. A smoothed mute in the *F-K* domain proved effective at suppressing the high amplitude linear noise (Figure 2-4).

2.3.5 Turbulence and swell noise suppression

Icebreaker operations in the Arctic Ocean often generate high amplitude, low frequency noise from turbulence due to propwash and also from tight turns as the ship navigates through difficult ice conditions. Turbulence can also be a problem in light ice or open water, where strong Arctic winds may cause considerable ocean swell. Signal-to-noise ratios on some records is so poor that, if it were a conventional survey, the records would be rejected and re-acquired. However, the operational complexity and expense of a two-ship icebreaker program precludes such measures. Instead, noisy traces were flagged using a semi-quantitative index, and then replaced with strongly filtered version. Truly erroneous traces caused by missed shots or equipment malfunction were edited manually.

The noise index was calculated as follows:

1. sort to common receiver gathers;
2. apply a 3:1 running mix and a coherency filter;
3. subtract the original from the filtered gather to obtain an estimate of noise;
4. apply a low-pass filter, effectively eliminating frequencies above 21 Hz;
5. normalize each trace with respect to the median amplitude of the common receiver gather within the interval of 1.0 to 4.0 s below the seafloor;
6. zero trace samples within the interval of 0.1 to 0.5 s with respect to the seafloor;
7. within the interval of 2.0 to 12.0 s below the seafloor, calculate the noise index for each trace as follows:

$$I = 100\left(\frac{a - \hat{a}}{\hat{a}}\right)^2, \text{where}$$

a is the cumulative absolute difference of the trace samples between 2.0 and 12.0 s, and $\hat{a}$ is the median of this value for the entire gather. A summary plot of the noise indices for the entire survey is shown on Figure 2-5.

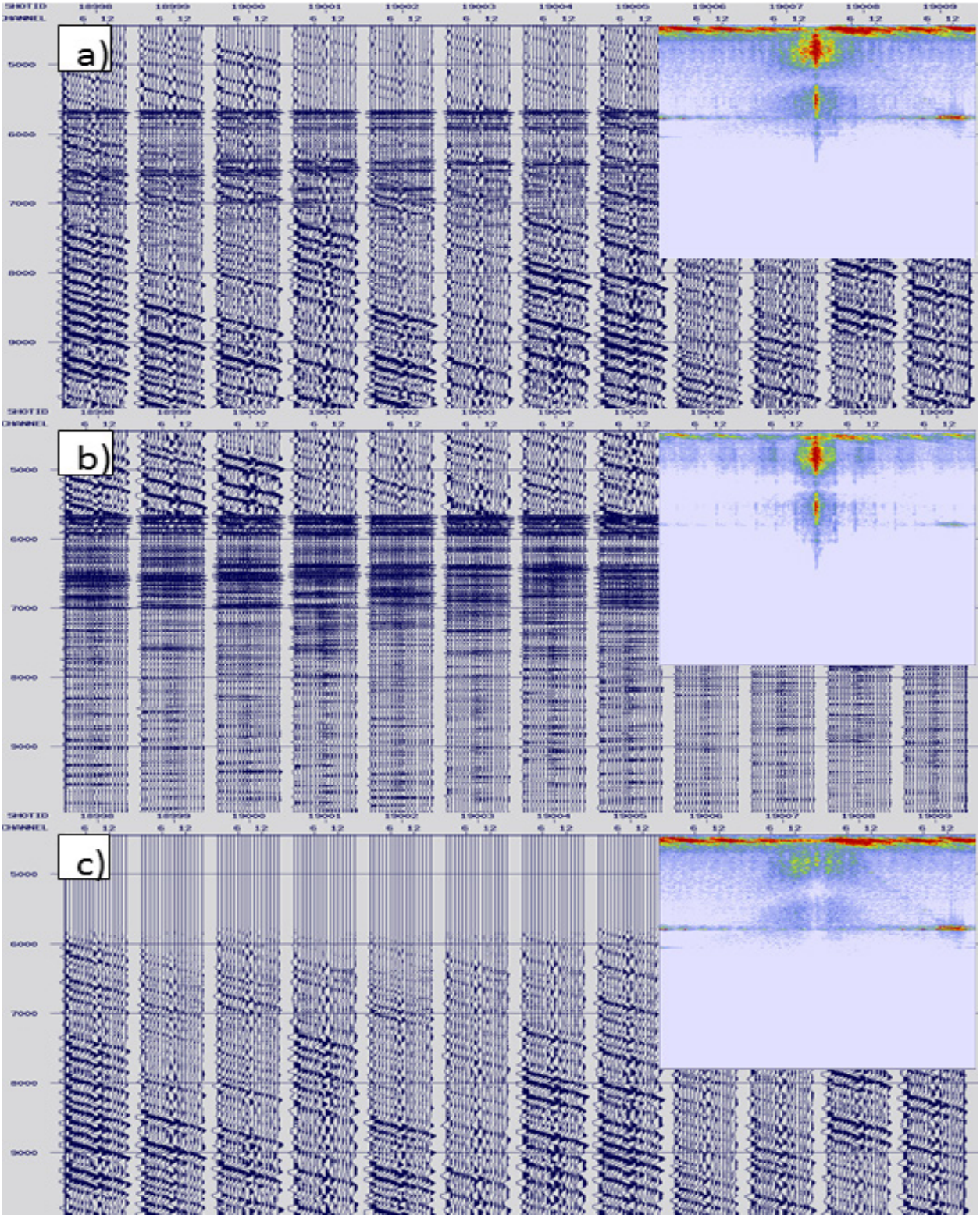

Figure 2-4: Example shot gathers from LSL1603 exhibiting high amplitude coherent cable noise. a) Bandpass filtered. b) Bandpass and F-K filtered. c) Residual. The colour inset images are plots of the F-K spectrum for frequencies and wavenumbers from 0 to Nyquist.

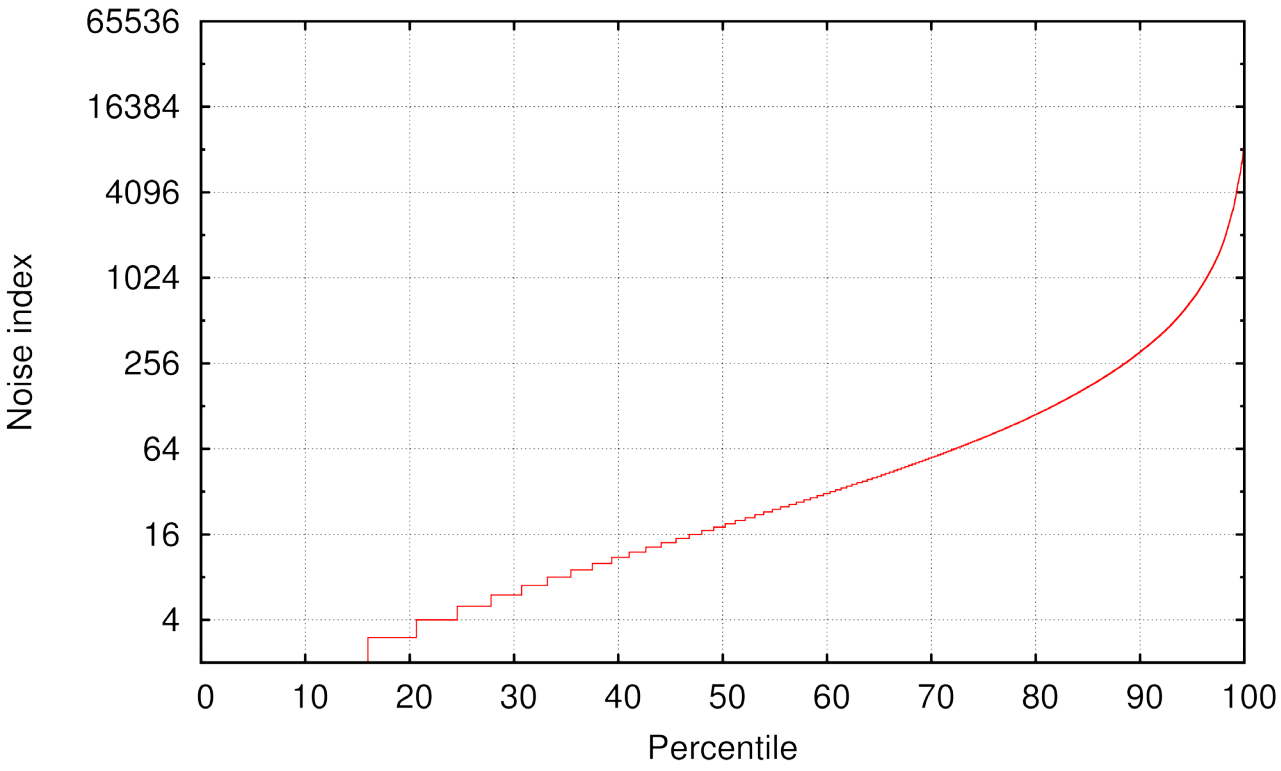

Figure 2-5: Semi-quantitative noise index plotted against trace percentile for the entire survey.

A noise index threshold of 200 was used to flag the noisiest 14% of the entire data set. These noisy traces were replaced with an *F-K* filtered version in which frequencies of less than 5 Hz and dips of greater than 16 ms/trace (on the common receiver gathers) where highly attenuated. Before applying the *F-K* filter, automatic gain control with a 1.0 s window was used to suppress noise bursts that might create artifacts. The automatic gain functions were then removed from the *F-K* filtered traces before swapping them with the noisy traces.

Swell noise and other random noise bursts were suppressed by applying an *F-X* domain coherency filter with a width of 19 traces to the common receiver gathers. Two passes of horizontal de-spiking were also applied in which three adjacent traces in the common receiver gather were compared within a 30 ms sliding window. The de-spiking operation mutes samples in the centre trace for which the amplitude envelope is greater than 4.5 times that of the adjacent traces.

Typical results achieved through the combination of *F-K*, *F-X* and de-spike filtering of common receiver gathers are shown on Figure 2-6.

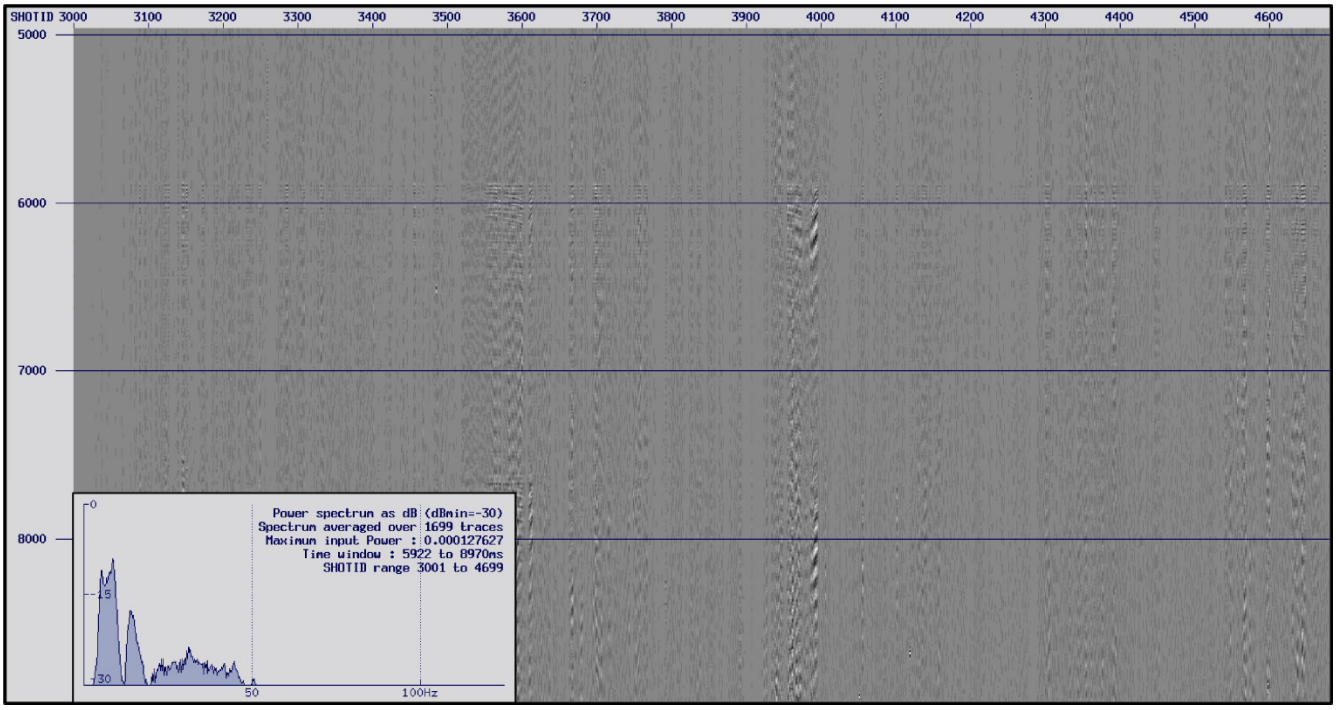

Figure 2-6: Turbulence and swell noise removed along a segment of LSL1601 through a combination of F-K, F-X, and de-spike filtering on common receiver gathers.

2.3.6 Multiple attenuation

A model of the primary multiples was constructed for the shot records using a technique known as surface-related multiple elimination (SRME; Vershuur et al., 1992). The results of this technique generally do not match exactly the amplitude and phase of the observations, but they are sufficiently close to be subtracted in an adaptive manner. For the present application, a residual time shift of between 0 and 8 ms was applied to each trace of the model in order to maximize the cross-correlation of the model with the data. Adaptive subtraction of the model from the data was then accomplished using an algorithm that is described by Wang (2003).

The SRME technique does not always perform well on data from deep-water or regions with a steeply dipping seafloor. Also the technique assumes a constant shotpoint interval, so it is not well-suited for the present dataset. An alternative approach was tested which involved interpretation of the first primary multiple horizon on poststack records. The stacked record was flattened on this multiple, and then an *F-K* filter was applied to remove essentially horizontal energy within a specified window of the multiple. This alternative approach is effective for abyssal plain settings where the seafloor and underlying layers are highly parallel. However it is not effective for slope settings where there are typically a wide range of dips beneath the seafloor. Also, the *F-K* filtering process has to be repeated for the second, third, and possibly higher primary multiples where they are present in shelf and mid- to upper-slope settings. SRME was chosen for the present study because: a) the objective was to simply reduce the multiple energy in deep-water, and b) a generalized technique was desired that could be applied to line segments over a wide range of water depths. An example of the results is shown on Figure 2-7.

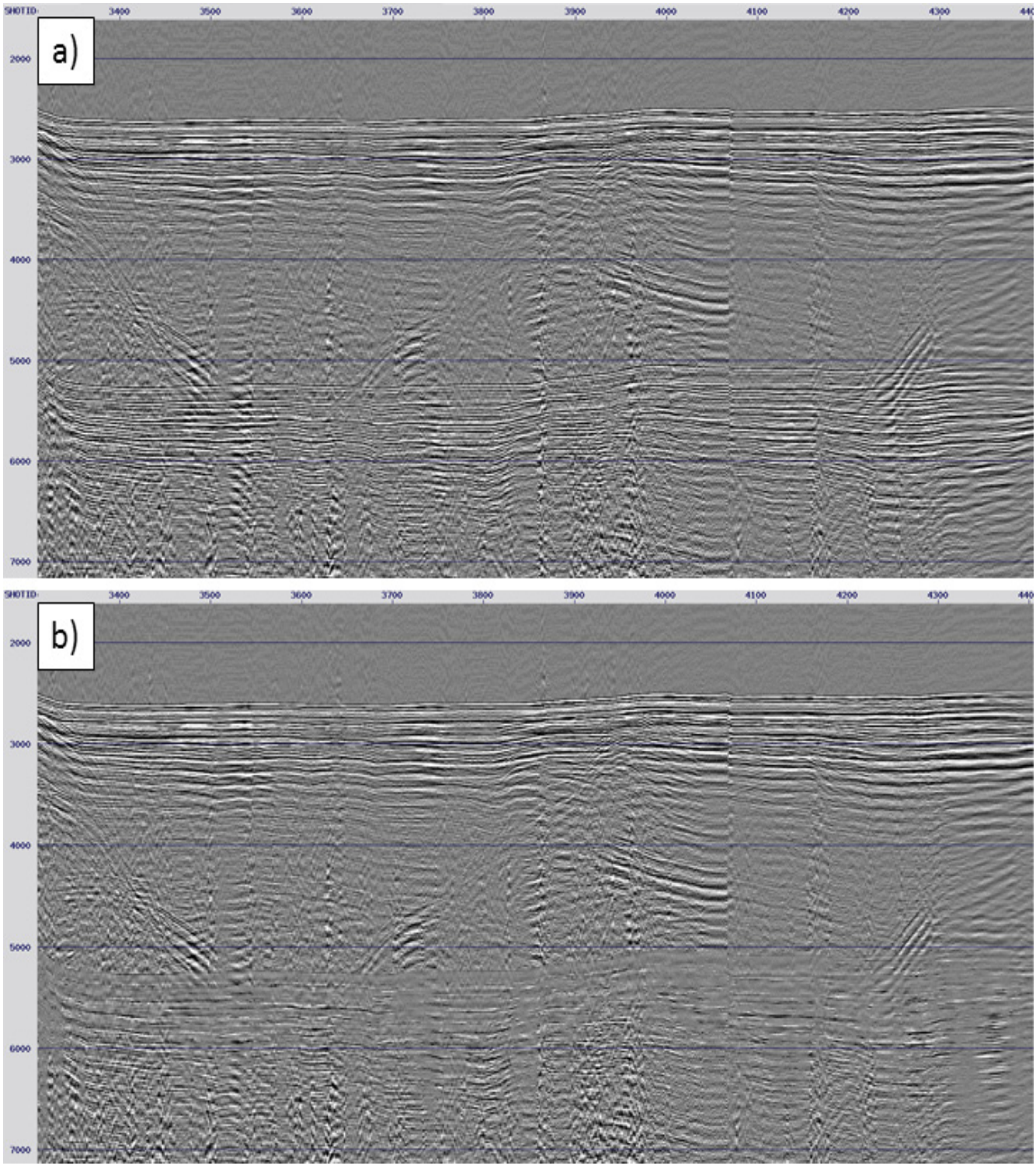

Figure 2-7: Example of results from the multiple attenuation technique. a) Near trace plot with t^2 amplitude scaling for a segment of line LSL1601. b) Same segment after adaptive subtraction of the multiple model.

2.3.7 Wavelet shaping deconvolution

Deterministic deconvolution was employed in a manner similar to that described by Sargent *et al.* (2011) to shape the seismic wavelet so that it is converted to zero phase and the bubble pulse is attenuated. Source signatures measured in the field were convolved with spikes of +1.0 at time zero and -0.7 at the time corresponding to the receiver depth in order to obtain a source wavelet with receiver ghost. A Weiner shaping filter was then designed for each trace to convert to a zero-phase band-limited Ormsby wavelet a frequency range defined by corner points 2, 5, 80, and 160 Hz. Numerical calculation of the shaping filter was stabilized through the addition of 1.0% white noise. Sample results are shown on Figure 2-8.

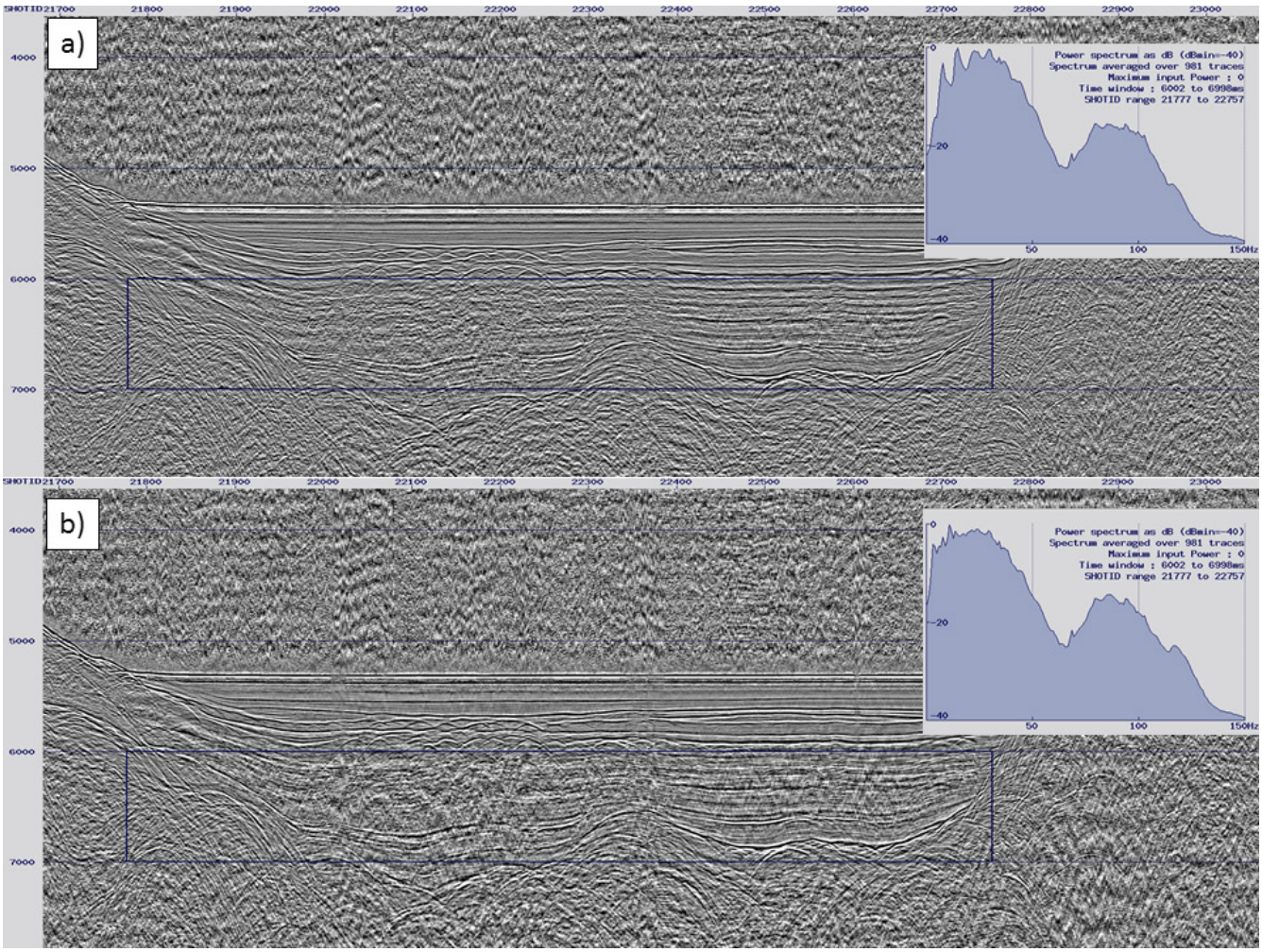

Figure 2-8: Example of results from deterministic deconvolution. a) Brute stack record section with automatic gain control for a segment of line LSL1604. b) Same record section after converting the wavelet to zero-phase and attenuating the bubble pulse. Power spectra averaged within the blue rectangles are shown on the inset plots.

2.3.8 Further random noise suppression

After deconvolution, a second round of pre-stack random noise suppression was applied to the common receiver gathers. This involved re-calculation of the noise index and *F-K/F-X* filtering as described in section 2.3.5, this time flagging and filtering the noisiest 5% of the traces in the survey. Horizontal and vertical despiking was then applied, followed by a zero-phase Butterworth bandpass filter in the frequency domain using 1.0% additive noise, a 7 Hz low-cut with a slope of 24 dB/octave, and a 93 Hz high-cut with a slope of 24 dB/octave.

2.3.9 Common midpoint binning and stacking

Shot records were sorted to common midpoint ensembles and a correction for normal moveout was applied although, as explained earlier, it is significant only for water depths of less than about 1500 m. Residual static shifts of up to 6 ms were determined through cross-correlations with an average pilot trace for each CMP ensemble. A surface consistent balance determined within the interval of 0 to 4 s beneath the seafloor was applied to the trace amplitudes, and the ensembles were then stacked.

2.3.10 Finite difference migration

Finite difference time migration was applied to the stacked records using a three-layer velocity model. As illustrated on Figure 2-9, the water layer was assigned a constant average interval velocity based on oceanographic CTD measurements for specific regions of the Arctic Ocean, and the sedimentary layer was assigned a discrete interval velocity function based on exponential slowness models by Shimeld *et al.* (2016). The crystalline basement beneath the sedimentary layer was assigned a constant velocity of 4500 m/s. Velocity interfaces between the three layers were smoothed using a 500 ms cosine taper to avoid migration artifacts.

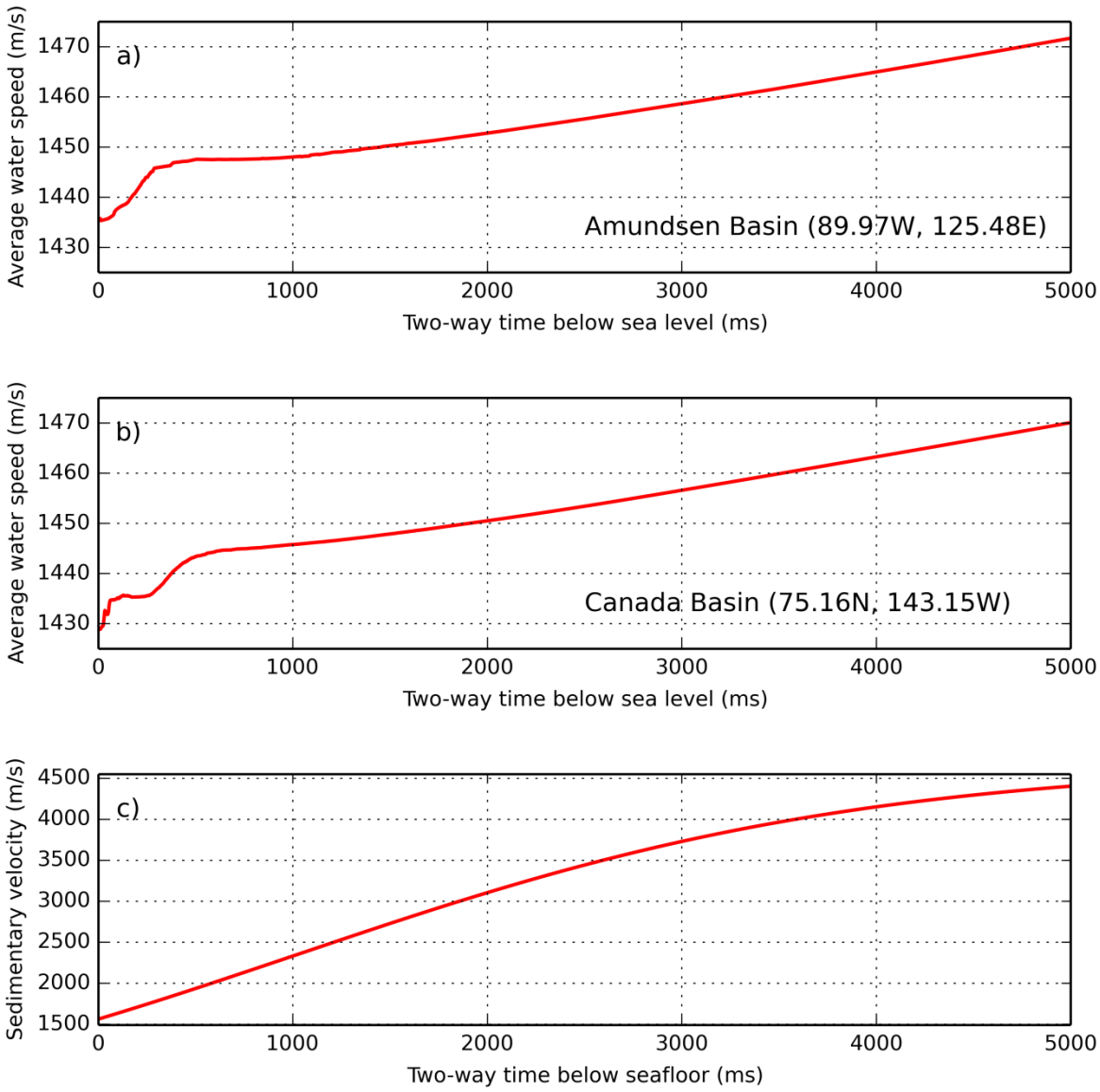

Figure 2-9: Example information used to construct a three-layer velocity model for finite difference time migration. a) Average water velocity versus two-way travel time below sea level from CTD measurements in the Amundsen Basin (Jane Eert 2016, pers. comm.). b) water velocity for Canada Basin (Jane Eert 2014, pers. comm.). c) Sedimentary velocity versus two-way time beneath the seafloor generate using the regional reference model of Shimeld et al. (2016) for the Canada Basin and southern Alpha Ridge.

2.3.11 Amplitude recovery

The following scalar function was applied to each trace in order to compensate for attenuation of the seismic amplitudes due to geometrical spreading and energy dissipation of the seismic wavefront with increasing distance from the source:

$$S(t) = t^2 V^2(t)$$

where V(t) is a linearly interpolated discrete function of the root-mean-square velocity with two-way travel time below the seafloor. The RMS velocities were calculated using the sedimentary velocity models of Shimeld *et al.* (2016) for the Canada Basin and southern Alpha Ridge. To avoid creating high noisy amplitudes near the bottom of the record sections, a linear amplitude scalar of -3 dB/s was applied starting at the time of the first primary seafloor multiple.

2.3.12 Time-varying bandpass filter and final output of SEG-Y record sections

A final time-varying zero-phase bandpass filter was applied in the frequency domain using the corner frequencies listed in Table 2-5. The final traces were resampled to a 4 ms time interval and output in digital standard SEG-Y format. Latitude and longitude coordinates are stored, respectively, in byte locations 81 and 85 of the trace headers as arcseconds (x 100). The mid-point bin numbers are in byte location 21, and the shotpoint numbers are in byte location 17.

Table 2-5: Corner frequencies for zero-phase, time-varying bandpass filter in the frequency domain.

f1 (Hz)	*f2 (Hz)*	*f3 (Hz)*	*f4 (Hz)*	*two-way time (ms below seafloor)*
4.5	7.5	100	115	0:200
4.5	7.5	80	300	300:1400
4.5	7.5	55	75	1500:2500
4.5	7.5	35	55	3500:4500

2.4 Comments

An example of the filtered and migrated data is shown on Figure 2-10. The overall high quality of these results, compared with other published data sets from the region, demonstrates that techniques such as multiple attenuation, deterministic deconvolution and migration are feasible even when icebreaker seismic data are contaminated with high amplitude noise. These techniques greatly enhance seismic resolution and interpretability, offering the potential to generate new knowledge about a poorly understood region of the Earth.

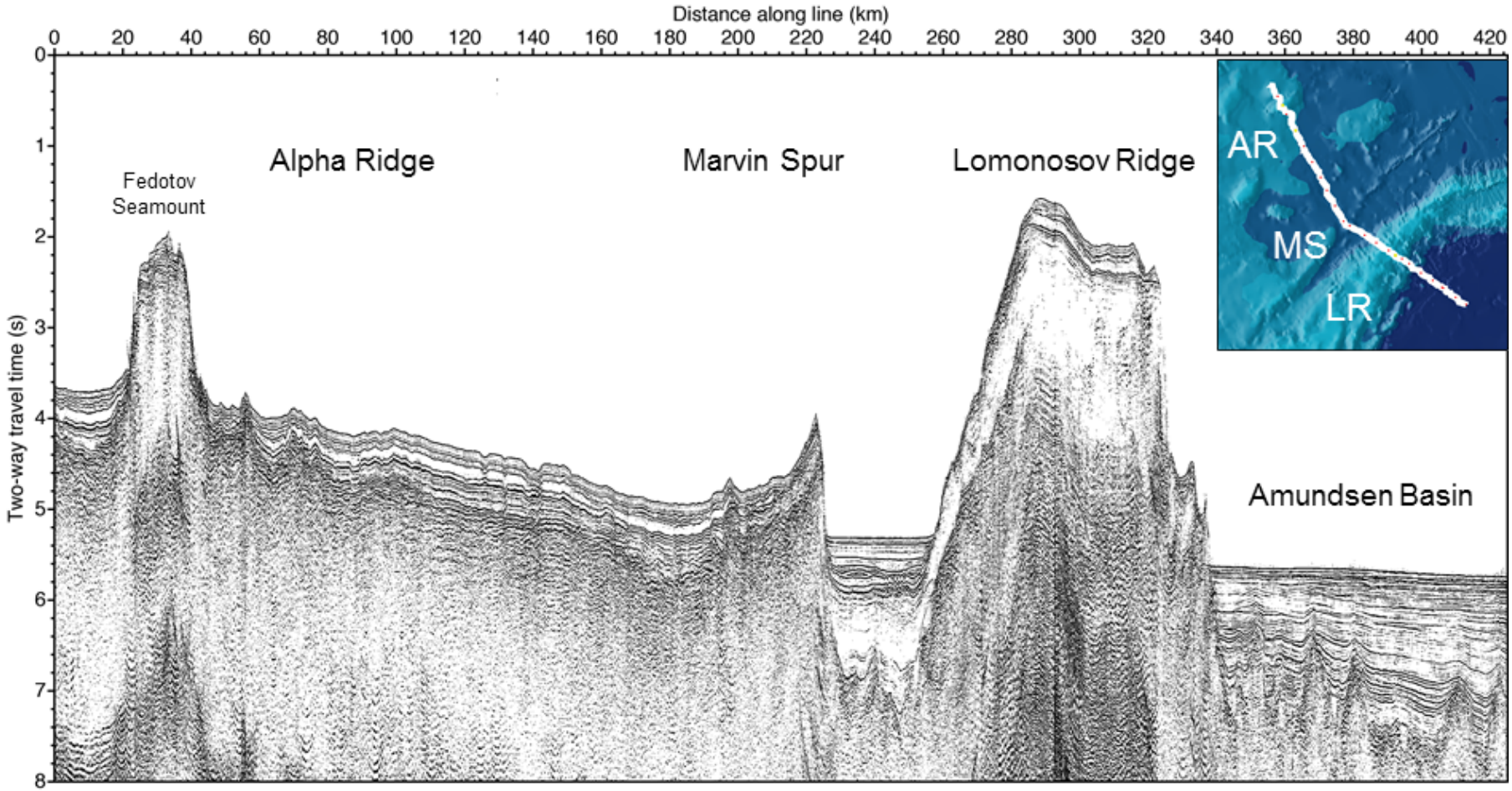

Figure 2-10: Sample record section illustrating the filtered and migrated results along merged lines LSL1603 and LSL1604.

References

Applanix Ltd., 2015. POS-MV V5 Installation and operation guide. Document no. PUBS-MAN-004291, revision 10.

Bruvoll, V., Kristoffersen, Y., Coakley, B.J., Hopper, J., Planke, S., Kandilarov, A. 2012. The nature of the acoustic basement on Mendeleev and northwestern Alpha ridges, Arctic Ocean. Tectonophysics, **514-517**, 123–145.

Cunningham, J., 2014. Vessel reference frame survey for the installation and operation of the Kongsberg multibeam echosounder EM122 (1° x 2°), and the Applanix POS/MV 320 position, heading, and attitude sensor, and all associated antennae and ancillary sensors, CCGS Louis S. St-Laurent. Unpublished report for Kongsberg Maritime, Dartmouth, Nova Scotia, Canada.

Eittreim, S. and Grantz, A. 1979. CDP seismic sections of the western Beaufort continental margin. Tectonophysics, **59**, 251–262.

Hutchinson, D.R., Jackson, H.R., Shimeld, J.W., Chapman, C.B., Childs, J.R., Funck, T., and Rowland, R.W., 2009. Acquiring marine data in the Canada Basin, Arctic Ocean. Eos, Transactions, American Geophysical Union, 90(23), 197–204.

Funck, T., Jackson, H.R., and Shimeld, J., 2011. The crustal structure of the Alpha Ridge at the transition to the Canadian Polar Margin: Results from a seismic refraction experiment. Journal of Geophysical Research, 116(B12101), 1–26, doi: 10.1029/2011JB008411.

Jackson, H.R., Grantz A., Reid, I., May, S.D., and Hart, P.E. 1995. Observations of anomalous oceanic crust in the Canada Basin, Arctic Ocean. Earth and Planetary Science Letters **134**, 99–106.

Jokat, W. and Buravtsev V., and Miller, H. 1995. Marine seismic profiling in ice covered regions. Polarforschung **64(1)**, 9–15.

Lykke-Andersen, H., Funck, T., Trinhammer, P., Marcussen, C., Gunvald, A., and Jørgensen, E. 2010. Seismic Acquisition Report - LOMROG II in 2009. Geological Survey of Denmark and Greenland, Report 2010/53.

Mosher, D.C., Shimeld, J.W. and Hutchinson, D.R., 2009. 2009 Canada Basin seismic reflection and refraction survey, western Arctic Ocean: CCGS Louis S. St-Laurent expedition report, Open File 6343, Natural Resource Canada, Ottawa, 266 p.

Mosher, D.C., Shimeld, J.W. and Chapman, C.B., 2011. 2010 Canada Basin seismic reflection and refraction survey, western Arctic Ocean: CCGS Louis S. St-Laurent expedition report. Geological Survey of Canada, Open File 6720, Natural Resources Canada, Ottawa, 252 p.

Sargent, C., and Hobbs, R.W., and Gröke, D.R., 2011. Improving the interpretability of air-gun seismic reflection data using deterministic filters: A case history from offshore Cape Leeuwin, southwest Australia. Geophysics, **76(3)**, B113–B125.

Shimeld, J., Li, Q., Chian, D., Lebedeva-Ivanova, N., Jackson, R., Mosher, D., and Hutchinson, D. 2016. Seismic velocities within the sedimentary succession of the Canada Basin and southern Alpha-Mendeleev Ridge, Arctic Ocean: evidence for accelerated porosity reduction? Geophysical Journal International, **204**, 1–20.

Verschuur, Berkhout, and Wapenaar, 1992. Adaptive surface-related multiple elimination. Geophysics, **57(9)**, 1166–1177.

Wang, Y., 2003. Multiple subtraction using an expanded multichannel matching filter. Geophysics, **68**(1), 346–356.

Appendix A: Listing of shotlog_create.py

```
# -*- coding: utf-8 -*-
"""
Created on Tue Jul 26 11:50:35 2016

Compiles a detailed shot log using information parsed from multiple log files.
Reads log files from GeoEel logging software for each line, and then locates and
indexes associated metadata to trigger times. Indexing of these
data uses the values from the closest logged string to the trigger time. Data are
pulled from the directory tree based on the SOL and EOL detected from the GeoEel
log file.

@author: kboggild
"""

import pandas as pd
import numpy as np
import os
from datetime import timedelta as td

def subsample_dates(matching,rng):
    subsampled = []
    for i in rng:
        day_string = i
        tmp = [s for s in matching if day_string in s]
        subsampled.extend(tmp)
    return subsampled

def binarySearch(alist, item):
    first = 0
    last = len(alist)-1
    found = False
    value = None
    while first<=last and not found:
        midpoint = (first+last)//2
        ender = midpoint==(len(alist)-1)
        if ender==True:
            c = abs(alist[midpoint]-item)<abs(alist[midpoint-1]-item)
            if c==True:
                found = True
                value = alist[midpoint]
            else:
                found = True
                value = alist[midpoint-1]
        else:
            a = abs(alist[midpoint]-item)<abs(alist[midpoint+1]-item)
            b = abs(alist[midpoint]-item)<abs(alist[midpoint-1]-item)
            if a==True and b==True:
                dd = alist[midpoint]<item                                    #
                yy = alist[midpoint+1]>item                                  #
                if dd==True and yy==True:                                    #
                    found = True                                             #
                    value = alist[midpoint+1]                                #
                else:
                    found = True
                    value = alist[midpoint]
            else:
                if item<alist[midpoint]:
```

```
                    last = midpoint - 1
                else:
                    first = midpoint + 1
    return value

def binarySearch_all(alist, item):
    first = 0
    last = len(alist)-1
    found = False
    value = None
    while first<=last and not found:
        midpoint = (first+last)//2
        ender = midpoint==(len(alist)-1)
        if ender==True:
            c = abs(alist[midpoint]-item)<abs(alist[midpoint-1]-item)
            if c==True:
                found = True
                value = alist[midpoint]
            else:
                found = True
                value = alist[midpoint-1]
        else:
            a = abs(alist[midpoint]-item)<abs(alist[midpoint+1]-item)
            b = abs(alist[midpoint]-item)<abs(alist[midpoint-1]-item)
            if a==True and b==True:
                    found = True
                    value = alist[midpoint]
            else:
                if item<alist[midpoint]:
                    last = midpoint - 1
                else:
                    first = midpoint + 1
    return value

#Read GeoEel shot log file

ffid1 = open('.\\2016_GeoEel_Logs\LSSL2016.01.log') #point to log for desired line
lines = ffid1.readlines()
ffid1.close()

ffid=[];geoeeltime=[]
for line in lines:
    lstrip=line.strip()
    if lstrip.startswith('File'):
        lstrip = lstrip.replace('\t',' ')
        lstrip = lstrip.replace('      ',' ')
        lstrip = lstrip.replace('     ',' ')
        lstrip = lstrip.replace('    ',' ')
        lstrip = lstrip.replace('   ',' ')
        lstrip = lstrip.replace('  ',' ')
        wordsz = lstrip.split(' ')
        ffid.append(int(wordsz[1]))
        tmpdatetime = wordsz[3] + ' ' + wordsz[2]
        geoeeltime.append(tmpdatetime)

geoeeltime = pd.to_datetime(geoeeltime, format='%m/%d/%Y %H:%M:%S.%f')
start_date = min(geoeeltime).date()
end_date = max(geoeeltime).date()
dfdf = pd.DataFrame({'GeoEelTime': geoeeltime, 'FFID':
```

```
ffid}).sort_values('GeoEelTime')

#Read streamer depth sensor log

streamerdepths = open('.\\2016_GeoEel_Logs\LSSL2016.01.Depth.txt','r')
lines = streamerdepths.readlines()
streamerdepths.close()

ffiddepth=[];depth1078=[];depth1122=[];emptystreamer=[]
for line in lines:
    lstrip=line.strip()
    lstrip = lstrip.replace(': ',',')
    lstrip = lstrip.replace('m',',')
    wordsr = lstrip.split(',')
    ffiddepth.append(int(wordsr[1]))
    depth1078.append(float(wordsr[4]))
    depth1122.append(float(wordsr[6]))
    emptystreamer.append(-999)
df7 = pd.DataFrame({'DepthFFID': ffiddepth, 'str01': depth1078, 'str09':
emptystreamer, 'str16':
depth1122}).sort_values('DepthFFID')#.reset_index(drop=True)
df2 = pd.merge(dfdf,df7,left_on='FFID',right_on='DepthFFID')

#Create list of all the data file paths for the other data logs located in the
working directory

file_list = []
for root, dirs, files in os.walk(".", topdown=True):
    for name in files:
        file_list.append(os.path.join(root, name))
gps_matching = [s for s in file_list if "GPS.txt" in s]
trigger_matching = [s for s in file_list if "Trigger.txt" in s]
depth_matching = [s for s in file_list if "DepthSounder.txt" in s]
heading_matching = [s for s in file_list if "Heading.txt" in s]
speed_matching = [s for s in file_list if "SpeedLog.txt" in s]
offset_matching = [s for s in file_list if "Offset.txt" in s]

#Create a list of paths to these files logged between the start and end of line

delta = end_date - start_date
rng=[]
for i in range(delta.days + 1):
    rng.append(str(start_date + td(days=i)))

gps_files = subsample_dates(gps_matching, rng)
trigger_files = subsample_dates(trigger_matching, rng)
depth_files = subsample_dates(depth_matching, rng)
heading_files = subsample_dates(heading_matching, rng)
speed_files = subsample_dates(speed_matching, rng)
offset_files = subsample_dates(offset_matching,rng)

print 'Assembling dataframes...'

#Read Trigger Log

trigger=[];clocktimebreak=[];fieldtimebreak=[]
for i in trigger_files:
    trig = open(i, 'r')
    lines = trig.readlines()
```

```
    trig.close()
    for line in lines:
        lstrip = line.strip()
        wordsA=lstrip.split('|')
        trigger.append(wordsA[4])

triggerarray = pd.to_datetime(trigger)
df1 = pd.DataFrame({'TriggerTime': triggerarray}).sort_values('TriggerTime')

#Read Knudsen Log

depth=[];depth_time=[]
for i in depth_files:
    knud = open(i, 'r')
    lines = knud.readlines()
    knud.close()
    for line in lines:
        lstrip = line.strip()
        lstrip = lstrip.replace(',','|')
        wordsB=lstrip.split('|')
        depth_time.append(wordsB[12])
        tmpdepth = wordsB[16]
        if tmpdepth == '0000.00' or tmpdepth == 'f':
            tmpdepth = '-999'
        depth.append(tmpdepth)

deptharray=np.asarray(depth, dtype='float64')
depth_time1=pd.to_datetime(depth_time)
df4 = pd.DataFrame({'KnudsenDepthTime': depth_time1, 'KnudsenDepth':
deptharray}).sort_values('KnudsenDepthTime')

#Read heading log

heading=[];heading_time=[]
for i in heading_files:
    head = open(i,'r')
    lines = head.readlines()
    head.close()
    for line in lines:
        lstrip = line.strip()
        finder5 = 'POS-MV' in lstrip
        if finder5 == True:
            lstrip = lstrip.replace('|',',')
            wordst = lstrip.split(',')
            heading.append(wordst[11])
            heading_time.append(wordst[9])
heading_time = pd.to_datetime(heading_time)
heading = np.asarray(heading, dtype='float64')
df8 = pd.DataFrame({'Heading': heading, 'HeadingTime':
heading_time}).sort_values('HeadingTime')

#Read speedlog

knots=[];kilometers=[];speed_time=[]
for i in speed_files:
    speed = open(i, 'r')
    lines = speed.readlines()
    speed.close()
    for line in lines:
```

```
        lstrip = line.strip()
        lstrip = lstrip.replace('|',',')
        wordso = lstrip.split(',')
        speed_time.append(wordso[8])
        knots.append(wordso[14])
        kilometers.append(wordso[16])
speed_time=pd.to_datetime(speed_time)
knots=np.asarray(knots, dtype='float64')
kilometers=np.asarray(kilometers, dtype='float64')
df9=pd.DataFrame({'SpeedTime': speed_time, 'SpeedKnots': knots, 'SpeedKilometers':
kilometers}).sort_values('SpeedTime')

#Read interpolated ODDI depth data

oddidepths = open('.\\2016_Interpolated_ODDI\Line01-
02_Reconverted_2.57m_262mbar_18S8026_interpolated.csv', 'r')
lines = oddidepths.readlines()
oddidepths.close()

odditime=[];forwardoddi=[];midoddi=[];aftoddi=[]
for line in lines:
    lstrip=line.strip()
    wordsE=lstrip.split(',')
    odditime.append(wordsE[0]+'.000000000')
    forwardoddi.append(-999)
    midoddi.append(round(float(wordsE[1]),2))
    #midoddi.append(-999)
    aftoddi.append(-999)
odditime=pd.to_datetime(odditime,format='%Y-%m-%d %H:%M:%S.%f')
#for i in xrange(0,len(triggerarray)):                          #Uncomment this and
comment out loop above if there is no ODDI data
#    forwardoddi.append(-999)
#    midoddi.append(-999)
#    aftoddi.append(-999)
#    odditime.append(triggerarray[i])
df6 = pd.DataFrame({'ODDITime': odditime, 'oddi01':forwardoddi, 'oddi09':
midoddi,'oddi16': aftoddi}).sort_values('ODDITime')

print 'Indexing dataframes...'

#Merge these all together. First need to append the closest values from each
dataframe to df1:
closest2=[];closest4=[];closest5=[];closest6=[];closest7=[];closest8=[];closest9=[]
;closest11=[]
for i in triggerarray:
    closestTimestamp2=binarySearch(geoeeltime,i) #use binarySearch_all for LSL1604
through LSL1612
    closestTimestamp4=binarySearch_all(depth_time1,i)
    closestTimestamp6=binarySearch_all(odditime,i)
    closestTimestamp7=binarySearch_all(heading_time,i)
    closestTimestamp8=binarySearch_all(speed_time,i)
    closest2.append(closestTimestamp2)
    closest4.append(closestTimestamp4)
    closest6.append(closestTimestamp6)
    closest7.append(closestTimestamp7)
    closest8.append(closestTimestamp8)
df1['Closest2']=closest2 #To connect to FFID dataframe (df2)
df1['Closest4']=closest4 #To connect to Depth dataframe (df4)
df1['Closest6']=closest6 #To connect to ODDI dataframe (df6)
```

```
df1['Closest7']=closest7 #To connect to Heading dataframe (df8)
df1['Closest8']=closest8 #To connect to SpeedLog dataframe(df9)
print 'Merging dataframes...'
dfout1 = pd.merge(df1, df2, left_on='Closest2',right_on='GeoEelTime')
dfout2 = pd.merge(dfout1, df6, left_on='Closest6', right_on='ODDITime')
dfout3 = pd.merge(dfout2, df4, left_on='Closest4', right_on='KnudsenDepthTime')
dfout5 = pd.merge(dfout3, df8, left_on='Closest7', right_on='HeadingTime')
dfout7 = pd.merge(dfout5, df9, left_on='Closest8', right_on='SpeedTime')
print 'Trimming output...'
dfout7 = dfout7.drop(dfout7.columns[[1,2,3,4,5,7,8,12,17,19,22]], axis=1)
print 'Saving output...'
dfout7.to_csv('.\\output\LSSL2016_0102_SHOTLOG_prelim.csv', index=None)
print 'Done!'
```

Appendix B: Listing of shotlog_interpolate.py

```
# -*- coding: utf-8 -*-
"""
Created on Fri Sep 09 11:00:10 2016

Takes the output of shotlogcreate.py and appends an interpolated latitude and
longitude from the GPS logs for a given GPS system. GPS logs are retrieved by
searching for file names based on keyword ('GPS.txt') and date range in the
NavNet directory structure.

@author: kboggild
"""

import pandas as pd
import os
from datetime import timedelta as td

def subsample_dates(matching,rng):
    subsampled = []
    for i in rng:
        day_string = i
        tmp = [s for s in matching if day_string in s]
        subsampled.extend(tmp)
    return subsampled

def binarySearch_post(alist, item):
    first = 0
    last = len(alist)-1
    found = False
    value = None
    while first<=last and not found:
        midpoint = (first+last)//2
        ender = midpoint==(len(alist)-1)
        if ender==True:
            c = abs(alist[midpoint]-item)<abs(alist[midpoint-1]-item)
            if c==True:
                found = True
                value = alist[midpoint]
            else:
                found = True
                value = alist[midpoint-1]
        else:
            a = abs(alist[midpoint]-item)<abs(alist[midpoint+1]-item)
            b = abs(alist[midpoint]-item)<abs(alist[midpoint-1]-item)
            if a==True and b==True:
                dd = alist[midpoint]<item
                yy = alist[midpoint+1]>item
                uu = alist[midpoint-1]<item
                ii = alist[midpoint]>item
                if dd==True and yy==True:
                    found = True
                    value = alist[midpoint+1]
                else:
                    found = True
                    value = alist[midpoint]
            else:
                if item<alist[midpoint]:
                    last = midpoint - 1
```

```
                else:
                    first = midpoint + 1
    return value

def binarySearch_pre(alist, item):
    first = 0
    last = len(alist)-1
    found = False
    value = None
    while first<=last and not found:
        midpoint = (first+last)//2
        ender = midpoint==(len(alist)-1)
        if ender==True:
            c = abs(alist[midpoint]-item)<abs(alist[midpoint-1]-item)
            if c==True:
                found = True
                value = alist[midpoint]
            else:
                found = True
                value = alist[midpoint-1]
        else:
            a = abs(alist[midpoint]-item)<abs(alist[midpoint+1]-item)
            b = abs(alist[midpoint]-item)<abs(alist[midpoint-1]-item)
            if a==True and b==True:
                dd = alist[midpoint]<item
                yy = alist[midpoint+1]>item
                if dd==True and yy==True:
                    found = True
                    value = alist[midpoint]
                else:
                    found = True
                    value = alist[midpoint-1]
            else:
                if item<alist[midpoint]:
                    last = midpoint - 1
                else:
                    first = midpoint + 1
    return value

################################################################################

final_shotlog =
pd.read_csv('C:\\ShotLogCreate\input\LSSL2016_03_SHOTLOG.csv',header=0)
start_date = pd.to_datetime(min(final_shotlog['TriggerTime'].values))
start_date = start_date.date()
end_date = pd.to_datetime(max(final_shotlog['TriggerTime'].values))
end_date = end_date.date()

file_list = []
for root, dirs, files in os.walk("C:\ShotLogCreate", topdown=True):
    for name in files:
        file_list.append(os.path.join(root, name))
gps_matching = [s for s in file_list if "GPS.txt" in s]

delta = end_date - start_date
rng=[]
for i in range(delta.days + 1):
    rng.append(str(start_date + td(days=i)))
gps_files = subsample_dates(gps_matching, rng)
```

```
################################################################################

#Extract navigation data for the primary, secondary or auxiliary system:
navtime=[];lat=[];lon=[]
for i in gps_files:
    gps = open(i,'r')
    lines = gps.readlines()
    gps.close()
    for line in lines:
        lstrip=line.strip()
        finder2 = 'Marine' in lstrip     # Replace with 'POS-MV' for primary,
'Marine' for secondary, 'Trimble' for auxiliary
        finder4 = '$GPGGA' in lstrip     # Replace with '$INGGA' for primary,
'$GPGGA' for secondary and auxiliary
        if finder2==True and finder4==True:
            lstrip = lstrip.replace(',','|')
            wordsc = lstrip.split('|')
            navtime.append(wordsc[11])
            tmplat = wordsc[14]
            tmplon = wordsc[16]
            deglat = float(tmplat[0:2])
            minlat = float(tmplat[2:10])
            deglon = float(tmplon[0:3])
            minlon = float(tmplon[3:11])
            tmplat = float(deglat + (minlat/60.0))
            tmplon = float(deglon + (minlon/60.0))
            if wordsc[17] == 'W':
                tmplon=tmplon*(-1.0)
            lat.append(tmplat)
            lon.append(tmplon)

trmtime = pd.to_datetime(navtime)
trmtime_cln = trmtime.drop_duplicates()

#Identical DataFrames created with different header names to make searching easier:
dfpre = pd.DataFrame({'TimePre': trmtime, 'LatPre':lat,
'LonPre':lon}).sort_values('TimePre')
dfpre = dfpre.drop_duplicates(subset='TimePre',keep='first')
dfpost = pd.DataFrame({'TimePost': trmtime, 'LatPost':lat,
'LonPost':lon}).sort_values('TimePost')
dfpost = dfpost.drop_duplicates(subset='TimePost',keep='first')

#Check for and remove duplicates by assigning a 'coordinate code':
coord_duplicate=[0]
for i in xrange(1,len(dfpre['TimePre'].values)):
    lat_now = dfpre['LatPre'].values[i]
    lat_last = dfpre['LatPre'].values[i-1]
    lon_now = dfpre['LonPre'].values[i]
    lon_last = dfpre['LonPre'].values[i-1]
    lat_check = lat_now == lat_last
    lon_check = lon_now == lon_last
    if lat_check==True and lon_check==True:
        coord_duplicate.append(int(-10))
    else:
        coord_duplicate.append(i)

dfpre['CoordinateCode']=coord_duplicate
dfpre = dfpre.drop_duplicates(subset='CoordinateCode', keep=False)
```

```
dfpost['CoordinateCode']=coord_duplicate
dfpost = dfpost.drop_duplicates(subset='CoordinateCode', keep=False)

pre_index = pd.to_datetime(dfpre['TimePre'].values)
post_index = pd.to_datetime(dfpost['TimePost'].values)

#Search for a timestamp before and after and determine the position relative to
each in terms of a multiplier:
trimblepre=[];trimblepost=[];multiplier=[]
for i in final_shotlog['TriggerTime'].values:
    tester = pd.to_datetime(i)
    pre = binarySearch_pre(pre_index,tester)
    post = binarySearch_post(post_index,tester)
    trimblepre.append(pre)
    trimblepost.append(post)
    trigger_delta = tester - pre
    trimble_delta = post - pre
    multiplier.append(trigger_delta/trimble_delta)

final_shotlog['ClosestPre']=trimblepre
final_shotlog['ClosestPost']=trimblepost
final_shotlog['Multiplier']=multiplier

dfout1=pd.merge(final_shotlog,dfpre,left_on='ClosestPre',right_on='TimePre')
final_shotlog=pd.merge(dfout1,dfpost,left_on='ClosestPost',right_on='TimePost')

#Merge DataFrames and create the interpolated coordinates. Name output
'MarineStar', 'Trimble' or 'POSMV':
final_shotlog['DiffLat']=(final_shotlog['LatPost']-
final_shotlog['LatPre'])*final_shotlog['Multiplier']
final_shotlog['Interpolated_MarineStarLat']=final_shotlog['LatPre']+final_shotlog['
DiffLat']
final_shotlog['DiffLon']=(final_shotlog['LonPost']-
final_shotlog['LonPre'])*final_shotlog['Multiplier']
final_shotlog['Interpolated_MarineStarLon']=final_shotlog['LonPre']+final_shotlog['
DiffLon']

#Trim excess information:
#final_shotlog=final_shotlog.drop(final_shotlog.columns[[18,19,20,21,22,23,24,25,26
,27,28,29,31]], axis=1) #for POSMV
#final_shotlog=final_shotlog.drop(final_shotlog.columns[[20,21,22,23,24,25,26,27,28
,29,30,31,33]], axis=1) #Trimble
final_shotlog=final_shotlog.drop(final_shotlog.columns[[22,23,24,25,26,27,28,29,30,
31,32,33,35]], axis=1) #MarineStar
final_shotlog.to_csv('C:\\ShotLogCreate\output\LSSL2016_03_SHOTLOG_interpolated_3.c
sv', index=None)

print 'Done!'
```

Appendix C: Listing of shotlog_finalize.py

```
# -*- coding: utf-8 -*-
"""
Created on Fri Sep 09 11:00:10 2016

Uses interpolated coordinates appended by shotlog_interpolate.py to project the
seismic source position. This calculation uses PyProj to assign a local projection,
apply an offset in meters, and take the inverse projection of the offset points
to determine the coordinates of the seismic source.

##IMU point relative to CRP: 0.54 m port, 54.56 m fwd
##COG point relative to CRP: 0.0 m port, 56.51 m fwd
##Trimble relative to CRP: 5.45 m port, 34.77 m fwd
##MarineStar relative to CRP: 1.57 m port, 79.72 m fwd
##Source located 0.5 m aft of CRP

@author: kboggild
"""

import pandas as pd
from pyproj import Proj
import math

def project_source_marinestar(lon1,lat1,heading):
    bearing = heading-180-math.degrees(math.atan(1.57/80.22))
    p = Proj(proj='stere',ellps='WGS84', lon_0=lon1,lat_0=lat1)
    x,y = p(lon1,lat1)
    offsetx =
(80.22/(math.cos(math.atan(1.57/80.22))))*math.sin(math.radians(bearing))
    offsety =
(80.22/(math.cos(math.atan(1.57/80.22))))*math.cos(math.radians(bearing))
    x = x + offsetx
    y = y + offsety
    output_lon,output_lat= p(x,y,inverse=True)
    return output_lon,output_lat
def project_source_posmv(lon1,lat1,heading):
    bearing = heading-180-math.degrees(math.atan(0.0/57.01))
    p = Proj(proj='stere',ellps='WGS84', lon_0=lon1,lat_0=lat1)
    x,y = p(lon1,lat1)
    offsetx =
(57.01/(math.cos(math.atan(0.00/57.01))))*math.sin(math.radians(bearing))
    offsety =
(57.01/(math.cos(math.atan(0.00/57.01))))*math.cos(math.radians(bearing))
    x = x + offsetx
    y = y + offsety
    output_lon,output_lat= p(x,y,inverse=True)
    return output_lon,output_lat
def project_source_trimble(lon1,lat1,heading):
    bearing = heading-180-math.degrees(math.atan(5.45/35.27))
    p = Proj(proj='stere',ellps='WGS84', lon_0=lon1,lat_0=lat1)
    x,y = p(lon1,lat1)
    offsetx =
(35.27/(math.cos(math.atan(5.45/35.27))))*math.sin(math.radians(bearing))
    offsety =
(35.27/(math.cos(math.atan(5.45/35.27))))*math.cos(math.radians(bearing))
    x = x + offsetx
    y = y + offsety
    output_lon,output_lat= p(x,y,inverse=True)
```

```
    return output_lon,output_lat

final_shotlog =
pd.read_csv('C:\\ShotLogCreate\input\LSSL2016_03_shotlog_interpolated.csv',header=0
)

src_lon=[];src_lat=[]
for i in xrange(0,len(final_shotlog['FFID'].values)):
    if float(final_shotlog['FFID'].values[i])>float(17593.5) and
float(final_shotlog['FFID'].values[i])<float(19647.5):
        calc_lon,calc_lat =
project_source_marinestar(final_shotlog['Interpolated_MarineStarLon'].values[i],fin
al_shotlog['Interpolated_MarineStarLat'].values[i],final_shotlog['Heading'].values[
i])
        calc_lon = format(round(calc_lon, 6), '.6f')
        calc_lat = format(round(calc_lat, 6), '.6f')
        src_lon.append(calc_lon)
        src_lat.append(calc_lat)
    else:
        calc_lon,calc_lat =
project_source_posmv(final_shotlog['Interpolated_POSMVLon'].values[i],final_shotlog
['Interpolated_POSMVLat'].values[i],final_shotlog['Heading'].values[i])
        calc_lon = format(round(calc_lon, 6), '.6f')
        calc_lat = format(round(calc_lat, 6), '.6f')
        src_lon.append(calc_lon)
        src_lat.append(calc_lat)
#out_ffid=[]                                    #commented section used to
accommodate formatting of LSL1603 FFIDs
#for i in final_shotlog['FFID'].values:
#    tmp = format(i, '.3f')
#    out_ffid.append(tmp)

#final_shotlog['FFID'] = out_ffid
final_shotlog['Src_Lat'] = src_lat
final_shotlog['Src_Lon'] = src_lon
final_shotlog =
final_shotlog.drop(final_shotlog.columns[[9,10,11,12,16,17,18,19,20,21,22,23]],
axis=1)

final_shotlog.to_csv('C:\\ShotLogCreate\output\LSL1603_shotlog_final.csv',
index=None)

print 'Done!'
```

Appendix D: Listing of shotlog entries that have been edited because of errors in the GeoEel controller logs, extraneous entries in the Zyfer trigger log, or shots that were triggered before the record length of the previous shot had elapsed (*e.g.* due to a change in firing interval).

Line #	Duplicated FFID	Day	Timestamp	Comments
LSL1601	1705	2016-08-17	18:59:12.008064000	Erroneous trigger log entry
LSL1601	1913	2016-08-17	19:40:51.563878400	Erroneous trigger log entry
LSL1601	5506	2016-08-18	08:17:47.692121600	Erroneous trigger log entry
LSL1601	5713	2016-08-18	08:59:09.217651200	Erroneous trigger log entry
LSL1601	5868	2016-08-18	09:30:06.229670400	Erroneous trigger log entry
LSL1601	6339	2016-08-18	11:20:00.047590400	Shot triggered before the previous shot's record length had elapsed (i.e. no shot file was recorded)
LSL1601	6891	2016-08-18	13:47:31.155788800	Erroneous trigger log entry
LSL1601	7489	2016-08-18	16:26:57.887462400	Erroneous trigger log entry
LSL1601	10650	2016-08-19	Multiple	Coincides with error messages in GeoEel log - was not able to log .sgd until final entry
LSL1601	13240	2016-08-19	12:06:00.041843200	Shot triggered before the previous shot's record length had elapsed (i.e. no .sgd file was recorded for this trigger)
LSL1603	17597	2016-08-22	08:52:20.046784000	1 minute gap between 17596-17597
LSL1603	17597	2016-08-22	08:52:40.047859200	1 minute gap between 17596-17597
LSL1603	18067	2016-08-22	11:29:41.617881600	Erroneous trigger log entry
LSL1603	18650	2016-08-22	15:23:00.049996800	Triggered but not saved, coincides with change in record length
LSL1603	18793	2016-08-22	16:34:52.601574400	Erroneous trigger log entry
LSL1603	20616	2016-08-23	07:46:39.703577600	Erroneous trigger log entry
LSL1603	21244	2016-08-23	13:00:13.567987200	Erroneous trigger log entry
LSL1604	26105	2016-08-25	07:04:03.788902400	Erroneous trigger log entry
LSL1604	27746	2016-08-25	15:04:08.285708800	Erroneous trigger log entry
LSL1604	30760	2016-08-26	07:48:44.393600000	Erroneous trigger log entry
LSL1604	30786	2016-08-26	07:57:12.946278400	Erroneous trigger log entry
LSL1605	31354	2016-08-27	19:37:21.926822400	Erroneous trigger log entry
LSL1605	32840	2016-08-28	02:13:45.623756800	Erroneous trigger log entry
LSL1605	33458	2016-08-28	04:58:28.482713600	Erroneous trigger log entry
LSL1606	37294	2016-09-03	04:51:01.058342400	Erroneous trigger log entry
LSL1607	40201	2016-09-03	21:03:01.586457600	Erroneous trigger log entry
LSL1607	40251	2016-09-03	21:19:48.464064000	Erroneous trigger log entry
LSL1608	43455	2016-09-05	14:17:34.008204800	Erroneous trigger log entry
LSL1608	43455	2016-09-05	14:17:46.192678400	Erroneous trigger log entry
LSL1608	45145	2016-09-05	23:40:57.797260800	Erroneous trigger log entry
LSL1608	45787	2016-09-06	03:15:03.759654400	Erroneous trigger log entry
LSL1608	48631	2016-09-06	19:03:01.896089600	Erroneous trigger log entry

LSL1609	54178	2016-09-08	18:41:12.370726400	Erroneous trigger log entry
LSL1609	54700	2016-09-08	21:35:23.072102400	Erroneous trigger log entry
LSL1610	54823	2016-09-08	22:19:49.885299200	Erroneous trigger log entry
LSL1610	55771	2016-09-09	03:35:43.672972800	Erroneous trigger log entry
LSL1610	55783	2016-09-09	03:39:44.073856000	Erroneous trigger log entry
LSL1610	57441	2016-09-09	12:52:19.379200000	Erroneous trigger log entry
LSL1610	58008	2016-09-09	16:00:09.870643200	Erroneous trigger log entry
LSL1610	58560	2016-09-09	19:03:57.701030400	Erroneous trigger log entry
LSL1610	58797	2016-09-09	20:23:06.287347200	Erroneous trigger log entry
LSL1611	59001	2016-09-09	21:32:41.648614400	Erroneous trigger log entry
LSL1611	59267	2016-09-09	23:01:15.343347200	Erroneous trigger log entry
LSL1611	59365	2016-09-09	23:34:00.591910400	Erroneous trigger log entry
LSL1611	62053	2016-09-10	14:30:11.631833600	Erroneous trigger log entry
LSL1611	62228	2016-09-10	15:28:17.793177600	Erroneous trigger log entry
LSL1612	65665	2016-09-11	14:03:44.578227200	Erroneous trigger log entry
LSL1612	65806	2016-09-11	14:50:47.217907200	Erroneous trigger log entry
LSL1612	65937	2016-09-11	15:34:30.781849600	Erroneous trigger log entry
LSL1612	66044	2016-09-11	16:09:51.988121600	Erroneous trigger log entry
LSL1612	66102	2016-09-11	16:29:18.065881600	Erroneous trigger log entry
LSL1612	66285	2016-09-11	17:30:19.792704000	Erroneous trigger log entry
LSL1612	66377	2016-09-11	18:01:10.990284800	Erroneous trigger log entry
LSL1612	66382	2016-09-11	18:02:47.948697600	Erroneous trigger log entry
LSL1612	66394	2016-09-11	18:06:40.178137600	Erroneous trigger log entry
LSL1612	66446	2016-09-11	18:23:53.413222400	Erroneous trigger log entry
LSL1612	66515	2016-09-11	18:47:06.387929600	Erroneous trigger log entry
LSL1612	66634	2016-09-11	19:26:34.155392000	Erroneous trigger log entry

Appendix E: Listing of partial file errors that were encountered during acquisition of lines LSL1602 and LSL1610.

Line #	Initial FFID	Contents	Linked FFID	Contents
1	12477	Channels 9-16 w/ auxiliary	12479	Channels 1-8
1	12478	Channels 9-16 w/ auxiliary	12481	Channels 1-8
10	57629	Channels 1-16	57633	Auxiliary channels
10	57630	Channels 1-16	57635	Auxiliary channels
10	57631	Channels 1-16	57636	Auxiliary channels
10	57632	Channels 1-16	57637	Auxiliary channels

Note: Linked FFIDs have been omitted from the shot log since they are the result of the same shot as the Initial FFID.